Parametric Resonance Characteristics of Laminated Composite Twisted Cantilever Panels

A thesis submitted to

National Institute of Technology, Rourkela

For the award of degree of

Doctor of Philosophy

in

Engineering

by

A.V. Asha

Under the supervision of

Prof. Shishir K. Sahu

Department of Civil Engineering

National Institute of Technology

Rourkela-769008, India

April 2008

Dedicated

To My Parents

Certificate

This is to certify that the thesis entitled "**Parametric Resonance Characteristics of Laminated Composite Twisted Cantilever Panels"**, being submitted to the National Institute of Technology, Rourkela (India) by A.V.Asha for the award of the degree of **Doctor of Philosophy (CIVIL ENGINEERING)** is a record of bonafide research work carried out by her under my supervision and guidance. A.V.Asha has worked for more than three years on the above problem and it has reached the standard fulfilling the requirements of the regulations of the degree. The results embodied in this thesis have not been submitted in part or full to any other university or institute for the award of any degree or diploma.

Rourkela
Date:

(Dr.Shishir Kumar Sahu)
Professor
Department of Civil Engineering
National Institute of Technology
Rourkela-769008
Orissa, India.

Acknowledgement

I express my deep sense of gratitude and indebtedness to my thesis supervisor Dr.Shishir Kumar Sahu, Professor, Department of Civil Engineering, National Institute of Technology, Rourkela, for his invaluable encouragement, helpful suggestions and supervision throughout the course of this work.

I express my sincere thanks to the Director, Prof. S.K.Sarangi, National Institute of Technology, Rourkela for motivating me in this endeavor and providing me the necessary facilities for this study.

I would like to thank Prof. B.K.Rath, ex-head of the Civil Engineering Department and Prof. K.C.Patra, present head of the department for their help and cooperation during the progress of this work.

I would also like to thank Prof. R.K.Sahoo of Mechanical Engineering Department and Prof. M.R.Barik of Civil Engineering Department for their invaluable suggestions and help at various stages of the work.

I acknowledge with thanks the help rendered to me by all my colleagues and other staff of the Civil Engineering Department and am grateful for their continuous encouragement during the progress of my work.

Last but not least, I am extremely grateful to my husband and children, Arun and Aravind, for their support and patience during this period.

(A.V.Asha)

ABSTRACT

The twisted cantilever panels have significant applications in wide chord turbine blades, compressor blades, fan blades and particularly in gas turbines. Structural elements subjected to in-plane periodic forces may lead to parametric resonance, due to certain combinations of the applied in-plane load parameters and the natural frequency of transverse vibrations. The instability may occur below the critical load of the structure under compressive loads over wide ranges of excitation frequencies. Composite materials are increasingly used as load bearing structural components in aerospace and naval structures, automobiles, pressure vessels, turbine blades and many other engineering applications because of their high specific strength, specific stiffness and tailorability. Thus, the parametric resonance characteristics of laminated composite twisted cantilever panels are of great technical importance for understanding the dynamic behaviour of structures under in-plane periodic loads. This aspect of static and dynamic stability behaviour of laminated composite pretwisted cantilever panels is studied in the present investigation.

The analysis is carried out with the finite element method (FEM) using first order shear deformation theory (FSDT), considering the effects of transverse shear deformation and rotary inertia. An eight-node isoparametric quadratic element is employed in the present analysis with five degrees of freedom per node. Element elastic stiffness matrices, mass matrices and load vectors are derived using the principle of Stationery Potential Energy. They are evaluated using the Gauss quadrature numerical integration technique. Plane stress analysis is carried out using the finite element method to determine the stresses and these are used to formulate the geometric stiffness matrix. The overall stiffness and

mass matrices are obtained by assembling the corresponding element matrices using skyline technique. The eigenvalues are determined using Subspace iteration scheme.

In this analysis the effects of various parameters such as twisting angle, aspect ratio, thickness, curvature, number of layers, ply orientation, degree of orthotropy, etc on the buckling and vibration behaviour of homogeneous and laminated composite twisted cantilever panels are studied. The parametric instability characteristics of homogeneous and laminated composite pretwisted cantilever flat and curved panels subjected to in-plane harmonic loads are studied.

The study revealed that, due to static component of load, the instability regions tend to shift to lower frequencies. The onset of instability occurs earlier with increase of angle of twist of panel with wider instability regions. Unlike twisted plates, there is significant deviation of the instability behaviour of twisted cylindrical panels from that of untwisted cylindrical panels. Similar behaviour is also observed for the variation of instability region of twisted spherical and hyperbolic paraboloidal panels. The excitation frequency decreases from square to rectangular panels with increase of aspect ratio. The ply orientation significantly affects the onset of instability and the width of the zones of instability.

Thus the instability behaviour of twisted cantilever panels is influenced by the geometry, material, ply lay-up and its orientation. This can be used to the advantage of tailoring during design of composite twisted structures.

Keywords: parametric resonance, dynamic instability, pretwist, laminated composite cantilever panels.

Contents

Abstract v

Contents vii

List of tables ix

List of figures xiv

Nomenclature xviii

List of Publications xxi

1. INTRODUCTION 1

1.1: Introduction 1

1.2: Importance of the present structural stability study 1

1.3: Outline of the present work 2

2. REVIEW OF LITERATURE 4

2.1: Introduction 4

2.2: Vibration and buckling of twisted panels 4

2.3: Dynamic stability of twisted panels 19

2.4: Critical discussion 23

2.5: Objectives and scope of the present study 25

3. THEORY AND FORMULATION 26

3.1: The Basic Problem 26

3.2: Proposed Analysis..... 27

3.2.1: Assumptions of the analysis 28

3.3: Governing Equations..... 29

3.3.1: Governing Differential Equations 29

3.4: Dynamic stability studies 31

3.5: Energy Equations..... 32

3.5.1: Formulation of Vibration and Static Stability problems... 35

3.6: Finite Element Formulation 35

3.6.1: The shell element 36

3.6.2: Strain displacement relations 38

3.6.3: Constitutive Relations 39

3.6.4: Derivation of Element Matrices …….. 44

3.6.5: Geometric stiffness matrix ……... 45

3.7: Computer program ……... 48

4. RESULTS AND DISCUSSIONS ……. 49

4.1: Introduction.....……..... 49

4.2: Convergence study …… 50

4.3: Comparison with previous studies …….. 51

4.4: Numerical results …….. 55

4.5: Isotropic twisted panels …… 55

4.5.1: Non-dimensionalization of parameters …… 56

4.5.2: Boundary conditions ……. 56

4.5.3: Vibration and buckling studies ……... 56

4.5.4: Dynamic stability studies ……. 63

4.6: Cross ply twisted cantilever panels…… 66

4.6.1: Non-dimensionalization of parameters …… 66

4.6.2: Boundary conditions ……. 67

4.6.3: Vibration and buckling studies …… 67

4.6.4: Dynamic stability studies …….. 81

4.7: Angle-ply twisted cantilever panels……. 90

4.7.1: Non-dimensionalization of parameters …… 91

4.7.2: Boundary conditions …….. 91

4.7.3: Vibration and buckling studies …… 91

4.7.4: Dynamic stability studies …….. 103

5. CONCLUSIONS…….. 112

5.1: Isotropic twisted panels ……. 113

5.2: Cross-ply twisted cantilever panels …….. 115

5.3: Angle-ply twisted cantilever panels ……. 118

5.4: Scope for further work …….. 123

REFERENCES …… 124

APPENDIX ……. 135

List of Tables

No.	Title	Page
4.1	Convergence of non-dimensional fundamental frequencies of free vibration of isotropic twisted plates …….	50
4.2	Convergence of non-dimensional frequencies of vibration of composite twisted cantilever plates with 45°/-45°/45° lamination ……...	51
4.3	Comparison of non-dimensional frequency parameters (λ) of the initially twisted isotropic cantilever plate type blade ……..	52
4.4	Comparison of non-dimensional fundamental frequencies of vibration of graphite epoxy pretwisted cantilever [θ/-θ/θ] plates ……..	53
4.5	Comparison of buckling loads for a thin untwisted (Φ = 0°) angle-ply cylindrical panel with symmetric lay-up $[0°/-\alpha°/+\alpha°/-90°]_s$ ……	54
4.6	Variation of non-dimensional frequency parameter with angle of twist for a square isotropic cantilever plate ……..	57
4.7	Variation of non-dimensional frequency parameter with R_y/b ratio for a square isotropic cylindrical cantilever panel ……	58
4.8	Variation of non-dimensional frequency parameter with aspect ratio for an isotropic twisted cantilever plate ……..	58
4.9	Variation of frequency in Hz with b/h ratio for a square isotropic twisted cantilever plate ……...	59

4.10 Variation of non-dimensional frequency parameter for different twisted cantilever curved panels …….. 59

4.11 Variation of non-dimensional buckling load with angle of twist for a square isotropic cantilever plate ... 60

4.12 Variation of non-dimensional buckling load with angle of twist for a square isotropic cylindrical cantilever panel …… 61

4.13 Variation of non-dimensional buckling load with R_y/b ratio for a square isotropic twisted cylindrical cantilever panel …… 61

4.14 Variation of non-dimensional buckling load with aspect ratio for an isotropic twisted cantilever plate… 62

4.15 Variation of buckling load with b/h ratio for a square isotropic twisted cantilever plate ……... 62

4.16 Variation of non-dimensional frequency parameter with angle of twist for square cross-ply plates with different ply lay-ups …… 67

4.17 Non-dimensional free vibration frequencies of square cross-ply pretwisted cantilever plates with varying angles of twist ……... 69

4.18 Non-dimensional free vibration frequencies of square cross-ply pretwisted cantilever plates with varying angles of twist (E-glass/epoxy) …… 70

4.19 Variation of non-dimensional frequency parameter with R/a ratio for square cross-ply cylindrical and spherical twisted cantilever shells …….. 71

4.20 Comparison of non-dimensional frequency parameter of square cross-ply twisted plates and square cross-ply twisted spherical shells ($b/R_y = 0.25$) ……... 72

4.21 Variation of non-dimensional frequency parameter with aspect ratio for cross-ply twisted cantilever plates with different ply lay-ups ……. 73

4.22 Variation of frequency in Hz with b/h ratio for square cross-ply twisted cantilever plates with different ply lay-ups ……..... 73

4.23 Variation of non-dimensional frequency parameter with geometry for cross-ply twisted cantilever plates with different ply lay-ups …… 74

4.24 Variation of non-dimensional frequency parameter with degree of orthotropy of different square cross-ply twisted cantilever plates ……..... 75

4.25 Variation of non-dimensional buckling load with angle of twist for square cross-ply plates with different ply lay-ups …… 76

4.26 Variation of non-dimensional buckling load with R/a ratio for square cylindrical and spherical twisted cross-ply shells ……. 77

4.27 Non-dimensional buckling load for square cross-ply twisted plates and spherical twisted shells (b/R_y = 0.25) with different ply lay-ups …….. 78

4.28 Variation of non-dimensional buckling load with aspect ratio for cross-ply twisted cantilever plates with different ply lay-ups …… 79

4.29 Variation of buckling load with b/h ratio for square cross-ply twisted cantilever plates with different ply lay-ups …….. 80

4.30 Variation of non-dimensional buckling load with geometry for square cross-ply twisted cantilever panels with different ply lay-ups …… 80

4.31 Variation of non-dimensional buckling load with degree of orthotropy (E_1/E_2) for different square cross-ply twisted cantilever plates ……. 81

4.32 Variation of non-dimensional free vibration frequencies with angle of twist and ply orientation of angle-ply (θ/-θ/θ) pretwisted cantilever plates …….. 92

4.33 Variation of non-dimensional free vibration frequencies with angle of twist and ply orientation of angle-ply (θ/-θ/θ) pretwisted cantilever panels ……. 94

4.34 Variation of non-dimensional free vibration frequencies with R_y/b ratio of square angle-ply (θ/-θ/θ) pretwisted cantilever panels …… 95

4.35 Variation of non-dimensional frequency with aspect ratio of laminated composite angle-ply (θ/-θ/θ) pretwisted cantilever plates …… 95

4.36 Variation of frequency in Hz with b/h ratio for square laminated composite angle-ply (θ/-θ/θ) pretwisted cantilever plates ……... 96

4.37 Variation of non-dimensional frequency with degree of orthotropy of square angle-ply (θ/-θ/θ) pretwisted cantilever plates ……... 97

4.38 Variation of non-dimensional buckling load with angle of twist of square angle-ply(θ/-θ/θ) pretwisted cantilever plates ……... 98

4.39 Variation of non-dimensional buckling load with angle of twist of square angle-ply(θ/-θ/θ) pretwisted cantilever plates with camber 99

4.40 Variation of non-dimensional buckling load with angle of twist of square laminated composite angle-ply (θ/-θ/θ) pretwisted thick cantilever plates …….. 99

4.41 Variation of non-dimensional buckling load with aspect ratio of laminated composite angle-ply (θ/-θ/θ) pretwisted cantilever plates ……... 100

4.42 Variation of non-dimensional buckling load with angle of twist of rectangular angle-ply (θ/-θ/θ) pretwisted cantilever plates …… 101

4.43 Variation of non-dimensional buckling load with b/h ratio of square angle-ply (θ/-θ/θ) pretwisted cantilever plates ……. 102

4.44 Variation of non-dimensional buckling load with degree of orthotropy of angle-ply (θ/-θ/θ) pretwisted cantilever plates ……... 102

List of Figures

No	Title	Page
3.1	Laminated composite twisted curved panel subjected to in-plane harmonic loads …….	27
3.2	Force and moment resultants of the twisted panel …..	30
3.3	Isoparametric quadratic shell element ……..	36
3.4	Laminated shell element …….	40
4.1	Comparison of results of instability regions of square untwisted angle-ply panels(45°/-45°, 45°/-45°/45°/-45°)of present formulation with Moorthy *et al*. ……	54
4.2	Variation of instability region with angle of twist of the isotropic cantilever panel, a/b = 1, Φ = 0°, 15° and 30°, α = 0.2 ……	63
4.3	Variation of instability region with static load factor for a square isotropic twisted cantilever panel, a/b = 1, Φ = 15°, α = 0.0, 0.2, 0.4 and α = 0.6 ……..	64
4.4	Variation of instability region with R_y/b ratio for a square isotropic cylindrical twisted cantilever panel, a/b = 1, Φ = 15°, α = 0.2 …….	64
4.5	Variation of instability region with b/h ratio for a square isotropic twisted cantilever plate, a/b = 1, Φ = 15°, α = 0.2 ……...	65
4.6	Variation of instability region with curvature for a square isotropic twisted cantilever panel, a/b = 1, Φ = 15°, α = 0.2, b/R_y = 0.25 ……..	66
4.7	Variation of instability region with angle of twist of the four layer cross-ply twisted plate [0°/90°/90°/0°], a/b = 1, Φ = 0°, 15° and 30°, α = 0.2 ……...	82

4.8 Variation of instability region with number of layers of the cross-ply twisted plate (2, 4, and 8 layers), a/b = 1, Φ = 15°, α = 0.2 ……... 83

4.9 Variation of instability region with static load factor of a cross-ply twisted plate[0°/90°/90°/0°], a/b = 1, Φ = 15°, α = 0.0, 0.2, 0.4 and α = 0.6 …….. 84

4.10 Variation of instability region with static load factor of a cross-ply twisted plate [0°/90°/0°/90°/0°/90°/0°/90°], a/b = 1, Φ =15°, α = 0.0, 0.2, 0.4 and α = 0.6 ……... 84

4.11 Variation of instability region with aspect ratio of the cross-ply twisted plate[0°/90°/90°/0°], Φ = 15°, α = 0.2, a/b = 0.5, 1.0, 1.5 …….. 85

4.12 Variation of instability region with b/h ratio of the four layer cross-ply twisted plate[0°/90°/90°/0°], a/b = 1 , Φ = 15°, α = 0.2, b/h = 200, 250 and 300 ……... 86

4.13 Variation of instability region with b/h ratio of the cross-ply twisted plate[0°/90°/0°/90°/0°/90°/0°/90°], a/b = 1 , Φ = 15°, α = 0.2, b/h = 200, 250 and 300 …… 86

4.14 Variation of instability region with number of layers of the cross-ply twisted cylindrical panel, a/b = 1, Φ = 15°, α = 0.2 and b/R_y = 0.25 ……. 87

4.15 Variation of instability region with number of layers of the cross-ply twisted spherical panel, a/b = 1, Φ = 15°, α = 0.2 and b/R_y = 0.25, b/R_x = 0.25 ……..... 87

4.16 Variation of instability region with number of layers of the cross-ply twisted hyperbolic panel, a/b = 1, Φ = 15°, α = 0.2 and b/R_y = 0.25, b/R_x = −0.25 ……. 88

4.17 Variation of instability region with curvature for a cross-ply twisted cantilever panel [0°/90°], a/b = 1, Φ = 15°, α = 0.2, b/R_y = 0.25 ……..... 89

4.18 Variation of instability region with curvature for a cross-ply twisted cantilever panel [0°/90°/90°/0°], a/b = 1, Φ = 15°, α = 0.2, b/R_y = 0.25 ……... 89

4.19 Variation of instability region with degree of orthotropy of the cross-ply twisted cantilever panel [0°/90°/90°/0°], a/b = 1, Φ = 15°, α = 0.2 ……... 90

4.20 Variation of instability region with angle of twist of the angle-ply flat panel [30°/-30°/30°/-30°], a/b = 1, Φ = 0°, 15° and 30°, α = 0.2 ……. 103

4.21 Variation of instability region with number of layers of the angle-ply twisted panel [45°/-45°/45°/-45°], a/b = 1, b/h = 250, Φ = 15°, α = 0.2 ……... 104

4.22 Variation of instability region with static load factor of an angle-ply twisted panel [30°/-30°/30°/-30°], a/b = 1, Φ = 15°, α = 0.0, 0.2, 0.4 and α = 0.6 ……. 105

4.23 Variation of instability region with ply orientation of an angle-ply twisted panel [θ/−θ/ θ/−θ], a/b = 1, Φ = 15°, α = 0.2, θ = 0° to 90° …… 106

4.24 Variation of instability region with aspect ratio of the angle-ply twisted panel [30°/-30°/30°/-30°], a/b = 1, 2 and 4, Φ = 15°, α = 0.2 ……. 107

4.25 Variation of instability region with b/h ratio of the angle-ply twisted panel [30°/-30°/30°/-30°], a/b = 1, b/h =200, 250 and 300, Φ = 15°, α = 0.2 ……. 107

4.26 Variation of instability region with angle of twist of the angle-ply cylindrical twisted panel [30°/-30°/30°/-30°], a/b = 1, Φ = 0°, 15° and 30°, α = 0.2, b/R_y = 0.25.. 108

4.27 Variation of instability region with angle of twist of the angle-ply spherical twisted panel [30°/-30°/30°/-30°], a/b = 1, Φ = 0°, 15° and 30°, α = 0.2, b/R_y = 0.25, b/R_x = 0.25 …… 109

4.28 Variation of instability region with angle of twist of the angle-ply hyperbolic paraboloidal twisted panel [30°/-30°/30°/-30°], a/b = 1, Φ = 0°, 15° and 30°, α = 0.2, b/R_y = 0.25, b/R_x = −0.25 ……... 109

4.29 Variation of instability region with geometry for an angle-ply twisted panel [30°/-30°/30°/-30°], a/b = 1, Φ = 15°, α = 0.2, b/R_y = 0.25 …… 110

4.30 Variation of instability region with degree of orthotropy for an angle-ply twisted panel [30°/-30°/30°/-30°], a/b = 1, Φ = 15°, α = 0.2, h = 2mm …….. 111

6.1 Flow chart of computer programme ……. 137

Nomenclature

The principal symbols used in this thesis are presented for easy reference. A single symbol is used for different meanings depending on the context and defined in the text as they occur.

English

a, b	dimensions of the twisted panel
a/ b	aspect ratio of the twisted panel
A_{ij}, B_{ij}, D_{ij} and S_{ij}	extensional, bending-stretching coupling, bending and transverse shear stiffnesses
b/ h	width to thickness ratio of the twisted panel
[B]	Strain-displacement matrix for the element
[D]	stress-strain matrix
$[D_p]$	stress-strain matrix for plane stress
dx, dy	element length in x and y-direction
dV	volume of the element
E_{11}, E_{22}	modulii of elasticity in longitudinal and transverse directions
G_{12}, G_{13}, G_{23}	shear modulii
h	thickness of the plate
$\lvert J \rvert$	Jacobian
k	shear correction factor
$[K_e]$	global elastic stiffness matrix
$[k_e]$	element bending stiffness matrix with shear deformation of the panel
$[K_g]$	global geometric stiffness matrix
$[K_p]$	plane stiffness matrix
k_x, k_y, k_{xy}	bending strains
[M]	global consistent mass matrix
$[m_e]$	element consistent mass matrix

M_x, M_y, M_{xy}	moment resultants of the twisted panel
n	number of layers of the laminated panel
[N]	shape function matrix
N_i	shape functions
N (t)	in-plane harmonic load
N_s	static portion of load N (t)
N_t	amplitude of dynamic portion of load N (t)
N_{cr}	critical load
N_x, N_y, N_{xy}	in-plane stress resultants of the twisted panel
N_x^0, N_y^0, N_{xy}^0	external loading in the X and Y directions respectively
[P]	mass density parameters
q	vector of degrees of freedom
Q_x , Q_y	shearing forces
R_x, R_y, R_{xy}	radii of curvature of shell in x and y directions and radius of twist
T	transformation matrix
u, v, w	displacement components in the x, y, z directions at any point
u_o, v_o, w_o	displacement components in the x, y, z directions at the midsurface
U_0	strain energy due to initial in-plane stresses
U_1	strain energy associated with bending with transverse shear
U_2	work done by the initial in-plane stresses and the nonlinear strain
V	kinetic energy of the twisted panel
w	out of plane displacement
x_i, y_i	cartesian nodal coordinates
X, Y, Z	global coordinate axis system

Greek

α	static load factor
β	dynamic load factor
γ	shear strains
$\varepsilon_x, \varepsilon_y, \gamma_{xy}$	strains at a point
ε_{xnl}, ε_{ynl}, ε_{xynl}	non-linear strain components
θ_x, θ_y	rotations of the midsurface normal about the x- and y- axes respectively
λ	non-dimensional buckling load
ν	Poisson's ratio
ξ, η	local natural coordinates of the element
$(\rho)_k$	mass density of k_{th} layer from mid-plane
ρ	mass density of the material
$\sigma_x, \sigma_y, \tau_{xy}$	stresses at a point
σ_x^0, σ_y^0 and σ_{xy}^0	in-plane stresses due to external load
τ_{xy}, τ_{xz}, τ_{yz}	shear stresses in xy, xz and yz planes respectively
ω	frequencies of vibration
ϖ	non-dimensional frequency parameter
Ω	frequency of excitation of the harmonic load
$\overline{\Omega}$	excitation frequency in radians/second
Φ	angle of twist of the twisted panel

Mathematical Operators

$[\ ]^{-1}$	Inverse of the matrix
$[\ ]^T$	Transpose of the matrix
$\frac{\partial}{\partial x}, \frac{\partial}{\partial y}$	Partial derivatives with respect to x and y

List of Publications out of this Work

Papers in International Journals

1. S. K. Sahu and A.V. Asha (2008): Parametric resonance characteristics of angle- ply twisted curved panels, *International Journal of Structural Stability and Dynamics*, Vol.**8**(1), pp.61-76

2. S. K. Sahu, A. V. Asha and R. N. Mishra (2005): Stability of Laminated Composite Pretwisted Cantilever Panels, Journal *of Reinforced Plastics and Composites*, Vol.**24** (12), pp.1327-1334.

Papers Presented in Conferences

1. S. K. Sahu and A. V. Asha: Dynamic Stability of twisted laminated Composite cross-ply panels, International Conference on *Theoretical, Applied, Computational and Experimental Mechanics (ICTACEM 2007)*, Dec 27-29, 2007 at IIT, Kharagpur

2. S. K .Sahu and A. V. Asha: Vibration and Stability of Cross-ply laminated twisted cantilever plates, *International conference on Vibration Problems*, Feb 1-3, 2007 at B.E College, Shibpur, Kolkata.

3. S. K.Sahu and A. V. Asha: Dynamic Stability of Laminated Composite twisted curved Panels, IXth *International conference on "Recent advances in Structural Dynamics"*, July 2006, Institute of Sound and Vibration Research, University of Southampton, UK.

CHAPTER 1

INTRODUCTION

1.1: Introduction

The twisted cantilever panels have significant applications in wide chord turbine blades, compressor blades, fan blades, aircraft or marine propellers, helicopter blades, and particularly in gas turbines. This range of practical applications demands a proper understanding of their vibration, static and dynamic stability characteristics. The damage caused by blades failing due to vibratory fatigue can be catastrophic at worst and at the very least result in additional engine development costs due to redesign and repair. Due to its significance, a large number of references deal with the free vibration of twisted plates.

1.2: Importance of the present structural stability study

The blades are often subjected to axial periodic forces due to axial components of aerodynamic or hydrodynamic forces acting on the blades. Structural elements subjected to in-plane periodic forces may lead to parametric resonance, due to certain combinations of the values of load parameters. The instability may occur below the critical load of the structure under compressive loads over wide ranges of excitation frequencies. Composite materials are being increasingly used in turbo-machinery blades because of their specific strength, stiffness and these can be tailored through the variation of fiber orientation and stacking sequence to obtain an efficient design. Thus the parametric resonance characteristics of laminated composite twisted cantilever panels are of great importance for

understanding the systems under periodic loads. The distinction between good and bad vibration regimes of a structure, subjected to in-plane periodic loading can be distinguished through an analysis of dynamic instability region (DIR) spectra. The calculation of these spectra is often provided in terms of natural frequencies and the static buckling loads. So, the calculation of these parameters with high precision is an integral part of dynamic stability analysis of twisted plates.

A comprehensive analysis of the vibration problems of homogeneous turbomachinery blades, modeled as beams has been studied exhaustively. Some studies are available on dynamic stability of untwisted plates and shells. The vibration aspects of laminated composite pretwisted blades, which have increasing application in recent years, are scanty in literature. The static and dynamic stability studies on twisted structures are the subject of renewed interest by various researchers. It is clear from the above discussion, that the process of investigating the different aspects of vibration and stability studies on twisted panels is a current problem of interest. A thorough review of earlier works done in this area becomes essential to arrive at the objective and scope of the present investigation. The detailed review of literature along with critical discussions is presented in the next chapter.

1.3: Outline of the present work

The present study mainly deals with the parametric resonance characteristics of homogeneous and laminated composite twisted cantilever panels. The influence of various parameters like angle of twist, curvature, side to thickness ratios, number of layers, lamination sequence, and ply orientation, degree of orthotropy, static and dynamic load factors on the vibration and instability behaviour of twisted panels are examined.

The governing equations for the dynamic stability of laminated composite doubly curved twisted panels/shells subjected to in-plane harmonic

loading are developed. The equation of motion represents a system of second order differential equations with periodic coefficients of the Mathieu-Hill type. The development of the regions of instability arises from Floquet's theory and the solution is obtained using Bolotin's approach using finite element method. The governing differential equations have been developed using the first order shear deformation theory (FSDT).

This thesis contains five chapters. In this chapter, a brief introduction of the importance of this study has been outlined.

In chapter 2, a detailed review of the literature pertinent to the previous works done in this field has been listed. A critical discussion of the earlier investigations is done. The aim and scope of the present study is also outlined in this chapter.

In chapter 3, a description of the theory and formulation of the problem and the finite element procedure used to analyse the vibration, buckling and parametric instability characteristics of homogeneous and laminated composite twisted cantilever panels is explained in detail. The computer program used to implement the formulation is briefly described.

In chapter 4, the results and discussions obtained in the study have been presented in detail. The effects of various parameters like twist angle, lamination sequence, ply orientation, degree of orthotropy, aspect ratio, width to thickness ratio and in-plane load parameters on the vibration, buckling and dynamic instability regions is investigated. The studies have been done for homogeneous, cross-ply and angle-ply laminated composite twisted cantilever panels separately.

Finally, in chapter 5, the conclusions drawn from the above studies are described. There is also a brief note on the scope for further study in this field.

CHAPTER 2

REVIEW OF LITERATURE

2.1: Introduction

The vast use of turbomachinery blades lead to significant amount of research over the years. Due to its wide range of application in the practical field, it is important to understand the nature of deformation, vibration and stability behaviour of cantilever twisted plates. Though the present investigation is mainly focused on stability studies of twisted panels, some relevant researches on vibration, static stability and dynamic stability of untwisted plates are also studied for completeness. The literature reviewed in this chapter are grouped into

- **Vibration and buckling of twisted panels**
- **Dynamic stability of twisted panels**

for homogeneous and laminated composite applications.

2.2: Vibration and buckling of twisted panels

With the continually increasing use of turbomachinery at higher performance levels, especially in aircraft, the study of vibration problems arising in twisted blades has become increasingly important. Free vibration frequencies and mode shapes are essential for the analysis of resonant response and flutter. Due to its

significance in structural mechanics, many researchers have worked on the vibration characteristics of turbomachinery blades.

An excellent survey of the earlier works in the free vibration of turbomachinery blades was carried out by Rao [1973, 1977[a], and 1980], Leissa [1980, 1981] and Rosen [1991] through 1991 for both stationary and rotating conditions. The vast majority of earlier researchers studied the vibration characteristics of turbine blades using assumptions of simple beam theory. The most thorough work to develop a comprehensive set of equations representing the vibrating blade as a beam was presented in a sequence of papers by Carnegie [1957, 1959, 1972] and his co-workers. Carnegie [1957] derived the potential energy functions for a twisted blade of arbitrary cross-section and variational methods were then employed to obtain static equations of equilibrium describing bending about two axes and torsion. Numerical results were obtained for blades of rectangular and aerofoil cross-section. Carnegie [1959[a]] developed a set of equations defining the dynamic motion of a pretwisted aerofoil blade and investigated the effect of pretwist on the frequencies of vibration using the Rayleigh-Ritz method. The dynamic effects due to blade rotation while mounted on a disk were addressed by Carnegie [1959[b]]. This work studied the effects of both the stabilizing (frequency increasing) primary and destabilizing (frequency decreasing) secondary centrifugal force effects. The additional torsional stiffening of twisted blades was expounded upon further by Carnegie [1962] and the effects of shear deformation and rotary inertia were also discussed [1964]. The most general potential and kinetic energy functions, along with corresponding equations of motion were summarized by Carnegie [1966]. Dawson [1968] used the Rayleigh–Ritz method and transformation techniques to study the effects of uniform pretwist on the frequencies of cantilever blades. Carnegie and Dawson [1969[a]] studied the modal curves of pretwisted beams of rectangular cross-section and the vibration characteristics of straight and pretwisted asymmetrical aerofoil blades [1969[b], 1971]. This was done by transforming the equations of motion to a set of simultaneous first-order differential equations and by integration using

Runge-Kutta method. Carnegie and Thomas [1972] and Rao [1972, 1977[b]] used the Rayleigh–Ritz method and Ritz–Galerkin method to study the effects of uniform pretwist and the taper ratio respectively on the frequencies of cantilever blades. Ansari [1975] analysed the evaluation of the nonlinear modes of vibration of a pretwisted non-uniform cantilever blade of unsymmetrical cross section mounted on the periphery of a rotating disk. The effect of shear deformation, rotary inertia and coriolis forces were included. Gupta and Rao [1978[b]] calculated the frequencies of a cantilever beam of varying width and depth at varying angles of twist. The effects of shear deformation and rotary inertia were considered in deriving the elemental matrices. Subrahmanyam and Rao [1982] used the Reissner method to determine the natural frequencies of uniformly pretwisted tapered cantilever blading. Chen and Jeng [1993] utilized the finite element method to analyze the vibration behaviour of a pretwisted blade with a single edge crack. The influence of crack locations and crack size on dynamic characteristics of twisted blades was studied. The dynamic response of twisted, non-uniform rotating blades was investigated by Hernried and Bian [1993] neglecting torsional, axial and warping deformations. Choi and Chu [2001] proposed the modified differential quadrature method to study the vibration of elastically supported turbomachinery blades. A pretwisted blade with varying cross-section was modelled as a Timoshenko beam. The equations of motion and the boundary conditions for the coupled flexural and torsional vibration of the blade were obtained by using Hamilton's principle. Equations of motion for the vibration analysis of rotating pretwisted blades were derived by a modelling method which employed hybrid deformation variables by Yoo, Park and Park [2001]. The derived equations were transformed into dimensionless forms in which dimensionless parameters were identified. The effects of the dimensionless parameters on the modal characteristics of rotating pretwisted blades were investigated. In particular, eigenvalue loci veering phenomena and associated mode shape variations were observed and discussed in this work. Yoo, Kwak and Chung [2001] investigated the vibration of a pretwisted blade with a concentrated

mass, using beam model. The equations of motion were derived based on a modelling method that employed hybrid deformation variables. The effects of the dimensionless parameters on the modal characteristics of the rotating blade were investigated through numerical analysis.

While these works were complete in their own right, their techniques treated the blades as beams i.e. as a one-dimensional case. A beam model represents a turbine engine blade reasonably well if the blade has high aspect ratio or the blade is reasonably thick and only the first few vibration frequencies and mode shapes are needed accurately. Many blades in sections of turbomachinery have a small aspect ratio and are thin blades. The beam idealization is highly inaccurate for the blade with moderate to low aspect ratio. Dynamic response studies require results for many modes of vibration. This earlier idealization could also not adequately handle the newer light weight, low aspect ratio turbine blading where the blades are more likely to behave as plates or shells rather than beams.

The emergence of digital computers with their enormous computing speed and core memory capacity changed the outlook of structural analysts and led to the application of the finite element method to blade vibration problems. This approach is widely used in all areas of modern structural analysis, and is particularly well suited to cope with blades of general configuration, including arbitrary curvatures and twist, variable thickness and irregular shapes. All types of finite element formulation can be found in the literature of turbomachinery blade vibration analysis, including elements which are triangular, quadrilateral, flat plate or shell, conforming or nonconforming. Dokainish and Rawtani [1969] studied the vibration characteristics of pretwisted cantilever plates using a flat triangular element. The twisted plate model shows not only the chord wise bending modes found in plates but also the increasing frequency of torsional modes with increasing angle of twist.

A twisted plate may be considered as a shell in which the curvature of the mid-surface in two orthogonal directions is zero, but there is an angle of twist. Many of the earlier works also included the rotational aspects of blades in the vibration analysis. These effects were studied by Dokainish and Rawtani [1971] who investigated the effects of rotation on untwisted plates. They analyzed the effect of various plate geometries and velocity on the frequencies of untwisted plates. All three components of centrifugal body force which arise were utilized. The work showed the significant destabilization that could arise from the z-component of the force. The plate was modeled by a mesh of triangular finite elements. Convergence studies for various mesh sizes were made and numerical results for the frequencies and mode shapes were presented for the first five modes. Rawtani and Dokainish [1972] extended their rotating plate analysis to twisted rotating plates using the same flat triangular elements. The effects of static deformation due to angular rotation on the vibration frequencies were considered. Numerical results were given for aspect ratios from 1 to 3 and twist angles up to 90°. Similar results for rotating flat plates were obtained by Bossak and Zienkiewicz [1973] using 3D finite elements to study the vibration analysis of rotating untwisted plates. Henry and Lalanne [1974] investigated the effects of rotation using a finite element method with plate triangular elements. Results for the first five modes of an existing compressor blade at 0 and 10000 RPM were presented. MacBain [1975] conducted a combined numerical and experimental study of the effects of varying tip twist and increasing centrifugal loading on the resonant characteristics of cantilever plates. The patterns which were very clear were presented for the first ten modes of a particular blade. Numerical results for both rotating and non rotating blades were obtained using the NASTRAN finite element program and were compared to those obtained experimentally using holographic interferometer. Abbas [1979] used the finite element method to determine the natural frequencies of uniformly pretwisted tapered cantilever blading. Thomas and Sabuncu [1979] presented a finite element model for the dynamic analysis of an asymmetric cross-section blade. The stresses and

deformations of pretwisted and tapered rotating blades were examined using finite element method by Ramamurti and Sreenivasamurthy [1980]. Three-dimensional, twenty-node isoparametric elements were used for the analysis. Sreenivasamurthy and Ramamurthy [1980] studied the effect of tip mass on the frequencies of vibration of a rotating pretwisted cantilever plate. In addition, Ramamurti and Kielb [1984] predicted eigen frequencies of twisted rotating plates. Karada [1984] investigated the dynamic characteristics of rotating and non-rotating practical bladed disks by taking blade shear center effects into account using both thin and thick beam and plate theories and the finite element method in the analysis.

Leissa *et al.* [1984] observed that there was a wide disagreement among the twisted plate natural frequencies obtained by different analytical methods. Previously published literature showed widely different results for the free vibration frequencies of twisted cantilever plates. In the above study, numerical results were obtained for a set of twenty different twisted plates having various aspect ratios, thickness ratios and pretwist angles. Although some of the best-known computational procedures (especially finite element codes) were used by analysts with great experience, the numerical results obtained showed considerable disagreement. The disagreement among the frequencies obtained by analytical methods led to experimental and analytical investigations by Kielb *et al*. [1985[a], 1985[b], 1985[c]].The experimental portion of a joint government/ industry/ university research study on the vibrational characteristics of twisted cantilevered plates was presented by Kielb *et al*. [1985[a]]. The overall purpose of the study was to assess the capabilities and limitations of existing analytical methods in predicting the vibratory characteristics of twisted plates. The resulting non-dimensional frequencies and mode shapes were presented as a function of plate tip twist. The trends of the natural frequencies as a function of the governing geometric parameters were discussed. Leissa *et al.* [1986] also studied the twisted plate problem using a three dimensional model. The three dimensional solution yielded slightly higher frequencies than the experimental ones. This may have been due to the difficulty of satisfying the clamped edge conditions

experimentally. A three dimensional analytical model to compute the deflection, stress, and eigenvalues in rotor blades was proposed by El Chazly [1993] using a bending triangular plate finite element. Both membrane and bending stiffness were considered in deriving the element stiffness matrix. Lift and drag forces created in steady wind conditions were analyzed as normal and tangential forces on the blade sections at certain angles of attack. The results showed that the maximum stresses occurred at the root of the blades for all configurations in the spanwise direction and that the tapered blade, in addition to saving material weight, diminished the stresses obtained. It was found that the twisting of the blade led to the increase of the stiffness and the decrease of the stresses. However the three dimensional solution, in comparison, was considered lengthy.

Turbine engine blades are also made with cambered cross-sections, i.e., they could have a radius of curvature in one or both directions. A small amount of camber considerably increases the longitudinal stiffness of a blade and, correspondingly the frequencies of vibration modes that are primarily longitudinal bending. A plate model of a blade is of limited value in such cases because the plate is flat and has no curvature. Plate models are useful in identifying the existence of modes that cannot be found by beam analysis, particularly those involving chord wise bending and as a limiting case check for the results of shell analyses. In general, the geometry of the mid surface of the blade is considered more complicated than a plate element. The mid surface may have two components of curvature and one of twist. These components require three coefficients of curvature R_x, R_y and R_{xy}. Also R_x, R_y and R_{xy} may not be constants but may vary along the blade. These considerations prompted the use of shell theory in the study of vibration characteristics of twisted blades. Leissa [1980] reviewed the earlier works on vibration of turbomachinery blades using shell analysis. Petericone and Sisto [1971] used the Rayleigh-Ritz method based on thin shell theory to investigate the influence of pretwist and skew angle on nonrotating blades. They examined two types of twisted plates corresponding to rectangular and skewed plates pretwisted at a constant rate. Membrane strains and

curvature changes were based upon the helicoidal shell theory and their numerical results were obtained by Ritz method using orthogonal polynomials as admissible functions. Numerical results were obtained for twist angles up to 45°. Several other methods were also used for the analysis of turbo machinery blades. Toda [1971] investigated nonrotating pretwisted plates using the Galerkin method, beam functions and shallow shell theory to analyze rectangular forms. He compared his results with those from experiments. Beres [1974] also investigated nonrotating blades using Hamilton's equations, Novozhilov strain-displacement shell equations and power series trial functions. Nodal patterns and frequencies of the first five modes were given for several configurations of straight and skewed helicoidal shells. Gupta and Rao [1978[a]] used Hamilton's principle and shallow shell equations to analyze the torsional vibration of nonrotating twisted plates considering aspect ratio varying from 1 to 8 with pretwist angles form 0° to 90°. Leissa, Lee and Wang [1981] studied the vibrations of untwisted cantilevered shallow cylindrical shells of rectangular planform using shallow shell theory and Ritz formulation with algebraic polynomial trial functions for the displacements. The work presented accurate non-dimensional frequency parameters for wide ranges of aspect ratio, shallowness ratio and thickness ratio. Leissa, Lee and Wang [1982] employed the same approach to determine the frequencies of turbo-machinery blades (isotropic twisted plates) with twist for different degrees of shallowness and thickness. This study concluded that the shallow shell theory can be used for twisted plates with an angle of twist of not more than 45°. Leissa, Lee and Wang [1983] studied the vibrational characteristics of doubly curved shallow shells having rectangular planforms, clamped along one edge and free on the other three. The solution procedure used the Ritz method with algebraic polynomial trial functions. Convergence studies were made, and accurate frequencies and contour plots of mode shapes were presented for various curvature ratios, including spherical, circular cylindrical and hyperbolic paraboloidal shells. Leissa and Ewing [1983] investigated the free vibration of turbomachinery blades by the beam and shell theories which included cambered

and/or twisted blades of uniform thickness. The Ritz method was used to provide the results for the shell analysis and was compared to the published results by the beam theory with and without torsional warping constant. Tsuiji *et al*. [1987] derived the fundamental equations needed to investigate the free vibrations of thin pretwisted plates. The strain-displacement relationships were derived by employing assumptions of the thin shell theory, and their simplified forms were proposed for plates having relatively large length-to-width ratios. The principle of virtual work for the free vibration of the thin pretwisted plates was formulated. The equation derived was used to analyze the free vibrations of thin pretwisted plates by the Rayleigh-Ritz procedure. Rao and Gupta [1987] investigated the free vibration characteristics of rotating pretwisted small aspect ratio blades using classical bending theory of thin shells. Variation of natural frequencies with various parameters like pretwist, speed of rotation, stagger angle and disc radius were presented in this study. Theoretical natural frequencies and mode shapes of the first four coupled modes of a uniform pretwisted cantilever blade and the first five coupled flexural frequencies of pretwisted tapered blades were determined.

Walker [1978] studied the free vibration of cambered helicoidal fan blades. A conforming finite shell element suitable for the analysis of curved twisted fan blades was developed and applied to a number of fan blade models. The element was assumed to be a doubly curved right helicoidal shell, in which the curvature is shallow with respect to the twisted base plane defining the helicoid. Element stiffness and mass formulations were based on Mindlin's theory and included the effects of transverse shear and rotary inertia. The thin shell element was used to predict the natural frequencies and mode shapes of a number of fabricated fan blade structures and the results were correlated with experiment. It was found that the finite element predictions converged very rapidly in a monotonic fashion towards the experimental results, even for coarse finite element meshes. Sreenivasamurthy and Ramamurti [1981] used the finite element technique to determine the natural frequencies of a pretwisted and tapered plate mounted on the periphery of a rotating disc. The pretwisted plate was idealized as

an assemblage of three noded triangular shell elements with six degrees of freedom at each node. In the analysis the initial stress effect (geometric stiffness) and other rotational effects except the Coriolis acceleration effect were included. The eigenvalues were extracted by using a simultaneous iteration technique. Computation of frequencies was carried out for plates of aspect ratios 1 and 2. Other parameters considered were pretwist, taper, skew angle and disc radius. From the results of computations an extension to the existing empirical formulae derived by Dokainish and Rawtani [1971] was suggested for computing natural frequencies of rotating pretwisted and tapered cantilever plates. Naim and Ghazi [1990] developed a ten-node triangular shell element for vibration analysis and applied it to study the free vibration of rectangular untwisted as well as twisted plates and shells of different boundary conditions.

In almost all the literature on the vibrations of turbomachinery blades in the earlier years, the material of the blade was taken to be isotropic. Efforts to improve the operating capabilities of turbine engine blades with composite materials were also being made. To tailor the structural properties, fibre reinforced composite laminates are increasingly used for designing turbomachinery blades requiring higher strength, more durability and less weight. There are unlimited ways of tailoring the mechanical properties of laminated composites to suit design requirements. Classical methods of analysis were being used to study the free vibration of composite twisted cantilever blades by many early researchers since these methods were well suited for parameter studies showing the effects of changing aspect ratio, thickness, shallowness, pretwist, disk radius and angular velocity upon the frequencies and mode shapes. These methods were particularly useful in obtaining a physical understanding of the problem and in preliminary design. In addition, many researchers also analysed composite plates using finite element methods. Chamis and his coworkers [1974, 1975] studied the free vibration characteristics of composite fan blades using the finite element method. Chamis [1977] also carried out a free vibration analysis complete with natural frequencies and mode shapes of composite fan blades

(graphite fibre reinforced polymide matrix- HTS/K601) for high speed applications. He tested HTS/K601 laminated composite blades using holographic technique and compared the test data with the theoretical results obtained using the finite element package NASTRAN. This was the first known study of the effects of twist angle upon the frequencies and mode shapes of laminated composite twisted cantilever plates. Theoretical results showed that different laminate configurations from the same composite system had only small effects on the blade frequency. White and Bendiksen [1987] studied the aeroelastic behaviour of titanium and composite flat blades of low aspect ratio using a Rayleigh-Ritz formulation. The blade mode included plate type mode to account for chordwise bending. Bhumbla *et al.* [1990] studied the natural frequencies and mode shapes of spinning laminated composite plates using finite element method. A first order shear deformation plate theory was used to predict the free vibration frequencies and mode shapes in spinning laminated composite plates. The natural frequencies and mode shapes of isotropic and laminated composite plates as functions of angular velocity, pitch angle, and sweep angle were presented. A complete and mathematically consistent set of equations for laminated composite shallow shells including equations of motion, boundary conditions and energy functionals was presented by Leissa and Qatu [1991]. It was shown that the energy functionals derived were consistent with the equations of motion and boundary conditions, and therefore could be used with energy approaches such as the Ritz method. These equations were successfully applied to the vibrations of laminated composite twisted cantilevered plates and shallow shells by Qatu and Leissa [1991]. The Ritz method with algebraic polynomial displacement functions was used. The effect of the angle of twist, thickness ratio and fiber orientation angle upon the natural frequencies and mode shapes of three-layer, E-glass/epoxy and graphite/epoxy angle-ply plates were studied. The experimental behaviour of spinning, pretwisted laminated composite plates was investigated by Lapid *et al.* [1993]. The purpose of these experiments was to establish an experimental database consisting of strains, deflections, and natural frequencies as a function of

rotational velocity. Six different plate sets were tested which included three different stacking sequences (two symmetric, one asymmetric), two different initial twist levels (0 deg, 30 deg), and two different initial twist axis locations (midchord, quarter-chord). The plates were spin tested at four different combinations of pitch and sweep. It was observed that the location of the pretwist axis and the level of pretwist greatly affected the strains and deflections of the spinning plate, while the pretwist level affected only the measured natural frequencies. The vibration and damping behaviour of cantilevered pretwisted composite blades of glass fiber reinforced plastics was studied by Nabi and Ganesan [1993] using a three noded triangular cylindrical shell element. The effects of pretwist, fiber orientation, skew angle, taper and aspect ratio on natural frequency and damping were investigated. Lim and Liew [1993] investigated the vibratory characteristics of pretwisted composite symmetric laminates with trapezoidal planform. A governing eigenvalue equation was derived based on the Ritz minimization procedure. This formulation showed that the bending and stretching effects of these symmetric laminates were coupled by the presence of twisting curvature. This method was applied to determine the vibration response of the problem. The effects of angles of twist and lamination parameters upon the vibration frequencies were examined. Vibration characteristics of pretwisted metal matrix composite blades were analyzed by using beam and plate theories by Nabi and Ganesan [1996]. A beam element with eight degrees of freedom per node was developed with torsion -flexure, flexure -flexure and shear -flexure couplings which are encountered in twisted composite beams. A triangular plate element was used for the composite material to model the beam as a plate structure. Both theories were validated for the isotropic case. This work summarized the quantitative comparison of natural frequencies of composite blades obtained by these theories. A parametric study was carried out for the beam and plate elements, the parameters being twist angle, fiber orientation, taper ratio and lamination scheme. A study of combined effect of initial twist and composite induced elastic couplings was presented by Rand and Barkai [1997] in

addition to nonlinear experimental data. Karmakar and Sinha [1997] analyzed the free vibration of laminated composite pretwisted cantilever plates using finite element method. A nine-node three-dimensional degenerated composite shell element was used for the analysis. Plates with exponentially varying thickness and variable chordwise width were studied. Effects of angle of pretwist, thickness ratio, fiber orientation, aspect ratio, skew angle and precone angle on the natural frequencies of graphite/epoxy plates were investigated. Parhi, Bhattacharya and Sinha [1999] studied the dynamic analysis of multiple delaminated composite twisted plates using the finite element method. Using the principle of virtual work and the Rayleigh–Ritz method with two dimensional algebraic polynomial displacement functions, the governing equation of vibration for a laminated composite cylindrical thin panel with twist and curvature was presented by Hu and Tsuiji [1999]. The effects of angle of twist, curvature, characteristics of material, the number of layers, stacking sequence and fiber orientation on vibration frequency parameters of laminated cylindrical thin panels with twist and curvature were studied, and some vibration mode shapes were also plotted to explain the variations of the vibration caused by them. He, Lim and Kitipornchai [2000] presented the free vibration of symmetric as well as anti-symmetric laminates explaining the limit of linear twisting curvature. They used a computational method for characterizing the resonant frequency properties of cantilever pretwisted plates composed of fibre-reinforced laminated composites. It aimed to simulate a laminated turbomachinery blade or a fan blade with a relatively small aspect ratio for which the conventional beam model failed to provide accurate solutions. Numerical solutions were presented and the effects of angle of pretwist, aspect ratio, and symmetric and antisymmetric lamination for two different composite laminates were analyzed. Kuang and Hsu [2002] investigated the effects of the fiber orientation, damping, inclined angle and rotation speed on the natural frequencies of tapered pretwisted composite blades, employing the differential quadrature method (DQM). Hu *et al.* [2002] investigated the vibration of twisted laminated composite conical shells by the

energy method. A methodology for free vibration of a laminated composite conical shell with twist was proposed, in which the strain–displacement relationship of a twisted conical shell was given by considering the Green strain tensor on the general thin shell theory. The principle of virtual work was utilized and the governing equation was formulated by the Rayleigh–Ritz procedure with algebraic polynomials in two elements as admissible displacement functions. Lee *et al.* [2002] studied the vibration of twisted cantilevered conical composite shells, using finite element method based on the Hellinger-Reissner principle. This study presented the twisting angle effect on vibration characteristics of conical laminated shells. For shells with a large curvature, the fundamental frequency, which was always characterized by the bending mode, was almost constant and independent of twisting angle. It was found that the twisting angle greatly affected the twisting frequency and mode shape. Considering transverse strain and rotary inertia, Hu *et al*. [2004] studied the vibration of angle-ply laminated plates with twist using a Rayleigh-Ritz procedure. An accurate strain–displacement relationship of a twisted plate was derived using the Green strain tensor on the general shell theory and the Mindlin plate theory. The equilibrium equation for free vibration was given by the principle of virtual work and was solved by using the Rayleigh–Ritz procedure with normalized characteristic orthogonal polynomials generated by the Gram–Schmidt process. The parametric effects of fibre angle, twist angle, thickness ratio and stacking sequence on the vibration frequencies and mode shapes of laminated plates were studied. Although extensive free vibration frequencies and mode shapes were studied, the results were however confined to symmetric laminates only.

McGee and Chu [1994] presented the three dimensional continuum vibration analysis for rotating, laminated composite blades. The Ritz method was used to minimize the dynamic energies with the displacements approximated by mathematically complete polynomials satisfying the vanishing displacement conditions at the blade root section. Non-dimensional frequency parameters are presented for various rotating, truncated quadrangular pyramids which served as

first approximations of practical blades. The influence of a number of blade parameters on the frequency parameters was studied. Chandiramani *et al.* [2003] studied the free and forced vibration of rotating pretwisted composite blades, including transverse shear flexibility, centrifugal and coriolis effects. Kee and Kim [2004] analyzed the vibration characteristics of initially twisted rotating shell type composite blades. The blade was assumed to be a moderately thick open cylindrical shell, and was oriented arbitrarily with respect to the axis of rotation to consider the effects of disc radius and setting angle. A general formulation was derived for the initially twisted rotating shell structure including the effect of centrifugal force and Coriolis acceleration and the transverse shear deformation and rotary inertia. The effects of various parameters like initial twisting angles, thickness to radius ratios, layer lamination and fiber orientation of composite blades were investigated.

Since Coulomb's and Saint-Venant's fundamental work, many researchers have studied the effect of twisting on elastic bodies. The study on stability characteristics of twisted plates is however relatively new. Crispino and Benson [1986] studied the stability of thin, rectangular, orthotropic plates which were in a state of tension and twist. A transfer matrix method was used to obtain numerical solutions to the linearized von Kármán plate equations, and to determine critical angles of twist per unit length which buckle the plate. Results were presented, in a compact non-dimensional form, for a range of material, geometric and loading parameters. It was found that orthotropism significantly affected the stability of the plate. The effect of thermal gradient and tangency coefficient on the stability of a pretwisted, tapered, rotating cantilever with a tip mass and subjected to a concentrated partial follower force at the free end was investigated by Kar and Neogy [1989]. The non-self adjoint boundary value problem was formulated with the aid of a conservation law using Euler-Bernoulli theory. The associated adjoint boundary value problem was introduced and an apposite variational principle was derived. Approximate values of critical load

were calculated on the basis of this variational principle and the influence of different parameters on the stability of the system was studied.

Piezoelectric materials are becoming increasingly popular in the emerging field of adaptive structures. In particular, active control of wings and helicopter rotors using these materials is being pursued currently. Thirupathi *et al.* [1997] made an effort at modeling piezoelectric actuated blades for turbomachinery applications. A laminated general quadrilateral shell finite element with eight nodes and curved edges was developed for this purpose. The mathematical formulation of the element was described. Experiments were conducted on a commercially available piezoceramic bimorph. The finite-element and experimental results were shown to match very well. The laminated element developed was then used to perform a static analysis of typical turbomachinery blades. Effects of the angle of pretwisting and aspect ratio were studied. PVDF and PZT piezoelectric materials were compared. The work presented by Mockensturm [2001] investigated instabilities that could occur when thin bodies were subjected to large twists and extended work by Green published in 1937. Because large twists were considered, a fully nonlinear plate theory was used. This theory gave results for compressive lateral membrane stresses not predicted by Green's weakly nonlinear theory. These stresses could significantly alter the twist angle at which buckling occurred. The buckling modes and critical twist angles varied significantly depending on the support conditions used.

2.3: Dynamic stability of twisted panels

Turbine blades are subjected to axial periodic forces due to axial components of aerodynamic or hydrodynamic forces acting on the blades. The increased utilization of composite materials in thin-walled structural components of aircrafts, submarines, automobiles and other high-performance application areas have necessitated a strong need to understand their dynamic characteristics under different loading conditions. Composite materials are being increasingly used in many applications because of their specific strength and stiffness and these can be

tailored through the variation of fiber orientation and stacking sequence to obtain an efficient design. Structural elements subjected to in-plane periodic forces may lead to parametric resonance, due to certain combinations of the values of load parameters and disturbing frequency. The above phenomenon is called dynamic instability or parametric resonance. The instability may occur below the critical load of the structure under compressive loads over wide ranges of excitation frequencies. Thus the parametric resonance characteristics of laminated composite twisted cantilever panels are of great importance for understanding the systems under periodic loads.

The general theory of dynamic stability of elastic systems of deriving the coupled second order differential equations of the Mathiew-Hill type and the determination of the regions of instability by seeking a periodic solution using Fourier series expansion was explained by Bolotin [1964]. Since Bolotin introduced the subject of dynamic stability under periodic loads, the topic has attracted much interest. The parametric instability characteristics of laminated composite untwisted plates were studied by a number of investigators. The instability of untwisted composite laminated plates under uniaxial, harmonically-varying, in-plane loads was investigated by Moorthy *et al.* [1990] using a first-order shear deformation theory. Both symmetric cross-ply laminates and antisymmetric angle-ply laminates were analyzed. The resulting linear equations of motion were transformed into small, uncoupled sets of equations, and instability regions in the plane of load amplitude versus load frequency were determined using the finite element method. The effects of damping, ratio of edge length to thickness of the plate, orthotropy, boundary conditions, number of layers and lamination angles on instability regions were examined. The dynamic instability of antisymmetric angle-ply and cross-ply laminated plates subjected to periodic in-plane loads was investigated using a higher order shear deformation lamination theory and the method of multiple-scale analysis by Cederbaum [1991]. Ganapathi *et al.* [1994] investigated the dynamic instability of composite curved panels without twist subjected to uniform in-plane periodic loads. The

dynamic instability of laminated composite cylindrical shells due to periodic loads was studied using a C^0 shear flexible QUAD-9 shell element. The boundaries of the principal instability regions were conveniently represented in the non-dimensional excitation frequency-nondimensional load amplitude plane. The effects of various parameters such as ply-angle, number of layers, thickness and radius-to-side ratio on the dynamic stability were brought out. Ng, Lam and Reddy [1998] investigated the parametric resonance of untwisted cross-ply cylindrical panels under combined static and periodic axial forces using Love's classical theory of thin shells. A normal-mode expansion of the equations of motion yielded a system of Mathieu–Hill equations. Bolotin's method was then employed to obtain the dynamic instability regions. The study examined the dynamic stability of antisymmetric cross-ply circular and cylindrical shells of different lamination schemes. The effect of the magnitude of the axial load on the instability regions was also examined. Sahu and Datta [2000] investigated the dynamic instability of untwisted laminated composite rectangular plates subjected to non-uniform harmonic in-plane edge loading. Sahu and Datta [2001] studied the parametric resonance characteristics of laminated composite doubly curved shells subjected to non-uniform loading. Sahu and Datta [2003] also investigated the dynamic stability of untwisted laminated composite curved panels with cutouts. The dynamic stability analysis of composite skew plates subjected to periodic in-plane load was studied by Dey and Singha [2006]. Here, the dynamic stability characteristics of simply supported laminated composite skew plates subjected to a periodic in-plane load were investigated using the finite element approach. The formulation included the effects of transverse shear deformation, in-plane and rotary inertia. The boundaries of the instability regions were obtained using the Bolotin's method and were represented in the non-dimensional load amplitude-excitation frequency plane. The principal and second instability regions were identified for different parameters such as skew angle, thickness-to-span ratio and fiber orientation.

A few studies have been made to investigate the dynamic stability of twisted blades. Ray and Kar [1995] analyzed the dynamic stability of pretwisted sandwich beams. Their work dealt with the parametric instability of a pretwisted, cantilevered, three-layered symmetric sandwich beam subjected to a periodic axial load at the free end. The non-dimensional governing equations of motion and the associated boundary conditions were derived by Hamilton's principle and were reduced to the time domain by the use of the generalized Galerkin method. This gave rise to a set of coupled Hill's equations with complex coefficients. The regions of instability were determined by using Hsu's method, modified for the complex case. The effects of pre-twist angle and geometric, shear and static load parameters on the regions of parametric instability were studied. Chen and Peng [1995] studied the dynamic stability of twisted rotating blades subjected to axial periodic forces, by using Lagrange's equation and the Galerkin finite element method. The effects of geometric non-linearity, shear deformation and rotary inertia were considered. The iterative method was used to get the mode shapes and frequencies of the non-linear system. Dynamic instability regions of the blade with different reference amplitudes of vibration were illustrated graphically. An analytical model was presented by Yang and Tsao [1997] to investigate the vibration and stability of a pretwisted blade under nonconstant rotating speed which was characterized by a periodic perturbation. The time-dependent rotating speeds led to a system with six parametric instability regions in primary and combination resonances. Each instability region was predicted using the multiple scale method and validated by the numerical results of a more detailed model. The analyses showed that the combination resonance at about twice the fundamental frequency was the most critical aspect and was sensitive to system parameter variation. It was shown that this instability could be minimized by either increasing the pretwist angle or decreasing the stagger angle. Lin and Chen [2003] studied the dynamic stability problems of a pretwisted blade with a viscoelastic core constrained by a laminated face layer subjected to a periodic axial load by using the finite element method. A 2-node element was used and shear

deformation and rotary inertia were neglected. The complex modulus representation was used for the viscoelastic material. A set of equations of motion governing the bending and extensional displacements were derived by Hamilton's principle. The regions of instability were determined by using Bolotin's procedure modified for the complex case. The effects of rotating speed, pre-twist angle, setting angle and static axial load on the first static buckling load under different shear parameters and core loss factors were presented. The influence of core loss factor, core thickness ratio and stiffness parameter on the unstable regions were also studied. The above dynamic stability studies idealized the twisted blade as a beam.

The study of the dynamic instability of twisted panels using shell formulation is relatively new and there were no references found in this area.

2.4: Critical Discussion

Many investigators worked on vibration behaviour of turbomachinery blades. Carnegie [1959[a], 1959[b]], Rao [1982, 1987] and many others studied extensively the free vibration of turbomachinery blades using several analytical methods. However, these studies involve idealization of blades as one dimensional beams. The beam idealization is highly erroneous for the blade with moderate to low aspect ratio. Dynamic studies require results for many modes of vibration. This earlier model could also not handle the newer composite low aspect ratio turbine blading where the blades are more likely to behave as plates or shells rather than beams. Studies were conducted using plate idealization by finite element (Rawtani and Dokainish [1972], Macbain [1975], Ramamurti and Sreenivasmurthy [1980] and Karada [1984]) and other numerical methods. The wide disagreements among the frequencies of vibration by different finite element analysis lead to experimental investigations (Macbain [1975], Walker [1978]) and analytical methods (Kielb *et al*. [1985]). Studies involving 3D models were also conducted (Leissa *et al*. [1986], El Chazly [1993], McGee and Chu [1994]) for comparison with other methods. The geometry of the mid surface of the turbine

blade is more complicated than the plate element and may have components of curvature in one or both directions. Thus the focus of research shifted towards thin shell models (Petericone and Sisto [1971], Toda [1971], Gupta and Rao [1978], Beres [1974], Leissa *et al*. [1982], Leissa and Ewing [1983], Tsuiji *et al*. [1987]). Choi and Chu [2001] used the modified differential quadrature method for analysis of elastically supported turbomachinery blades. Composite materials were also used by many investigators (Chamis [1977], White and Bendiksen [1987], Qatu and Leissa [1991], Lim and Liew [1993], Nabi and Ganesan [1996] and He *et al*. [2000]) to improve the operating capabilities of turbine engine blades by different methods. McGee and Chu [1994] presented the three dimensional continuum vibration analysis for rotating, laminated composite blades. Thirupathi *et al.* [1997] made an effort at modeling piezoelectric actuated blades for turbomachinery applications. Parhi, Bhattacharya and Sinha [1999] studied the dynamic analysis of multiple delaminated composite twisted plates using the finite element method. Studies were also conducted for the vibration of laminated composite conical shells (Hu *et al.* [2002], Lee *et al.* [2002]). Kuang and Hsu [2002] investigated the effects of the fiber orientation, damping, inclined angle and rotation speed on the natural frequencies of tapered pretwisted composite blades, employing the differential quadrature method (DQM). Chandiramani *et al.* [2003] studied the free and forced vibration of rotating pretwisted blades, including transverse shear flexibility, centrifugal and coriolis effects. Kee and Kim [2004] analyzed the vibration characteristics of twisted plates. A few studies are made on stability of plates. Crispino and Benson [1986] studied the stability of thin, rectangular orthotropic plates which are in a state of tension and twist.

However, turbine blades are often subjected to axial periodic forces due to axial components of hydrodynamic forces acting on the blades and may undergo dynamic instability under in-plane periodic loads. Since Bolotin [1964] introduced the subject of dynamic stability under periodic loads, many researchers (Reddy *et al.* [1990], Ganapathi *et al.* [1994], Sahu and Datta [2001]) studied the

dynamic stability of untwisted plates. Some studies (Ray and Kar [1995], Chen and Peng [1995], Lin and Chen [2003]) are available on dynamic stability of twisted blades using beam idealization. No studies are available on parametric resonance behaviour of twisted panels and thus it becomes the subject of this investigation.

2.5: Objectives and scope of the present study

A review of the literature shows that a lot of work has been done on the vibration of laminated composite twisted cantilever panels. Very little work has been done on static stability of laminated composite twisted cantilever panels. However, no study is available on parametric resonance behaviour of twisted panels subjected to in-plane harmonic loads. The present study is mainly aimed at filling some of the lacunae that exist in the proper understanding of the dynamic stability of twisted panels.

Based on the review of literature, the different problems identified for the present investigation are presented as follows.

- Vibration, buckling and parametric resonance characteristics of isotropic twisted cantilever panels
- Vibration, buckling and parametric resonance characteristics of cross-ply twisted cantilever panels
- Vibration, buckling and parametric resonance characteristics of angle-ply twisted cantilever panels

The influence of various parameters such as angle of twist, curvature, side to thickness ratio, number of layers, lamination sequence, and ply orientation, degree of orthotropy, static and dynamic load factors on the vibration and instability behaviour of twisted panels are examined in detail.

CHAPTER 3

THEORY AND FORMULATION

3.1: The Basic Problem

This chapter presents the mathematical formulation for vibration, static and dynamic stability analysis of the twisted plate and shell structures. The basic configuration of the problem considered here is a composite laminated doubly curved twisted panel of sides ‘a’ and ‘b’ as shown in Figure 3.1. This panel may be subjected to harmonic in-plane edge loading N (t) as shown in the figure.

The twisted panel is modeled as a doubly curved panel with twisting curvature so that the analysis can be done for twisted plates, cylindrical and differently curved panels such as spherical, hyperbolic and elliptical paraboloid configurations by changing the value of the curvature. The boundary conditions are taken to be that of a cantilever, that is fixed at the left end and free at the other edges.

The basic composite twisted curved panel is considered to be composed of composite material laminates. ‘n’ denotes the number of layers of the laminated composite twisted panel.

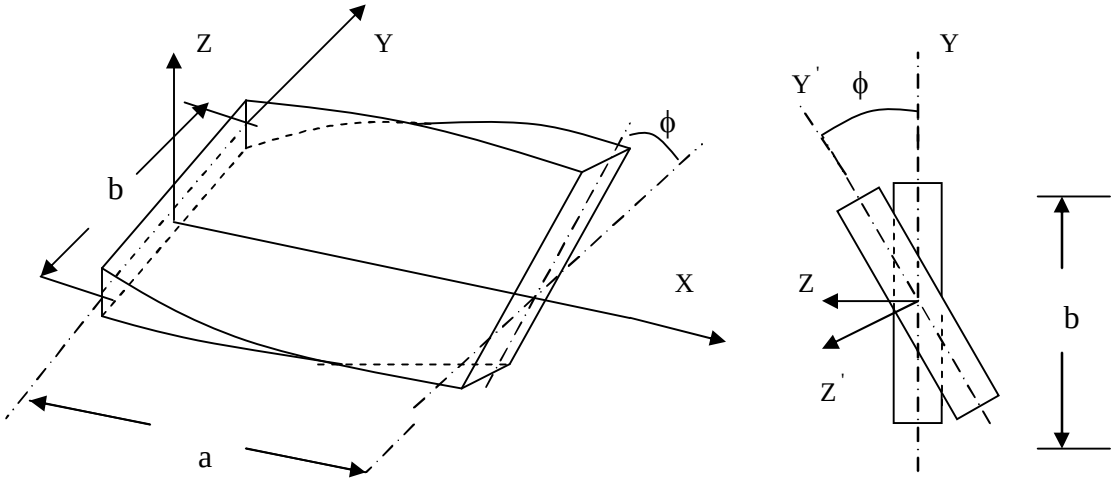

(a) twisted cantilever panel

(b) the lamination

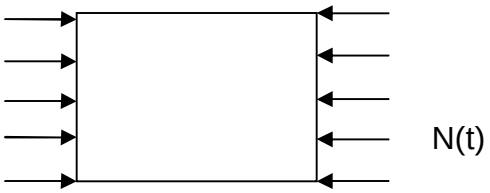

(c) planform subjected to in-plane load

Figure 3.1: Laminated composite twisted curved panel subjected to in-plane harmonic loads

3.2: Proposed Analysis

The governing equations for the dynamic stability of laminated composite doubly curved twisted panels/shells subjected to in-plane harmonic loading are developed. The presence of external in-plane loads induces a stress field in the structure. This necessitates the determination of the stress field as a prerequisite to the solution of problems like vibration, buckling and dynamic stability

behaviour of pretwisted plates and shells. As the thickness of the structure is relatively smaller, the determination of the stress field reduces to the solution of a plane stress problem. The equation of motion represents a system of second order differential equations with periodic coefficients of the Mathieu-Hill type. The development of the regions of instability arises from Floquet's theory and the solution is obtained by Bolotin's approach using finite element method. The governing differential equations have been developed using the first order shear deformation theory (FSDT). The assumptions made in the analysis are given below.

3.2.1: Assumptions of the analysis

1. The analysis is linear, in line with previous studies on the dynamic stability of untwisted panels (Bert and Birman [1988], Sahu and Datta [2003]) with a few exceptions. This implies both linear constitutive relations (generalized Hooke's law for the material and linear kinematics) and small displacements to accommodate small deformation theory.

2. The pretwisted curved panels have no initial imperfections. The consideration for imperfections is less important for dynamic loading and is consistent with the work of Bert and Birman [1988] for untwisted panels.

3. The straight line that is perpendicular to the neutral surface before deformation remains straight but not normal after deformation (FSDT). The thickness of the twisted panel is small compared with the principal radii of curvature. Normal stress in the z-direction is neglected.

4. The loading on the panel is considered as axial with a simple harmonic fluctuation with respect to time.

5. All damping effects are neglected.

3.3: Governing Equations

The governing differential equations, the strain energy due to loads, kinetic energy and formulation of the general dynamic problem are derived on the basis of the principle of potential energy and Lagrange's equation.

3.3.1: Governing Differential Equations

The equations of motion are obtained by taking a differential element of the twisted panel as shown in figure 3.2. The figure shows an element with internal forces like membrane forces (N_x, N_y, and N_{xy}), shearing forces (Q_x, and Q_y) and the moment resultants (M_x, M_y and M_{xy}).

The governing differential equations of equilibrium for vibration of a shear deformable doubly curved pretwisted panel subjected to external in-plane loading can be expressed as (Chandrashekhara[1989], Sahu and Datta [2003]):

$$\frac{\partial N_x}{\partial x}+\frac{\partial N_{xy}}{\partial y}-\frac{1}{2}\left(\frac{1}{R_y}-\frac{1}{R_x}\right)\frac{\partial M_{xy}}{\partial y}+\frac{Q_x}{R_x}+\frac{Q_y}{R_{xy}}=P_1\frac{\partial^2 u}{\partial t^2}+P_2\frac{\partial^2 \theta_x}{\partial t^2}$$

$$\frac{\partial N_{xy}}{\partial x}+\frac{\partial N_y}{\partial y}+\frac{1}{2}\left(\frac{1}{R_y}-\frac{1}{R_x}\right)\frac{\partial M_{xy}}{\partial x}+\frac{Q_y}{R_y}+\frac{Q_x}{R_{xy}}=P_1\frac{\partial^2 v}{\partial t^2}+P_2\frac{\partial^2 \theta_y}{\partial t^2}$$

$$\frac{\partial Q_x}{\partial x}+\frac{\partial Q_y}{\partial y}-\frac{N_x}{R_x}-\frac{N_y}{R_y}-2\frac{N_{xy}}{R_{xy}}+N_x^0\frac{\partial^2 w}{\partial x^2}+N_y^0\frac{\partial^2 w}{\partial y^2}=P_1\frac{\partial^2 w}{\partial t^2} \qquad (3.3.1)$$

$$\frac{\partial M_x}{\partial x}+\frac{\partial M_{xy}}{\partial y}-Q_x=P_3\frac{\partial^2 \theta_x}{\partial t^2}+P_2\frac{\partial^2 u}{\partial t^2}$$

$$\frac{\partial M_{xy}}{\partial x}+\frac{\partial M_y}{\partial y}-Q_y=P_3\frac{\partial^2 \theta_y}{\partial t^2}+P_2\frac{\partial^2 v}{\partial t^2}$$

where N_x^0 and N_y^0 are the external loading in the X and Y directions respectively. The constants R_x, R_y and R_{xy} identify the radii of curvature in the x and y directions and the radius of twist.

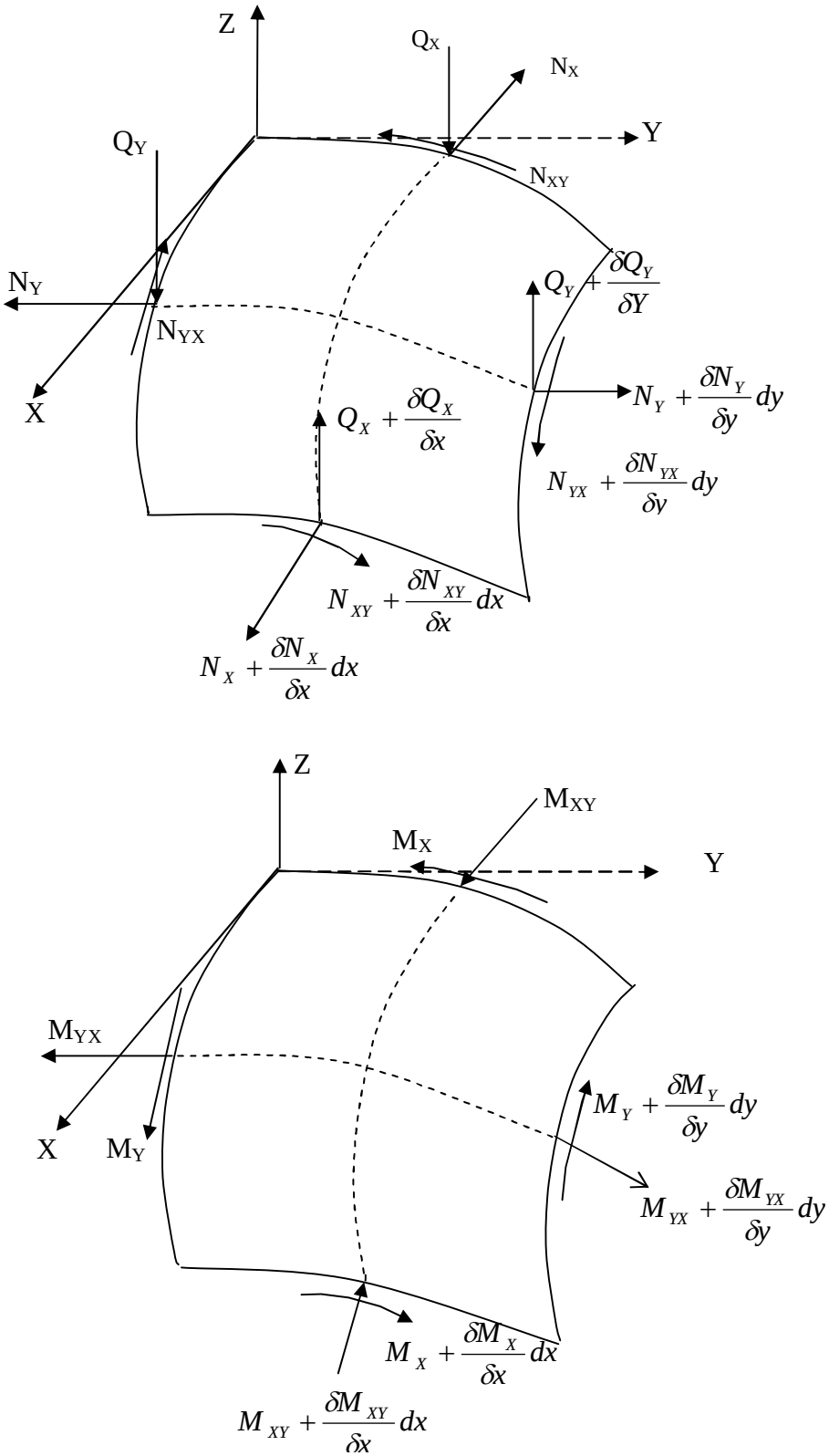

Figure 3.2: Force and moment resultants of the twisted panel

$(P_1, P_2, P_3) = \sum_{k=1}^{n} \int_{z_{k-1}}^{z_k} (\rho)_k (1, z, z^2) dz$ where n = number of layers of the laminated composite twisted curved panel, $(\rho)_k$ = mass density of k_{th} layer from the mid-plane.

3.4: Dynamic stability studies

The equation of motion for vibration of a laminated composite twisted cantilever panel, subjected to in-plane loads can be expressed as:

$$[M]\{\ddot{q}\} + [[K_e] - N(t)[K_g]]\{q\} = 0 \quad (3.4.1)$$

'q' is the vector of degrees of freedom (u, v, w, θ_x, θ_y). The in-plane load 'N (t)' may be harmonic and can be expressed in the form:

$$N(t) = N_s + N_t Cos\Omega t \quad (3.4.2)$$

where N_s is the static portion of the load N(t), N_t is the amplitude of the dynamic portion of N(t) and Ω is the frequency of the excitation. Considering the static and dynamic components of load as a function of the critical load,

$$N_s = \alpha N_{cr}, N_t = \beta N_{cr} \quad (3.4.3)$$

where α and β are the static and dynamic load factors respectively. Using equation (3.4.3), the equation of motion for the twisted curved panel under periodic loads in matrix form may be obtained as:

$$[M]\{\ddot{q}\} + [[K_e] - \alpha N_{cr}[K_g] - \beta N_{cr}[K_g] Cos\Omega t]\{q\} = 0 \quad (3.4.4)$$

The above equation (3.4.4) represents a system of differential equations with periodic coefficients of the Mathieu-Hill type. The development of regions of instability arises from Floquet's theory which establishes the existence of periodic solutions of periods T and 2T. The boundaries of the primary instability regions with period 2T, where T = 2 π/Ω are of practical importance [Bolotin, 1964] and the solution can be achieved in the form of the trigonometric series:

$$q(t) = \sum_{k=1,3,5,..}^{\infty} [\{a_k\} Sin(k\Omega t/2) + \{b_k\} Cos(k\Omega t/2)] \quad (3.4.5)$$

Putting this in equation (3.4.4) and if only the first term of the series is considered, and equating coefficients of Sin Ωt/2 and Cos Ωt/2, the equation (3.4.5) reduces to

$$[[K_e] - \alpha N_{cr}[K_g] \pm \frac{1}{2}\beta N_{cr}[K_g] - \frac{\Omega^2}{4}[M]]\{q\} = 0 \quad (3.4.6)$$

Equation (3.4.6) represents an eigenvalue problem for known values of α, β and N_{cr}. The two conditions under the plus and minus sign correspond to the two boundaries of the dynamic instability region. The eigenvalues are Ω, which give the boundary frequencies of the instability regions for given values of α and β. In this analysis, the computed static buckling load of the panel is considered as the reference load in line with many previous investigations (Ganapati *et al*. [1994], Moorthy, Reddy and Plaut [1990]).

This equation represents a solution to a number of related problems:

(1)Free vibration: α = 0, β = 0 and ω = Ω/2

$$[[K_e] - \omega^2 [M]]\{q\} = 0 \quad (3.4.7)$$

(2)Vibration with static axial load: β = 0 and ω = Ω/2

$$[[K_e] - \alpha N_{cr} [K_g] - \omega^2 [M]]\{q\} = 0 \quad (3.4.8)$$

(3)Static stability: α = 1, β = 0, Ω = 0

$$[[K_e] - \alpha N_{cr} [K_g]] \{q\} = 0 \quad (3.4.9)$$

3.5: Energy Equations

The laminated composite doubly curved twisted panel is subjected to initial in-plane edge loads N_x^0, N_y^0 and N_{xy}^0. These in-plane loads cause in-plane stresses of

σ_x^0, σ_y^0 and σ_{xy}^0 and are a plane stress problem. The doubly curved panels with the initial stresses undergo small lateral deformations. The total stresses at any layer are the sum of the initial stresses plus the stresses due to bending and shear deformation. The strain energy U_o due to initial in-plane stresses is written as

$$U_o = \frac{1}{2}\iint \{\varepsilon^0\}^T \{\sigma^0\} dA \tag{3.5.1}$$

where

$$\{\varepsilon^0\}^T = [\varepsilon_x^0 \varepsilon_y^0 \gamma_{xy}^0]^T = \left[\frac{\partial u^0}{\partial x}, \frac{\partial v^0}{\partial y}, \frac{\partial u^0}{\partial y} + \frac{\partial v^0}{\partial x}\right] \tag{3.5.2}$$

and the stresses are

$$\{\sigma^0\} = [D_p]\{\varepsilon^0\} \tag{3.5.3}$$

The strains can be expressed in terms of initial in-plane deformations u^0, v^0 as

$$\{\varepsilon^0\} = [B_P]\{q^0\} \tag{3.5.4}$$

Substituting the values of stress and strain in the equation (3.5.1), we get

$$U_0 = \frac{1}{2}\iint \{q^0\}^T [B_P]^T [D_P][B_P]\{q^0\} dA \tag{3.5.5}$$

The strain energy is expressed as

$$U_0 = \frac{1}{2}\{q^0\}^T [K_P]\{q^0\} \tag{3.5.6}$$

where

$$[K_P] = \iint [B_P]^T [D_P][B_P] dA \tag{3.5.7}$$

Considering the prestressed state as the initial state, the strain energy stored due to bending and shear deformation in the presence of initial stresses and neglecting higher order terms is given by

$$U = U_1 + U_2 \tag{3.5.8}$$

where U_1 = Strain energy associated with bending with transverse shear and

U_2 = Work done by the initial in-plane stresses and the nonlinear strain

$$U_1 = \frac{1}{2}\iiint [\{\varepsilon_l\}^T [D]\{\varepsilon_l\}]dV \tag{3.5.9}$$

where the strains can be expressed in terms of deformations as

$$\{\varepsilon_l\} = [B]\{q^0\} \tag{3.5.10}$$

and $$U_2 = \frac{1}{2}\iiint [\{\sigma^0\}^T \{\varepsilon_{nl}\}]dV \tag{3.5.11}$$

The method of explicit integration is performed through the thickness of the twisted panel and thus the generalized force and moment resultants can directly be related to the strain components through the laminate stiffness. The kinetic energy V of the curved panel can be derived as

$$V = \iint \left[\frac{h}{2}\left\{ \frac{\partial \overline{u}^2}{\partial t} + \frac{\partial \overline{v}^2}{\partial t} + \frac{\partial \overline{w}^2}{\partial t} \right\} + \frac{h^3}{12}\left\{ \frac{\partial \theta_x{}^2}{\partial t} + \frac{\partial \theta_y{}^2}{\partial t} \right\} \right] dxdy \tag{3.5.12}$$

The energies now can be written in matrix form as

$$U_0 = \frac{1}{2}\{q\}^T [K_P]\{q\}$$

$$U_1 = \frac{1}{2}\{q\}^T [K_e]\{q\} \tag{3.5.13}$$

$$U_2 = \frac{1}{2}\{q\}^T [K_g]\{q\}$$

$$V = \frac{1}{2}\{\dot{q}\}^T [M]\{\dot{q}\}$$

where $[K_p]$ = Plane stiffness matrix of the twisted panel

$[K_e]$ = Bending stiffness matrix with shear deformation of the panel

$[K_g]$ = Geometric stiffness or stress stiffness matrix of the twisted panel

[M] = Consistent mass matrix of the twisted panel

3.5.1: Formulation of Vibration and Static Stability problems

The governing equations for specified problems like plane stress, vibration and static stability are derived as below:

1. Plane stress problem

Using the principle of stationary potential energy the equilibrium equation for plane stress is expressed as

$$[K_P]\{q^0\}= \{p^0\} \tag{3.5.14}$$

2. Vibration with out in plane load

The governing equations for free vibrations are

$$[M]\ \{\ddot{q}\} + [K_e]\ \{q\} = \{0\} \tag{3.5.15}$$

3. Static stability or buckling

$$[[K_e] - N\ [K_g]]\{q\}= \{0\} \tag{3.5.16}$$

The eigenvalues of the above equations give the natural frequencies and buckling loads for different modes. The lowest values of frequency and buckling load are termed as the fundamental natural frequency and fundamental critical load of the twisted panel.

3.6: Finite Element Formulation

For problems involving complex geometrical and boundary conditions, analytical methods are not easily adaptable and numerical methods like finite element methods (FEM) are preferred. The finite element formulation is developed hereby for the structural analysis of isotropic as well as composite twisted shell panels using a curved shear deformable shell theory.

3.6.1: The shell element

The plate is made up of perfectly bonded layers. Each lamina is considered to be homogeneous and orthotropic and made of unidirectional fiber-reinforced material. The orthotropic axes of symmetry in each lamina are oriented at an arbitrary angle to the plate axes. An eight-noded isoparametric quadratic shell element is employed in the present analysis with five degrees of freedom u, v, w, θ_x and θ_y per node as shown in Figure 3.3. But the in-plane deformations u and v are considered for the initial plane stress analysis. The isoparametric element shall be oriented in the natural coordinate system and shall be transferred to the Cartesian coordinate system using the Jacobian matrix. In the analysis of thin shells, where the element is assumed to have mid-surface nodes, the shape function of the element is derived using the interpolation polynomial as follows

$$u(\xi,\eta) = \alpha_1 + \alpha_2\xi + \alpha_3\eta + \alpha_4\xi^2 + \alpha_5\xi\eta + \alpha_6\eta^2 + \alpha_7\xi^2\eta + \alpha_8\xi\eta^2 \qquad (3.6.1)$$

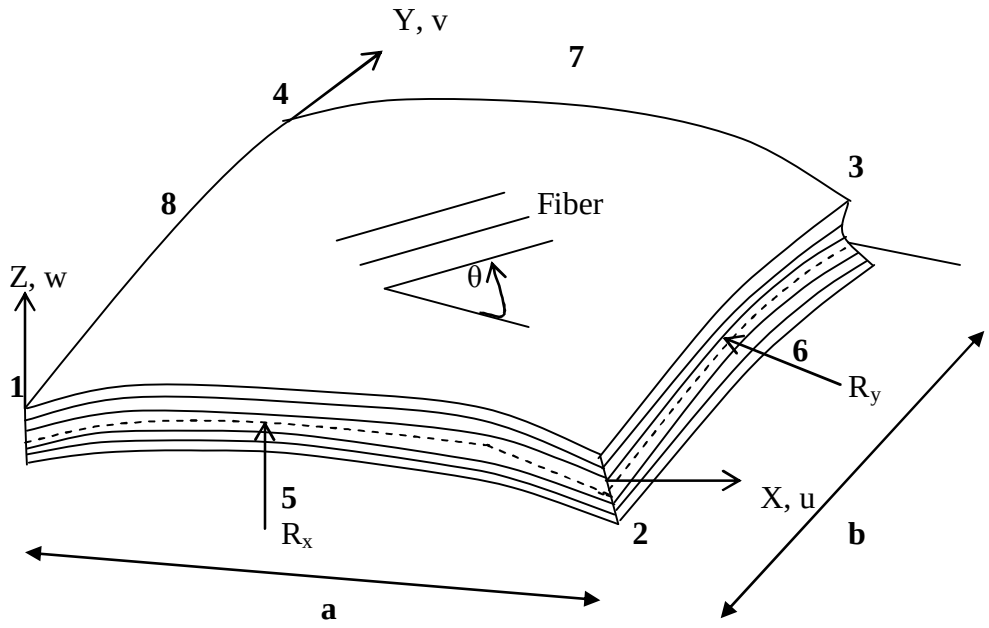

Figure 3.3: Isoparametric quadratic shell element

The element geometry and displacement field are expressed by the shape functions N_i.

The shape functions N_i are defined as

$$N_i = (1+\xi\xi_i)(1+\eta\eta_i)(\xi\xi_i+\eta\eta_i-1)/4 \qquad \text{i =1 to 4}$$

$$N_i = (1-\xi^2)(1+\eta\eta_i)/2 \qquad \text{i = 5, 7} \qquad (3.6.2)$$

$$N_i = (1+\xi\xi_i)(1-\eta^2)/2 \qquad \text{i = 6, 8}$$

where ξ and η are the local natural coordinates of the element and ξ_i and η_i are the values at i^{th} node.

The derivatives of the shape function N_i with respect to x and y are expressed in terms of their derivatives with respect to ξ and η by the following relationship.

$$\begin{bmatrix} N_{i,x} \\ N_{i,y} \end{bmatrix} = [J]^{-1} \begin{bmatrix} N_{i,\xi} \\ N_{i,\eta} \end{bmatrix} \qquad (3.6.3)$$

where

$$[J] = \begin{bmatrix} x_{i,\xi} & y_{i,\xi} \\ x_{i,\eta} & y_{i,\eta} \end{bmatrix} \qquad (3.6.4)$$

is the Jacobian matrix. The shell with the initial stresses undergoes small lateral deformations. First order shear deformation theory is used and the displacement field assumes that the mid-plane normal remains straight before and after deformation, but not necessarily normal after deformation, so that

$$\begin{aligned} u(x, y, z) &= u_o(x, y) + z\,\theta_y(x, y) \\ v(x, y, z) &= v_o(x, y) + z\,\theta_x(x, y) \\ w(x, y, z) &= w_o(x, y) \end{aligned} \qquad (3.6.5)$$

where u, v, w and u_o, v_o, w_o are displacement components in the x, y, z directions at any point and at the midsurface respectively. θ_x and θ_y are the rotations of the midsurface normal about the x and y axes respectively. Also

$$x = \sum N_i\, x_i, \qquad y = \sum N_i\, y_i$$

$$u_o = \sum N_i\, u_i \qquad v_o = \sum N_i\, v_i \qquad w_o = \sum N_i\, w_i \qquad (3.6.6)$$

$$\theta_x = \sum N_i\, \theta_{xi} \qquad \theta_y = \sum N_i\, \theta_{yi}$$

3.6.2: Strain displacement relations

Green-Lagrange's strain displacement relations are used throughout the structural analysis. The linear part of the strain is used to derive the elastic stiffness matrix and the nonlinear part of the strain is used to derive the geometric stiffness matrix. The linear strain displacement relations for a twisted shell element are:

$$\varepsilon_{xl} = \frac{\partial u}{\partial x} + \frac{w}{R_x} + zk_x$$

$$\varepsilon_{yl} = \frac{\partial v}{\partial y} + \frac{w}{R_y} + zk_y$$

$$\gamma_{xyl} = \frac{\partial u}{\partial y} + \frac{\partial v}{\partial x} + \frac{2w}{R_{xy}} + zk_{xy} \qquad (3.6.7)$$

$$\gamma_{xzl} = \frac{\partial w}{\partial x} + \theta_x - \frac{u}{R_x} - \frac{v}{R_{xy}}$$

$$\gamma_{yzl} = \frac{\partial w}{\partial y} + \theta_y - \frac{v}{R_y} - \frac{u}{R_{xy}}$$

where the bending strains k_j are expressed as

$$k_x = \frac{\partial \theta_x}{\partial x},\ k_y = \frac{\partial \theta_y}{\partial y} \text{ and}$$

$$k_{xy} = \frac{\partial \theta_x}{\partial y} + \frac{\partial \theta_y}{\partial x} + \frac{1}{2}\left(\frac{1}{R_y} - \frac{1}{R_x}\right)\left(\frac{\partial v}{\partial x} - \frac{\partial u}{\partial y}\right) \qquad (3.6.8)$$

The linear strains can be expressed in terms of displacements as,

$$\{\varepsilon\} = [B]\{d_e\} \qquad (3.6.9)$$

where

$\{d_e\} = \{u_1, v_1, w_1, \theta_{x1}, \theta_{y1}, \ldots\ldots\ldots\ldots\ldots\ldots u_8, v_8, w_8, \theta_{x8}, \theta_{y8}\}$ (3.6.10)

and $[B] = [[B_1], [B_2]\ldots\ldots\ldots\ldots\ldots\ldots\ldots\ldots [B_8]]$ (3.6.11)

$$[B_i] = \begin{bmatrix} N_{i,x} & 0 & \frac{N_i}{R_x} & 0 & 0 \\ 0 & N_{i,y} & \frac{N_i}{R_y} & 0 & 0 \\ N_{i,y} & N_{i,x} & 2\frac{N_i}{R_{xy}} & 0 & 0 \\ 0 & 0 & 0 & N_{i,x} & 0 \\ 0 & 0 & 0 & 0 & N_{i,y} \\ 0 & 0 & 0 & N_{i,y} & N_{i,x} \\ 0 & 0 & N_{i,x} & N_i & 0 \\ 0 & 0 & N_{i,y} & 0 & N_i \end{bmatrix} \quad (3.6.12)$$

3.6.3: Constitutive Relations

The basic composite twisted curved panel is considered to be composed of composite material laminates (typically thin layers). The material of each lamina consists of parallel, continuous fibers (e.g. graphite, boron, glass) of one material embedded in a matrix material (e.g. epoxy resin). Each layer may be regarded on a macroscopic scale as being homogeneous and orthotropic. The laminated fiber reinforced shell is assumed to consist of a number of thin laminates as shown in figure 3.4. The principal material axes are indicated by 1 and 2 and the moduli of elasticity of a lamina along these two directions are E_{11} and E_{22} respectively. For the plane stress state, $\sigma_z = 0$.

The stress strain relation becomes,

$$\begin{bmatrix} \sigma_x \\ \sigma_y \\ \tau_{xy} \\ \tau_{xz} \\ \tau_{yz} \end{bmatrix} = \begin{bmatrix} Q_{11} & Q_{12} & 0 & 0 & 0 \\ Q_{12} & Q_{22} & 0 & 0 & 0 \\ 0 & 0 & Q_{66} & 0 & 0 \\ 0 & 0 & 0 & Q_{44} & 0 \\ 0 & 0 & 0 & 0 & Q_{55} \end{bmatrix} \begin{bmatrix} \varepsilon_x \\ \varepsilon_y \\ \gamma_{xy} \\ \gamma_{xz} \\ \gamma_{yz} \end{bmatrix} \quad (3.6.13)$$

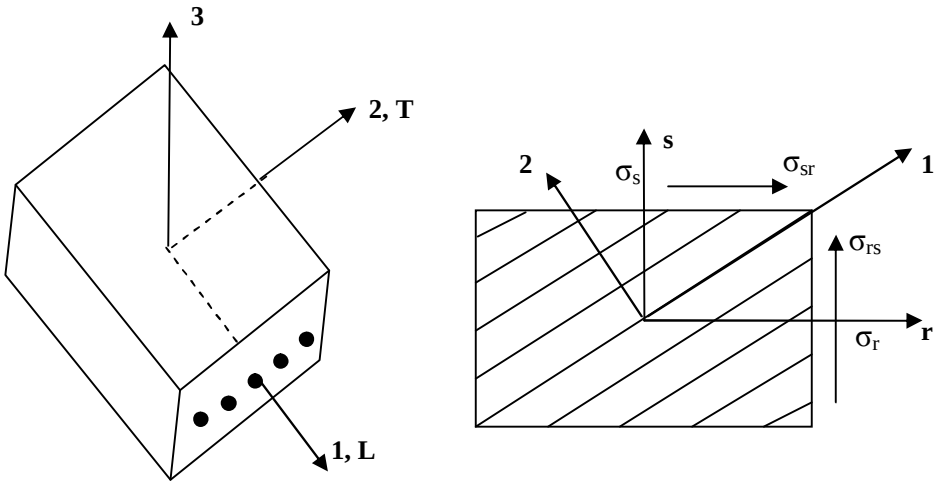

Figure 3.4: Laminated shell element

where $Q_{11} = \dfrac{E_{11}}{(1-\nu_{12}\nu_{21})}$

$$Q_{12} = \frac{E_{11}\nu_{21}}{(1-\nu_{12}\nu_{21})}$$

$$Q_{21} = \frac{E_{22}}{(1-\nu_{12}\nu_{21})}$$

$$Q_{22} = \frac{E_{22}}{(1-\nu_{12}\nu_{21})} \qquad (3.6.14)$$

$Q_{66} = G_{12}$

$Q_{44} = kG_{13}$

$Q_{55} = kG_{23}$

The on-axis elastic constant matrix corresponding to the fiber direction is given by

$$\left[Q_{ij}\right] = \begin{bmatrix} Q_{11} & Q_{12} & 0 & 0 & 0 \\ Q_{12} & Q_{22} & 0 & 0 & 0 \\ 0 & 0 & Q_{66} & 0 & 0 \\ 0 & 0 & 0 & Q_{44} & 0 \\ 0 & 0 & 0 & 0 & Q_{55} \end{bmatrix} \qquad (3.6.15)$$

If the major and minor Poisson's ratios are ν_{12} and ν_{21}, then using the reciprocal relation one obtains the following well known expression

$$\frac{\nu_{12}}{E_{11}} = \frac{\nu_{21}}{E_{22}} \tag{3.6.16}$$

Standard coordinate transformation is required to obtain the elastic constant matrix for any arbitrary principal axes with which the material principal axes makes an angle θ. Thus the off-axis elastic constant matrix is obtained from the on-axis elastic constant matrix as

$$\left[\overline{Q_{ij}}\right] = \begin{bmatrix} \overline{Q_{11}} & \overline{Q_{12}} & \overline{Q_{16}} & 0 & 0 \\ \overline{Q_{12}} & \overline{Q_{22}} & \overline{Q_{26}} & 0 & 0 \\ \overline{Q_{16}} & \overline{Q_{26}} & \overline{Q_{66}} & 0 & 0 \\ 0 & 0 & 0 & \overline{Q_{44}} & \overline{Q_{45}} \\ 0 & 0 & 0 & \overline{Q_{45}} & \overline{Q_{55}} \end{bmatrix}$$

$$\left[\overline{Q_{ij}}\right] = [T]^T [Q_{ij}][T] \tag{3.6.17}$$

where T is the transformation matrix. The elastic stiffness coefficients after transformation are

$$\begin{aligned}
\overline{Q_{11}} &= Q_{11} m^4 + 2(Q_{12} + 2Q_{66}) m^2 n^2 + Q_{22} n^4 \\
\overline{Q_{12}} &= (Q_{11} + Q_{22} - 4Q_{66}) m^2 n^2 + Q_{12}(m^4 + n^4) \\
\overline{Q_{22}} &= Q_{11} n^4 + 2(Q_{12} + Q_{66}) m^2 n^2 + Q_{22} m^4 \\
\overline{Q_{16}} &= (Q_{11} - Q_{12} - 2Q_{66}) nm^3 + (Q_{12} - Q_{22} + 2Q_{66}) n^3 m \\
\overline{Q_{26}} &= (Q_{11} - Q_{12} - 2Q_{66}) mn^3 + (Q_{12} - Q_{22} + 2Q_{66}) m^3 n \\
\overline{Q_{66}} &= (Q_{11} + Q_{22} - 2Q_{12} - 2Q_{66}) n^2 m^2 + Q_{66}(n^4 + m^4)
\end{aligned} \tag{3.6.18}$$

The elastic constant matrix corresponding to transverse shear deformation is

$$\begin{aligned}
\overline{Q_{44}} &= G_{13} m^2 + G_{23} n^2 \\
\overline{Q_{45}} &= (G_{13} - G_{23}) mn \\
\overline{Q_{55}} &= G_{13} n^2 + G_{23} m^2
\end{aligned} \tag{3.6.19}$$

Where $m = \cos\theta$ *and* $n = \sin\theta$

The stress strain relations are

$$\begin{Bmatrix} \sigma_x \\ \sigma_y \\ \tau_{xy} \\ \tau_{xz} \\ \tau_{yz} \end{Bmatrix} = \begin{bmatrix} \overline{Q_{11}} & \overline{Q_{12}} & \overline{Q_{16}} & 0 & 0 \\ \overline{Q_{12}} & \overline{Q_{22}} & \overline{Q_{26}} & 0 & 0 \\ \overline{Q_{16}} & \overline{Q_{26}} & \overline{Q_{66}} & 0 & 0 \\ 0 & 0 & 0 & \overline{Q_{44}} & \overline{Q_{45}} \\ 0 & 0 & 0 & \overline{Q_{45}} & \overline{Q_{55}} \end{bmatrix} \begin{Bmatrix} \varepsilon_x \\ \varepsilon_y \\ \gamma_{xy} \\ \gamma_{xy} \\ \gamma_{xy} \end{Bmatrix} \tag{3.6.20}$$

The forces and moment resultants are obtained by integration through the thickness h for stresses as

$$\begin{bmatrix} N_x \\ N_y \\ N_{xy} \\ M_x \\ M_y \\ M_{xy} \\ Q_x \\ Q_y \end{bmatrix} = \int_{-h/2}^{h/2} \begin{Bmatrix} \sigma_x \\ \sigma_y \\ \tau_{xy} \\ \sigma_x z \\ \sigma_y z \\ \tau_{xy} z \\ \tau_{xz} \\ \tau_{yz} \end{Bmatrix} dz \tag{3.6.21}$$

where σ_x, σ_y are the normal stresses along X and Y directions, τ_{xy}, τ_{xz} *and* τ_{yz} are shear stresses in xy, xz and yz planes respectively.

Considering only in-plane deformations, the constitutive relation for the initial plane stress analysis is

$$\begin{Bmatrix} N_x \\ N_y \\ N_{xy} \end{Bmatrix} = \begin{bmatrix} A_{11} & A_{12} & A_{16} \\ A_{21} & A_{22} & A_{26} \\ A_{31} & A_{32} & A_{66} \end{bmatrix} \begin{Bmatrix} \varepsilon_x \\ \varepsilon_y \\ \gamma_{xy} \end{Bmatrix} \tag{3.6.22}$$

The extensional stiffness for an isotropic material with material properties E and ν are

$$[D_P]=\begin{bmatrix} \frac{Eh}{1-\nu^2} & \frac{\nu Eh}{1-\nu^2} & 0 \\ \frac{\nu Eh}{1-\nu^2} & \frac{Eh}{1-\nu^2} & 0 \\ 0 & 0 & \frac{Eh}{2(1+\nu)} \end{bmatrix} \tag{3.6.23}$$

The constitutive relationships for bending with transverse shear of a doubly curved shell becomes

$$\begin{Bmatrix} N_x \\ N_y \\ N_{xy} \\ M_x \\ M_y \\ M_{xy} \\ Q_x \\ Q_y \end{Bmatrix} = \begin{bmatrix} A_{11} & A_{12} & A_{16} & B_{11} & B_{12} & B_{16} & 0 & 0 \\ A_{21} & A_{22} & A_{26} & B_{12} & B_{22} & B_{26} & 0 & 0 \\ A_{16} & A_{26} & A_{66} & B_{11} & B_{12} & B_{16} & 0 & 0 \\ B_{11} & B_{12} & B_{16} & D_{11} & D_{12} & D_{16} & 0 & 0 \\ B_{12} & B_{22} & B_{26} & D_{12} & D_{22} & D_{26} & 0 & 0 \\ B_{16} & B_{26} & B_{66} & D_{16} & D_{26} & D_{66} & 0 & 0 \\ 0 & 0 & 0 & 0 & 0 & 0 & S_{44} & S_{45} \\ 0 & 0 & 0 & 0 & 0 & 0 & S_{45} & S_{55} \end{bmatrix} \begin{Bmatrix} \varepsilon_x \\ \varepsilon_y \\ \gamma_{xy} \\ k_x \\ k_y \\ k_{xy} \\ \gamma_{xz} \\ \gamma_{yz} \end{Bmatrix} \tag{3.6.24}$$

This can also be stated as

$$\begin{Bmatrix} N_i \\ M_i \\ Q_i \end{Bmatrix} = \begin{bmatrix} A_{ij} & B_{ij} & 0 \\ B_{ij} & D_{ij} & 0 \\ 0 & 0 & S_{ij} \end{bmatrix} \begin{Bmatrix} \varepsilon_j \\ k_j \\ \gamma_m \end{Bmatrix} \tag{3.6.25}$$

or $$\{F\}=[D]\{\varepsilon\} \tag{3.6.26}$$

where A_{ij}, B_{ij}, D_{ij} and S_{ij} are the extensional, bending-stretching coupling, bending and transverse shear stiffnesses. They may be defined as:

$$
\begin{aligned}
A_{ij} &= \sum_{k=1}^{n} (\overline{Q_{ij}})_k \, (z_k - z_{k-1}) \\
B_{ij} &= \frac{1}{2} \sum_{k=1}^{n} (\overline{Q_{ij}})_k \, (z_k^2 - z_{k-1}^2) \\
D_{ij} &= \frac{1}{3} \sum_{k=1}^{n} (\overline{Q_{ij}})_k \, (z_k^3 - z_{k-1}^3); \; i, j = 1,2,6 \\
S_{ij} &= k \sum_{k=1}^{n} (\overline{Q_{ij}})_k \, (z_k - z_{k-1}); i, j = 4,5
\end{aligned}
\tag{3.6.27}
$$

and k is the transverse shear correction factor. The accurate prediction for anisotropic laminates depends on a number of laminate properties and is also problem dependent. A shear correction factor of 5/6 is used in the present formulation for all numerical computations.

3.6.4: Derivation of Element Matrices

The element matrices in natural coordinate system are derived as:

1. Element plane elastic stiffness matrix

$$
[k_p] = \int_{-1}^{1} \int_{-1}^{1} [B_P]^T [D_P] [B_P] |J| \, d\xi \, d\eta \tag{3.6.28}
$$

2. Element elastic stiffness matrix

$$
[k_e] = \int_{-1}^{1} \int_{-1}^{1} [B]^T [D] [B] |J| \, d\xi \, d\eta \tag{3.6.29}
$$

3. Generalized element mass matrix or consistent mass matrix

$$
[m_e] = \int_{-1}^{1} \int_{-1}^{1} [N]^T [P] [N] |J| \, d\xi \, d\eta \tag{3.6.30}
$$

where the shape function matrix

$$[N]=\begin{bmatrix} N_i & 0 & 0 & 0 & 0 \\ 0 & N_i & 0 & 0 & 0 \\ 0 & 0 & N_i & 0 & 0 \\ 0 & 0 & 0 & N_i & 0 \\ 0 & 0 & 0 & 0 & N_i \end{bmatrix} \quad \text{i =1, 2…….8} \tag{3.6.31}$$

$$[P]=\begin{bmatrix} P_1 & 0 & 0 & P_2 & 0 \\ 0 & P_1 & 0 & 0 & P_2 \\ 0 & 0 & P_1 & 0 & 0 \\ P_2 & 0 & 0 & P_3 & 0 \\ 0 & P_2 & 0 & 0 & P_3 \end{bmatrix} \tag{3.6.32}$$

and

$$(P_1, P_2, P_3)=\sum_{k=1}^{n}\int_{z_{k-1}}^{z_1}(\rho)_k(1, z, z^2)\,dz \tag{3.6.33}$$

where [B], [D], [N] are the strain-displacement matrix, stress-strain matrix and shape function matrix and $|J|$ is the Jacobian determinant. [P] involves mass density parameters as explained earlier.

3.6.5: Geometric stiffness matrix

The element geometric stiffness matrix for the twisted shell is derived using the non-linear in-plane Green's strains with curvature component using the procedure explained by Cook, Malkus and Plesha [1989]. The geometric stiffness matrix is a function of in-plane stress distribution in the element due to applied edge loading. Plane stress analysis is carried out using the finite element technique to determine the stresses and these stresses are used to formulate the geometric stiffness matrices.

$$U_2 = \int_v \left[\sigma^0\right]^T \{\varepsilon_{nl}\} dV \tag{3.6.34}$$

The non-linear strain components are as follows:

$$\varepsilon_{xnl} = \frac{1}{2}\left(\frac{\partial u}{\partial x}\right)^2 + \frac{1}{2}\left(\frac{\partial v}{\partial x}\right)^2 + \frac{1}{2}\left(\frac{\partial w}{\partial x} - \frac{u}{R_x}\right)^2 + \frac{1}{2}z^2\left[\left(\frac{\partial \theta_x}{\partial x}\right)^2 + \left(\frac{\partial \theta_y}{\partial x}\right)^2\right]$$

$$\varepsilon_{ynl} = \frac{1}{2}\left(\frac{\partial u}{\partial y}\right)^2 + \frac{1}{2}\left(\frac{\partial v}{\partial y}\right)^2 + \frac{1}{2}\left(\frac{\partial w}{\partial y} - \frac{v}{R_y}\right)^2 + \frac{1}{2}z^2\left[\left(\frac{\partial \theta_x}{\partial y}\right)^2 + \left(\frac{\partial \theta_y}{\partial y}\right)^2\right] \tag{3.6.35}$$

$$\gamma_{xynl} = \frac{\partial u}{\partial x}\left(\frac{\partial u}{\partial y}\right) + \frac{\partial v}{\partial x}\left(\frac{\partial v}{\partial y}\right) + \left(\frac{\partial w}{\partial x} - \frac{u}{R_x}\right)\left(\frac{\partial w}{\partial y} - \frac{v}{R_y}\right) +$$

$$z^2\left[\left(\frac{\partial \theta_x}{\partial x}\right)\left(\frac{\partial \theta_x}{\partial y}\right) + \left(\frac{\partial \theta_y}{\partial x}\right)\left(\frac{\partial \theta_y}{\partial y}\right)\right]$$

Using the non-linear strains, the strain energy can be written as

$$U_2 = \int_A \frac{h}{2}\left[\begin{array}{c}\sigma_x^0\left\{\left(\frac{\partial u}{\partial x}\right)^2 + \left(\frac{\partial v}{\partial x}\right)^2 + \left(\frac{\partial w}{\partial x} - \frac{u}{R_x}\right)^2\right\} + \sigma_y^0\left\{\left(\frac{\partial u}{\partial y}\right)^2 + \left(\frac{\partial v}{\partial y}\right)^2 + \left(\frac{\partial w}{\partial y} - \frac{v}{R_y}\right)^2\right\} + \\ 2\tau_{xy}^0\left\{\left(\frac{\partial u}{\partial x}\frac{\partial u}{\partial y}\right) + \left(\frac{\partial v}{\partial x}\frac{\partial v}{\partial y}\right) + \left(\frac{\partial w}{\partial x} - \frac{u}{R_x}\right)\left(\frac{\partial w}{\partial y} - \frac{v}{R_y}\right)\right\}\end{array}\right] dx\,dy +$$

$$\int_A \frac{h^3}{24}\left[\sigma_x^0\left\{\left(\frac{\partial \theta_x}{\partial x}\right)^2 + \left(\frac{\partial \theta_y}{\partial x}\right)^2\right\} + \sigma_y^0\left\{\left(\frac{\partial \theta_y}{\partial y}\right)^2 + \left(\frac{\partial \theta_x}{\partial y}\right)^2\right\} + 2\tau_{xy}^0\left\{\left(\frac{\partial \theta_y}{\partial x}\frac{\partial \theta_y}{\partial y}\right) + \left(\frac{\partial \theta_x}{\partial x}\frac{\partial \theta_y}{\partial y}\right)\right\}\right] dx\,dy$$

(3.6.36)

This can also be expressed as

$$U_2 = \frac{1}{2}\int_v [f]^T [S][f] dV \tag{3.6.37}$$

where

$$\{f\}=\left[\frac{\partial u}{\partial x},\frac{\partial u}{\partial y},\frac{\partial v}{\partial x},\frac{\partial v}{\partial y},\left(\frac{\partial w}{\partial x}-\frac{u}{R_x}\right),\left(\frac{\partial w}{\partial y}-\frac{v}{R_y}\right),\frac{\partial \theta_x}{\partial x},\frac{\partial \theta_x}{\partial y},\frac{\partial \theta_y}{\partial x},\frac{\partial \theta_y}{\partial y}\right]^T \quad (3.6.38)$$

$$\text{and}\,[S]=\begin{bmatrix}[s] & 0 & 0 & 0 & 0\\ 0 & [s] & 0 & 0 & 0\\ 0 & 0 & [s] & 0 & 0\\ 0 & 0 & 0 & [s] & 0\\ 0 & 0 & 0 & 0 & [s]\end{bmatrix}$$

(3.6.39)

$$\text{where}\,[s]=\begin{bmatrix}\sigma_x^0 & \tau_{xy}^0\\ \tau_{xy}^0 & \sigma_y^o\end{bmatrix}=\frac{1}{h}\begin{bmatrix}N_x^0 & N_{xy}^0\\ N_{xy}^0 & N_y^0\end{bmatrix} \quad (3.6.40)$$

The in-plane stress resultants N_x^0, N_y^0 *and* N_{xy}^0 at each Gauss point are obtained separately by plane stress analysis and the geometric stiffness matrix is formed for these stress resultants.

$$\{f\}=[G]\{q_e\} \quad (3.6.41)$$

$$\text{where}\,\{q_e\}=\begin{bmatrix}u & v & w & \theta_x & \theta_y\end{bmatrix}^T \quad (3.6.42)$$

The strain energy becomes

$$U_2=\frac{1}{2}\{q\}^T[G]^T[S][G]\{q\}dV=\frac{1}{2}\{q_e\}^T[K_g]_e[q_e] \quad (3.6.43)$$

where the element geometric stiffness matrix

$$[k_g]_e=\int_{-1}^{1}\int_{-1}^{1}[G]^T[S][G]|J|d\xi d\eta \quad (3.6.44)$$

$$\text{and}\,[G]=\begin{bmatrix} N_{i,}x & 0 & 0 & 0 & 0 \\ N_{i,}y & 0 & 0 & 0 & 0 \\ 0 & N_{i,}x & 0 & 0 & 0 \\ 0 & N_{i,}y & 0 & 0 & 0 \\ 0 & 0 & N_{i,}x & 0 & 0 \\ 0 & 0 & N_{i,}y & 0 & 0 \\ 0 & 0 & 0 & N_{i,}x & 0 \\ 0 & 0 & 0 & N_{i,}y & 0 \\ 0 & 0 & 0 & 0 & N_{i,}x \\ 0 & 0 & 0 & 0 & N_{i,}y \end{bmatrix} \qquad (3.6.45)$$

3.7: Computer program

A computer program has been developed to perform all necessary computations. The twisted panel is divided into a two-dimensional array of rectangular elements. The element elastic stiffness and mass matrices are obtained with 2×2 gauss points. The geometric stiffness matrix is essentially a function of the in-plane stress distribution in the element due to applied edge loading. The overall stiffness and mass matrices are obtained by assembling the corresponding element matrices using skyline technique. Subspace iteration method is used throughout to solve the eigen value problem. Reduced integration technique is adopted in order to avoid possible shear locking.

CHAPTER 4

RESULTS AND DISCUSSIONS

4.1: Introduction

The present chapter deals with the results of the analyses of the vibration, buckling and parametric resonance characteristics of homogeneous and laminated composite twisted cantilever panels using the formulation given in the previous chapter. As explained, the eight-node isoparametric quadratic shell element is used to develop the finite element procedure. The first order shear deformation theory is used to model the twisted panels considering the effects of transverse shear deformation and rotary inertia. The stability characteristics of homogeneous and laminated composite pretwisted cantilever panels subjected to in-plane loads are studied. The parametric instability studies are carried out for isotropic and laminated composite pretwisted panels subjected to in-plane periodic loads with static component of load to consider the effect of various parameters. The studies in this chapter are presented as follows:

- Convergence study
- Comparison with previous studies
- Numerical results

4.2: Convergence study

The convergence study is first done for four lowest non-dimensional frequencies of free vibration of square isotropic twisted cantilever plates with an angle of twist of 30° for different mesh divisions and is shown in Table 4.1. The convergence study is then performed for non-dimensional fundamental frequencies of vibration of laminated composite twisted cantilever plates for two thickness ratios (b/h =100, 20) and three angles of twist (Φ = 0°, 15° and 30°) for different mesh divisions as shown in Table 4.2. As observed, a mesh of 10 ×10 shows good convergence of the numerical solution for the free vibration of twisted cantilever plates and this mesh is employed throughout the study to idealize the panel in the subsequent vibration and stability analysis of the panel.

Table 4.1: Convergence of non-dimensional fundamental frequencies of free vibration of isotropic twisted plates

a /b =1, b/h = 20, ν = 0.3, Φ = 15°

Non-dimensional frequency $\varpi = \omega a^2 \sqrt{\frac{\rho h}{D}}$

Mesh division	Angle of twist	Non-dimensional frequency			
		1st frequency	2nd frequency	3rd frequency	4th frequency
4 × 4	30°	3.404	15.957	18.896	27.416
8 × 8		3.401	15.946	18.796	27.329
10 × 10		3.400	15.945	18.792	27.325

Table 4.2: Convergence of non-dimensional frequencies of vibration of composite twisted cantilever plates with 45°/- 45°/45° lamination

a /b = 1

E_{11} = 138GPa, E_{22} = 8.96GPa, G_{12} = 7.1GPa, ν_{12} = 0.3

Non-dimensional frequency $\varpi = \omega a^2 \sqrt{(\rho / E_{11} h^2)}$

Mesh	Non-dimensional fundamental frequencies of free vibration for different thickness ratios and angles of twist					
	a/h =100			a/h = 20		
	0°	15°	30°	0°	15°	30°
4×4	0.4615	0.5300	0.5165	0.4570	0.4744	0.4770
8×8	0.4596	0.5261	0.5123	0.4546	0.4719	0.4745
10×10	0.4592	0.5256	0.5118	0.4541	0.4714	0.4741

4.3: Comparison with previous studies

After the convergence study, the accuracy and efficiency of the present formulation are established through comparison with previous studies. The four lowest non-dimensional frequency parameters of square isotropic pretwisted cantilever plates obtained by the present formulation is compared with those obtained by Nabi and Ganesan [1996] using triangular plate element and with those of Kee and Kim [2004] using nine-node degenerated shell element as shown in Table 4.3. The study is made for an untwisted plate and a plate with an angle of twist of 30°. The symbols 'B', 'T', and 'CB' denote the bending, twisting and chordwise bending modes respectively. The present results show good comparison with the previous studies in the literature.

Table 4.3: Comparison of non-dimensional frequency parameters (λ) of the initially twisted isotropic cantilever plate type blade

a/b =1, b/h = 20, E = 200GPa, ν = 0.3,

Non dimensional frequency $\lambda = \omega a^2 \sqrt{\frac{\rho h}{D}}$

Angle of twist	Mode	Nabi & Ganesan [1996]	Kee & Kim [2004]	Present study
0°	1B	3.46	3.49	3.46
	2B	21.44	22.01	20.95
	1T	8.53	8.51	8.33
	1CB	27.05	27.33	26.64
30°	1B	3.41	3.42	3.25
	2B	18.88	19.51	19.10
	1T	16.88	14.43	15.93
	1CB	27.98	27.41	27.40

The present finite element formulation is validated for free vibration of twisted laminated plates by comparing the non-dimensional fundamental frequencies of vibration of graphite /epoxy [θ, -θ, θ] pretwisted (Φ =15°) cantilever plates with the results presented by Qatu and Leissa [1991] and He, Lim and Kitipornchai [2000], both of whom used the Ritz method for their analysis, as shown in Table 4.4. As shown, there exists good comparison between the results obtained by the present formulation and those presented by the previous investigators.

Table 4.4: Comparison of non-dimensional fundamental frequencies of vibration of graphite epoxy pretwisted cantilever [θ, -θ,θ] plates

a /b = 1, Φ =15°

E_{11} = 138GPa, E_{22} = 8.96GPa, G_{12} = 7.1GPa, ν_{12} = 0.3

Non-dimensional frequency, $\varpi = \omega a^2 \sqrt{(\rho / E_{11} h^2)}$

b/h	Reference	Non-dimensional fundamental frequencies of free vibration for different ply orientations (θ)						
		0	15	30	45	60	75	90
100	Qatu & Leissa [1991]	1.0035	0.9296	0.7465	0.5286	0.3545	0.2723	0.2555
	He *et al.*[2000]	1.0034	0.92938	0.74573	0.52724	0.35344	0.27208	0.25544
	Present FEM	1.00295	0.92798	0.74381	0.52560	0.35278	0.27200	0.25543
20	Qatu & Leissa [1991]	1.0031	0.8981	0.6899	0.4790	0.3343	0.2695	0.2554
	He *et al.*[2000]	1.0031	0.89791	0.68926	0.47810	0.33374	0.26934	0.25540
	Present study	0.99107	0.87025	0.67939	0.47143	0.33074	0.26786	0.25506

To validate the formulation further for stability studies, the buckling loads of untwisted (Φ = 0°) singly curved angle-ply panels with symmetric lay-up are compared in Table 4.5 with the results obtained by Moita *et al*. [1999].This comparative study also indicates good agreement between the results obtained by the present study and those of Moita *et al*. [1999] using an eight-node serendipity finite element with ten degrees of freedom per node.

To validate the formulation for dynamic stability, the principal instability regions of untwisted (ϕ = 0°) square anti-symmetric angle-ply flat panels subjected to in-plane periodic loads is plotted with the non-dimensional frequency Ω/ω (ratio of excitation frequency to the free vibration frequency) without static component of load and compared with the results of Moorthy *et al.* [1990] using finite element method. Two angle-ply panels with different stacking

sequences were compared: two layer (45°/-45°) and four layer (45°/-45°/45°/-45°). As observed from Figure 4.1, the present finite element results show excellent agreement with the previous instability studies.

Table 4.5: Comparison of buckling loads for a thin un-twisted (Φ = 0°) angle-ply cylindrical panel with symmetric lay-up $[0°/-\alpha°/+\alpha°/-90°]_s$

h =1.0mm, R/h =150, L/R =1.0, ϕ = 0

E_{11} = 181GPa, E_{22} = 10.3GPa, $G_{12} = G_{23} = G_{13}$ = 7.17GPa, ν_{12} = 0.28

Non dimensional buckling load, $\lambda = N_x R / E_{11} h^2$

α	b/L =1.309		b/L =1.047		b/L = 0.786	
	Present	Moita *et al.*[1999]	Present	Moita *et al.*[1999]	Present	Moita *et al.*[1999]
0	0.123	0.122	0.121	0.121	0.121	0.129
15	0.150	0.147	0.147	0.147	0.160	0.159
30	0.193	0.192	0.191	0.190	0.205	0.205
45	0.220	0.220	0.217	0.211	0.232	0.232
60	0.213	0.214	0.209	0.206	0.230	0.230
75	0.180	0.179	0.175	0.174	0.194	0.193
90	0.155	0.155	0.148	0.147	0.165	0.163

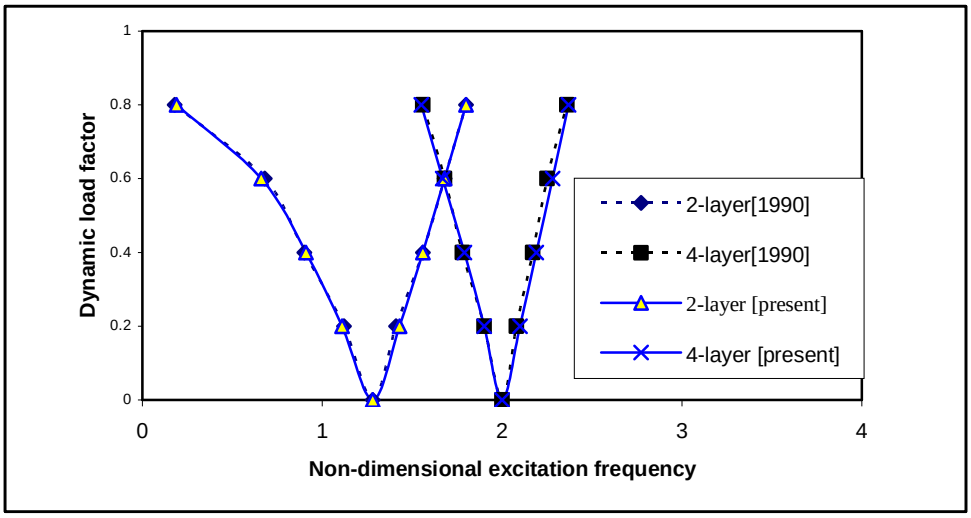

Figure 4.1: Comparison of results of instability regions of square untwisted angle-ply panels (45°/-45°, 45°/-45°/45°/-45) of present formulation with Moorthy *et al*.

4.4: Numerical results

After validation, the studies are extended to investigation of the vibration, buckling and dynamic stability characteristics of homogeneous and laminated composite pretwisted cantilever panels (plates with camber). Numerical results are presented to show the effects of various geometrical parameters like angle of twist, aspect ratio, shallowness ratio and lamination details (for composite panels) on the vibration and stability characteristics of isotropic and laminated composite twisted cantilever panels.

The numerical results based on the present formulation are grouped into:

- **Isotropic twisted cantilever panels**
- **Cross-ply twisted cantilever panels**
- **Angle-ply twisted cantilever panels**

The results of each group above are presented in subgroups as:

- **Vibration and buckling studies**
- **Dynamic stability studies**

4.5: Isotropic twisted panels

The study is first carried out for the analysis of the vibration and stability of isotropic pretwisted cantilever panels (plates with camber). The geometrical and material properties of the twisted panels (unless otherwise stated) are:

$a = b = 500mm$, $h = 5$ mm, $\rho = 2700$ kg/ m^3

$E = 70$ GPa and $\nu = 0.3$

4.5.1: Non-dimensionalization of parameters

The non-dimensionalization of the different parameters is carried out as follows:

Non-dimensional frequency $\varpi = \omega a^2 \sqrt{\frac{\rho h}{D}}$

Non-dimensional buckling load $\lambda = \frac{N_x b^2}{D}$ where D = $\frac{Eh^3}{12(1-\nu^2)}$

The non-dimensional excitation frequency $\Omega = \overline{\Omega} a^2 \sqrt{(\rho h / D)}$ (unless otherwise stated) is used throughout the dynamic instability studies, where $\overline{\Omega}$ is the excitation frequency in radians/second.

4.5.2: Boundary conditions

The clamped (C) boundary condition of the isotropic twisted panel using the first order shear deformation theory is:

u = v = w = θ_x = θ_y = 0 at the left edge.

4.5.3: Vibration and buckling studies

The first four frequencies of vibration of an isotropic twisted cantilever plate are presented in Table 4.6 for varying angles of twist. Introduction of an angle of twist of 10° to the untwisted plate is seen to reduce the fundamental frequency parameter by 0.5%. It is also seen that as the angle of twist increases, the fundamental frequency parameter decreases. When the angle of twist of the plate is 30°, the fundamental frequency parameter is lesser by 5.7% as compared to the untwisted plate. The 2nd frequency in bending mode decreases with the increasing angle of twist except the additional twisting mode for untwisted plates. The 3rd and the 4th frequency parameter increase with increase in the twisting angle.

Table 4.6: Variation of non-dimensional frequency parameter with angle of twist for a square isotropic cantilever plate

a/b =1, b/h = 100

Angle of twist	Non-dimensional frequency parameter			
	1st frequency	2nd frequency	3rd frequency	4th frequency
0°	3.4707	8.4838	21.2714	27.1573
10°	3.4528	21.3136	22.3154	31.2619
15°	3.4281	21.1392	31.4238	35.9028
20°	3.3908	20.8056	39.9847	41.6632
30°	3.2727	19.7639	54.7100	57.8757

The effect of changing the curvature of the twisted panel on the non-dimensional frequency parameter of a cylindrical twisted panel of square planform is studied and shown in Table 4.7. The angle of twist for all further studies is taken as 15°. As observed from the table, the fundamental frequency parameter decreases as the R_y/b ratio increases. Also introduction of curvature to the twisted panel increases the non-dimensional frequency parameter suggesting an increase in the stiffness of the panel due to addition of curvature. For an angle of twist of 15° and R_y/b ratio of 5, the frequency parameter increases by 23.85% as compared to the flat twisted plate.

The effect of increasing aspect ratio (a/b) on the non-dimensional frequency parameter is shown in Table 4.8. As the aspect ratio increases, the fundamental frequency parameter decreases. Comparing the square plate with the rectangular plate of a/b =3, there is a 1.5% decrease in the first non-dimensional frequency parameter.

Table 4.7: Variation of non-dimensional frequency parameter with R_y/b ratio for a square isotropic cylindrical cantilever panel

a/b =1**,** b/h = 100, Φ = 15°

R_y/b	Non-dimensional frequency parameter			
	1st frequency	2nd frequency	3rd frequency	4th frequency
5	4.2456	21.0855	35.5853	37.2419
10	3.6649	21.0583	33.1054	35.8822
20	3.4902	21.1128	31.8614	35.9132
50	3.4381	21.1347	31.4946	35.9027
100	3.4306	21.1381	31.4416	35.9028

Table 4.8: Variation of non-dimensional frequency parameter with aspect ratio for an isotropic twisted cantilever plate

b/h = 100, Φ = 15°

a/b	Non-dimensional frequency parameter			
	1st frequency	2nd frequency	3rd frequency	4th frequency
1	3.4281	21.1392	31.4240	35.9032
2	3.3968	20.9707	38.5154	59.7581
3	3.3758	20.8805	41.8687	59.5900

The variation of the frequency in Hz with decreasing thickness (increasing b/h ratio) of a square isotropic cantilever twisted plate is studied and is shown in Table 4.9. As the b/h ratio increases, the frequency is seen to decrease due to reduction in stiffness. Comparing the first frequencies for b/h = 50 and b/h =100, the frequency is seen to decrease by almost 50%.

Table 4.9: Variation of frequency in Hz with b/h ratio for a square isotropic twisted cantilever plate

a/b =1, Φ = 15°

b/h	frequency in Hz			
	1st frequency	2nd frequency	3rd frequency	4th frequency
50	32.9666	172.9527	201.8892	282.2533
100	16.5108	101.8148	151.3504	172.9240
200	8.2701	51.1583	127.5220	129.6366

The non-dimensional frequency parameters are compared for twisted panels with various geometries as shown in Table 4.10. The angle of twist is fixed at 15°. The b/R_y ratio is taken as 0.25, i.e., cylindrical ($b/R_y = 0.25$), spherical ($b/R_x = 0.25$, $b/R_y = 0.25$) and hyperbolic paraboloidal ($b/R_x = -0.25$, $b/R_y = 0.25$). The first frequency parameter is largest for the spherical twisted panel and is 35.1% greater than the twisted plate. Again all the twisted panels with curvature have greater frequency parameter than the plate.

Table 4.10: Variation of non-dimensional frequency parameter for different twisted cantilever curved panels

a/b =1, b/h = 100, Φ = 15°, $b/R_y = 0.25$

Geometry of plate	Non-dimensional frequency parameter			
	1st frequency	2nd frequency	3rd frequency	4th frequency
Plate	3.4281	21.1392	31.4240	35.9032
Cylindrical	4.6058	21.2605	35.2980	39.5362
Spherical	4.6322	17.5216	25.4093	40.9337
Hyperbolic paraboloid	4.4911	17.1455	27.7090	51.4189

The study is then extended to the static stability of isotropic twisted cantilever panels. The non-dimensional buckling loads are presented for a cantilever twisted plate of square plan form for different angles of twist. The lowest two buckling loads are shown in Table 4.11. As observed, the first non-dimensional buckling load decreases as the angle of twist of the plate increases. Introduction of an angle of twist of 10° to the untwisted plate decreases the buckling load by 1.9% and at an angle of twist of 30°, the decrease in the lowest buckling load is as much as 18.96% compared to the untwisted plate.

Table 4.11: Variation of non-dimensional buckling load with angle of twist for a square isotropic cantilever plate

a/b = 1, b/h = 100

Angle of twist	**Non-dimensional buckling load**	
	1st buckling load	**2nd buckling load**
0°	2.374	17.839
10°	2.330	20.970
20°	2.182	19.874
30°	1.924	18.119

The effect of curvature on the buckling load is next studied. Comparing the results of Tables 4.11 and 4.12, it is seen that the buckling load significantly increases with introduction of curvature to the plate. The buckling load for an untwisted square cylindrical panel is 726.9% more than the untwisted square plate. At a twisting angle of 10°, the non-dimensional buckling load for the twisted cylindrical panel is 119.5% more than the twisted plate (Φ =10°).As seen from Table 4.12, the buckling load of the cylindrical cantilever panel decreases as the angle of twist increases. There is an 88.6% decrease at an angle of twist of 30° as compared to the untwisted panel. So the effect of twist is more pronounced in a cylindrical panel than a flat panel.

Table 4.12: Variation of non-dimensional buckling load with angle of twist for a square isotropic cylindrical cantilever panel

a/b = 1, b/h = 100, b/ R_y = 0.25

Angle of twist	Non-dimensional buckling load	
	1st buckling load	2nd buckling load
0°	19.6296	19.8602
10°	5.1162	28.7320
20°	3.0927	24.5594
30°	2.3473	20.7555

Table 4.13 shows the variation of the non-dimensional buckling load with R_y/b ratio for a square panel with angle of twist taken as 15°. It is observed that as the R_y/b ratio increases, the non-dimensional buckling load decreases. When the R_y/b changes from 5 to 10, there is a 22.1% decrease in the non-dimensional buckling load.

Table 4.13: Variation of non-dimensional buckling load with R_y/b ratio for a square isotropic twisted cylindrical cantilever panel

a/b = 1, b/h = 100, Φ =15°

R_y/b	Non-dimensional buckling load	
	1st buckling load	2nd buckling load
5	3.2474	24.9409
10	2.5294	21.9130
20	2.3361	20.8944
50	2.2803	20.5827
100	2.2723	20.5372

Table 4.14 shows the variation of the non-dimensional buckling load with aspect ratio. As seen in Table 4.14, when the aspect ratio is doubled, the first buckling load decreases by 75.6%.

Table 4.14: Variation of non-dimensional buckling load with aspect ratio for an isotropic twisted cantilever plate

b/h =100, Φ =15°

a/b	Non-dimensional buckling load	
	1st buckling load	2nd buckling load
1	2.270	20.522
2	0.555	5.030
3	0.244	2.213

The effect of increasing b/h ratio on the buckling load is next studied. As observed in Table 4.15, the first buckling load decreases as the b/h ratio increases suggesting a decrease in stiffness as the thickness decreases. When the b/h ratio becomes half, there is an 87% decrease in the buckling load.

Table 4.15: Variation of buckling load with b/h ratio for a square isotropic twisted cantilever plate

a/b =1, Φ =15°

b/ h	Buckling load	
	1st buckling load	2nd buckling load
50	335.836	3026.843
100	42.191	381.498
200	5.304	48.012

4.5.4: Dynamic stability studies

The studies are then extended to the dynamic instability characteristics of the isotropic twisted cantilever panel. Figure 4.2 shows the variation of the instability regions with the angle of twist. A static load factor of 0.2 is considered for the twisted panel. The panel is studied for the untwisted case ($\Phi = 0°$) and angle of twists of $\Phi = 15°$ and $30°$. The instability occurs at a lower excitation frequency as the angle of twist of the plate increases and the width of the instability region is found to increase as the angle of twist increases from 0° to 30°.

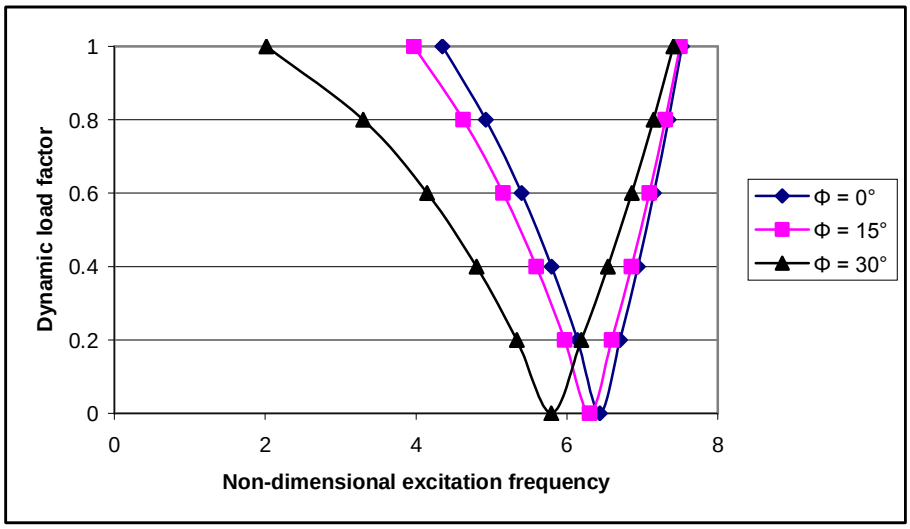

Figure 4.2: Variation of instability region with angle of twist of the isotropic cantilever panel, a/b =1, $\phi = 0°, 15°$ and $30°$, $\alpha = 0.2$.

The dynamic instability regions are plotted for an isotropic twisted panel with varying static load factor $\alpha = 0.0$, $\alpha = 0.2$, $\alpha = 0.4$ and $\alpha = 0.6$ for an angle of twist $\phi = 15°$ and are shown in Figure 4.3. The instability occurs earlier for higher static load factor and the width of instability zones decreases with the decrease in the static load factor. For all further studies, the angle of twist is taken as 15° and the static load factor α is taken as 0.2 (unless otherwise stated).

The effect of change in the R_y/b ratio of a twisted isotropic cylindrical panel is shown in Figure 4.4. As the R_y/b ratio increases, the instability occurs at

an earlier frequency and the width of the instability region decreases as the R_y/b ratio decreases.

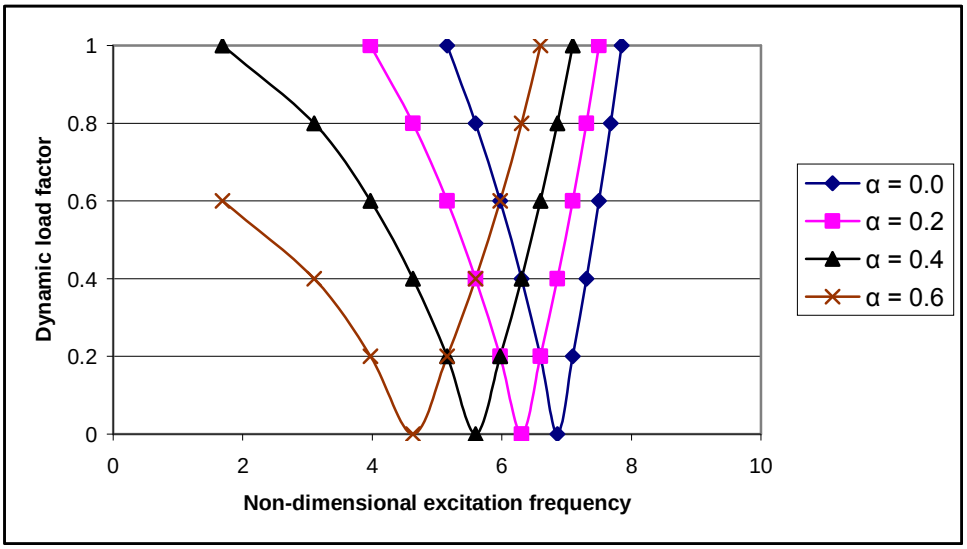

Figure 4.3: Variation of instability region with static load factor for a square isotropic twisted cantilever panel, a/b =1, ϕ =15°, α = 0.0, 0.2, 0.4 and α = 0.6.

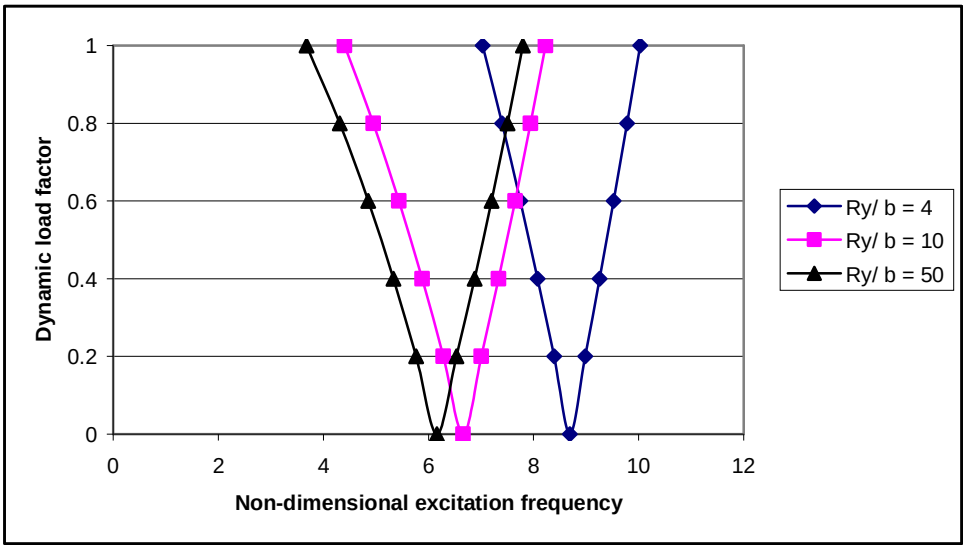

Figure 4.4: Variation of instability region with R_y/b ratio for a square isotropic cylindrical twisted cantilever panel, a/b =1, ϕ = 15°, α = 0.2

The effect of changing the thickness of a square isotropic twisted cantilever plate is studied in Figure 4.5. As the b/h ratio increases, the instability occurs earlier and the width of the instability region increases.

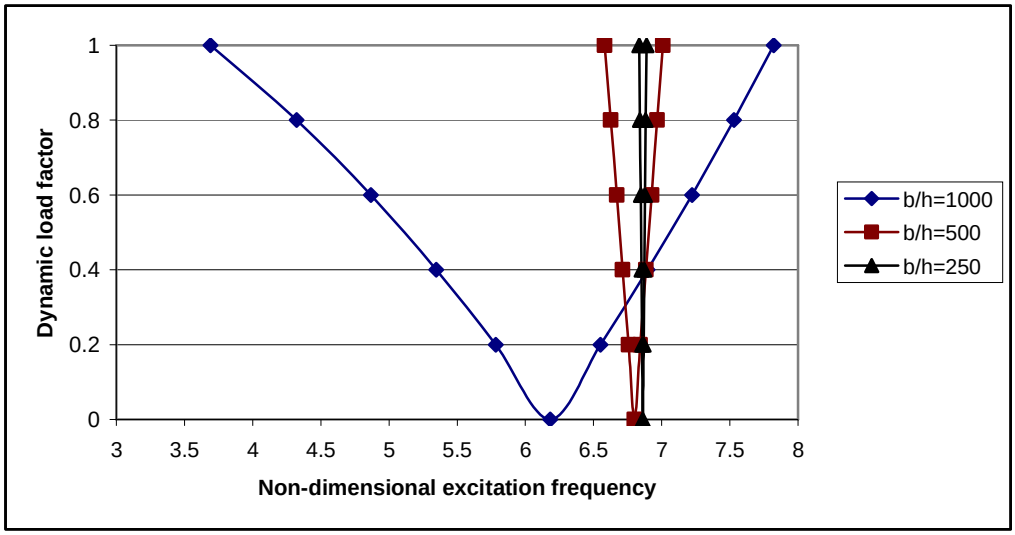

Figure 4.5: Variation of instability region with b/h ratio for a square isotropic twisted cantilever plate, a/b =1, ϕ =15°, α = 0.2

The studies are then extended to the study of the effect of curvature on the dynamic instability regions of different curved panels. The dynamic instability regions of different isotropic twisted curved panels, i.e., cylindrical ($b/R_y = 0.25$), spherical ($b/R_x = 0.25$, $b/R_y = 0.25$) and hyperbolic paraboloidal ($b/R_x = -0.25$, $b/R_y = 0.25$), for a particular angle of twist (ϕ =15°) are compared. As observed from Figure 4.6, the onset of instability occurs earlier for the flat panel. The instability occurs at a later excitation frequency for cylindrical panels than the hyperbolic paraboloidal twisted panels and latest for the spherical twisted panels, though the spherical and cylindrical twisted panels show little difference of excitation frequencies for instability. The width of the instability region is marginally smaller for the cylindrical panel than the hyperbolic paraboloidal twisted panel.

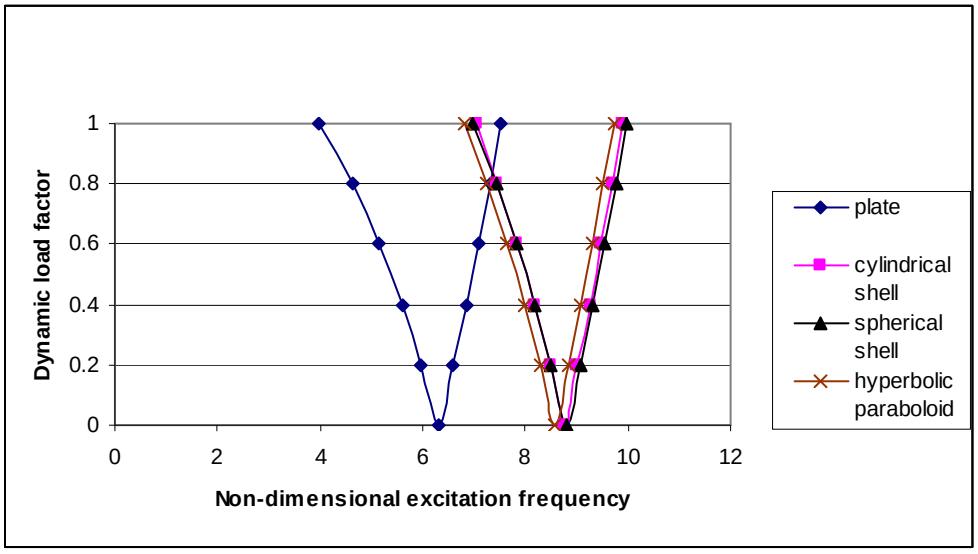

Figure 4.6: Variation of instability region with curvature for a square isotropic twisted cantilever panel, a/b =1, ϕ =15°, α = 0.2, b/R_y = 0.25

4.6: Cross ply twisted cantilever panels

The parametric study is then extended to laminated composite cross-ply twisted cantilever panels. The study is carried out extensively for vibration, buckling and parametric resonance characteristics of symmetric and anti-symmetric cross-ply lay-ups.

The geometrical and material properties of the twisted panels (unless otherwise stated) are

a = b = 500mm, h = 2mm, ρ = 1580 kg/ m^3

E_{11} = 141.0GPa, E_{22} = 9.23GPa, ν_{12} = 0.313, G_{12} = 5.95GPa, G_{23} = 2.96GPa.

4.6.1: Non-dimensionalization of parameters

Non-dimensional frequency $\varpi = \omega a^2 \sqrt{\frac{\rho}{E_{11} h^2}}$

Non-dimensional buckling load $\lambda = \frac{N_x b^2}{E_{22} h^3}$

Non-dimensional excitation frequency $\Omega = \overline{\Omega} a^2 \sqrt{(\rho / E_{22} h^2)}$ in line with many previous investigations, where $\overline{\Omega}$ is the excitation frequency in radians/second.

4.6.2: Boundary conditions

The clamped (C) boundary condition of the laminated composite twisted cross-ply panel using the first order shear deformation theory is:

$u = v = w = \theta_x = \theta_y = 0$ at the left edge.

4.6.3: Vibration and buckling studies

The non-dimensional fundamental frequencies of vibration of twisted cantilever plates for different cross-ply stacking sequences and for varying angles of twist are shown in Table 4.16. The laminate material properties are as mentioned earlier. Two, four and eight layer antisymmetric lay-ups as well as a four layer symmetric cross-ply lay-up were taken for the study. It is found that as the angle of twist increases for a particular cross-ply orientation, the frequency parameter decreases. This is true for both the symmetric as well as antisymmetric cross-ply stacking sequences. For both the symmetric as well as the antisymmetric lay-ups, there is roughly a 0.6% decrease in the non-dimensional frequency when an angle of twist of 10° is introduced to the plate while for an angle of twist of 30°; the decrease is about 6%.

Table 4.16: Variation of non-dimensional frequency parameter with angle of twist for square cross-ply plates with different ply lay-ups

a/b = 1, b/h = 250

Angle of twist	**Non-dimensional frequency parameter**			
	0°/90°	**0°/90°/0°/90°**	**0°/90°/90°/0°**	**0°/90°/0°/90°/0°/ 90°/0°/90°**
0°	0.4829	0.6872	0.9565	0.7294
10°	0.4800	0.6831	0.9508	0.7251
20°	0.4708	0.6700	0.9326	0.7112
30°	0.4540	0.6461	0.8993	0.6858

The first five non-dimensional frequency parameters for various cross-ply twisted cantilever plates are shown in Table 4.17. It is observed that the first frequency parameter decreases with increase in the angle of twist for all cross-ply stacking sequences. The second frequency parameter of twisted plate first increases and then decreases with the increase in the angle of twist. The third frequency parameter increases as the angle of twist increases except for the unsymmetrical cross-ply lay-ups which first increase and then decrease with increasing twist angle. This is also noticed for the three layer (90°/0°/90°) cross-ply. The fifth frequency parameter increases with increasing twist angle for all ply orientations.

Table 4.18 shows the first five frequency parameters for cross-ply cantilever twisted plates having different stacking sequences and different angles of twist. Here E-glass/epoxy composite is used and the laminates have a square plan form and a thickness ratio b/h = 100. As observed earlier, the first frequency of vibration decreases with increase of angle of twist. The third and fourth frequency parameters increase with increase in the angle of twist. However second frequency increases and then decreases with increase of angle of twist. The fifth frequency parameter increases with angle of twist, except for the antisymmetric lay-ups which increase and then decrease with the increasing twist angle. So there is some slight difference in the behaviour of the twisted plates on changing the material of the cross-ply lamina.

Table 4.19 shows the non-dimensional fundamental frequencies for various twisted cross-ply cylindrical and spherical shells of square plan form and increasing R/a (radius of curvature to length ratio) ratios. The angle of twist for all the shells is 15°. As the R/a ratio increases, the non-dimensional frequency parameter decreases. Also for a particular cross-ply orientation and low R/a ratio, the spherical shell shows slightly higher frequency parameter than the cylindrical shell. For higher R/a ratios there is very little difference in the non-dimensional frequencies of the spherical and cylindrical twisted shells for all cross-ply lay-ups.

Table 4.17: Non-dimensional free vibration frequencies of square cross-ply pretwisted cantilever plates with varying angles of twist

a/b = 1, h = 2mm

E_{11}=141.0GPa, E_{22} = 9.23GPa, υ_{12} = 0.313, G_{12} =5.95GPa, G_{23} = 2.96GPa

Angle of twist	**[0°/90°]**				
0°	0.4829	0.9402	3.0241	3.4614	3.7570
10°	0.4800	2.9935	7.7311	8.1922	8.4474
15°	0.4762	2.9535	8.3970	10.2132	11.2391
20°	0.4708	2.8982	8.3362	12.5956	13.9412
30°	0.4540	2.7455	8.1648	16.3130	17.5352
[0°/90°/0°]					
0°	1.0000	1.3081	2.8074	6.1770	6.2633
10°	0.9940	6.1958	7.4734	8.2290	11.5005
15°	0.9862	6.1131	9.9849	10.9231	15.7281
20°	0.9750	5.9984	12.4158	13.2571	17.2459
30°	0.9401	5.6811	16.8197	17.0853	17.9465
[90°/0°/90°]					
0°	0.3218	0.8382	2.0159	3.0164	5.6458
10°	0.3199	1.9953	5.6280	8.0581	9.3633
15°	0.3174	1.9690	5.5996	11.0498	11.4226
20°	0.3138	1.9323	5.5596	11.0079	14.3207
30°	0.3026	1.8307	5.4461	10.8894	18.2308
[0°/90°/0°/90°]					
0°	0.6872	1.0823	4.3018	4.7064	4.8675
10°	0.6831	4.2600	8.4202	8.9211	12.0089
15°	0.6778	4.2030	11.4073	11.9184	12.1588
20°	0.6700	4.1242	11.8568	13.9922	15.3056
30°	0.6461	3.9066	11.6123	19.2600	21.0679
[0°/90°/90°/0°]					
0°	0.9565	1.2777	3.3529	5.9918	6.3935
10°	0.9508	5.9270	7.6768	8.1607	12.0176
15°	0.9434	5.8477	10.0824	11.0935	16.2837
20°	0.9326	5.7378	12.4310	13.6267	16.4988
30°	0.8993	5.4342	16.1177	17.2414	18.2266
[0°/90°/0°/90°/0°/90°/0°/90°]					
0°	0.7294	1.1126	4.5655	4.9675	5.1053
10°	0.7251	4.5213	8.5146	9.0772	12.3580
15°	0.7194	4.4608	11.6137	12.2693	12.6963
20°	0.7112	4.3772	12.5822	14.2609	15.5157
30°	0.6858	4.1461	12.3230	19.5770	21.4796

Table 4.18: Non-dimensional free vibration frequencies of square cross-ply pretwisted cantilever plates with varying angles of twist (E-glass/epoxy)

a/b =1, b/h =100

E_{11}= 60.7GPa, E_{22} = 24.8GPa, υ_{12} = 0.23, G_{12} =12.0GPa

Angle of twist	[0°/90°]				
0°	0.7994	1.8673	4.9832	6.0764	6.8999
10°	0.7947	4.9459	5.3633	7.2392	10.1804
15°	0.7886	4.8849	7.5704	8.4886	12.8143
20°	0.7797	4.7956	9.6007	10.0053	13.7988
30°	0.7519	4.5438	13.0458	13.2241	13.8841
[0°/90°/0°]					
0°	1.0121	2.0015	5.4375	6.3691	7.9164
10°	1.0061	5.5399	6.2431	6.9268	10.7851
15°	0.9984	6.1821	7.7136	8.3482	13.0373
20°	0.9870	6.0698	9.6240	10.0230	15.0884
30°	0.9519	5.7501	12.8271	13.7178	17.1255
[90°/0°/90°]					
0°	0.6708	1.7881	4.1913	6.3482	7.2012
10°	0.6669	4.1521	5.1535	8.0837	9.8510
15°	0.6618	4.1001	7.3638	9.0795	11.6868
20°	0.6543	4.0259	9.5159	10.3288	11.6329
30°	0.6311	3.8159	11.3022	13.4669	13.6380
[0°/90°/0°/90°]					
0°	0.8444	1.8979	5.2613	6.3398	7.1203
10°	0.8394	5.2237	5.3851	7.4614	10.3318
15°	0.8329	5.1597	7.6215	8.6810	12.9836
20°	0.8235	5.0656	9.7106	10.1727	14.5766
30°	0.7942	4.7996	13.3078	13.5725	14.4437
[0°/90°/90°/0°]					
0°	0.9849	1.9853	5.6071	6.2184	7.7868
10°	0.9791	5.3968	6.0801	6.9415	10.7658
15°	0.9715	6.0160	7.5521	8.2328	13.1938
20°	0.9605	5.9068	9.4853	9.7821	15.3724
30°	0.9262	5.5956	12.6907	13.3041	16.6668
[0°/90°/0°/90°/0°/90°/0°/90°]					
0°	0.8552	1.9052	5.3285	6.4039	7.1740
10°	0.8502	5.2909	5.3900	7.5157	10.3690
15°	0.8436	5.2261	7.6328	8.7283	13.0232
20°	0.8341	5.1308	9.7350	10.2140	14.7654
30°	0.8044	4.8614	13.3682	13.6317	14.6043

Table 4.19: Variation of non-dimensional frequency parameter with R/a ratio for square cross-ply cylindrical and spherical twisted cantilever shells

a/b =1, Φ = 15°, h =2mm

E_{11}= 141.0GPa, E_{22} = 9.23GPa, υ_{12} = 0.313, G_{12} =5.95GPa, G_{23} = 2.96GPa

R/a	0°/90°		$0^o/90^o/0°/90°$		$0^o/90^o/90^o/0^o$		$0^o/90^o/0^o/90^o$ $/0^o/90^o/0^o/90^o$	
	C	S	C	S	C	S	C	S
5	0.6001	0.6150	0.8218	0.8343	1.1067	1.1165	0.8675	0.8796
10	0.5162	0.5172	0.7238	0.7248	0.9948	0.9959	0.7665	0.7676
20	0.4873	0.4874	0.6904	0.6905	0.9572	0.9573	0.7323	0.7324
50	0.4780	0.4780	0.6798	0.6798	0.9456	0.9456	0.7215	0.7215
100	0.4766	0.4766	0.6782	0.6783	0.9440	0.9439	0.7199	0.7199

C – cylindrical, S - spherical

The first five frequency parameters are obtained for various twisted cross-ply plates and spherical shells with curvature (b/R_y) ratio = 0.25 and having different ply orientations and are presented in Table 4.20. It is seen that the first frequency is more for the spherical shell as compared to the plate for all the cross-ply orientations suggesting an increase in stiffness with introduction of curvature. For example, for the two layer antisymmetric cross-ply lay-up, the non-dimensional frequency parameter of the spherical shell is 43.9% more than the twisted plate, whereas for the four layer symmetric cross-ply panel it is 25.4% more than the twisted plate. The symmetric cross-ply stacking sequences seem to be stiffer than the anti-symmetric lay-ups as their frequency parameters are more.

Table 4.20: Comparison of non-dimensional frequency parameter of square cross-ply twisted plates and square cross-ply twisted spherical shells($b/R_y = 0.25$)

a/b =1, h = 2mm, $\Phi = 15°$

E_{11}= 141.0GPa, E_{22} = 9.23GPa, υ_{12} = 0.313, G_{12} =5.95GPa, G_{23} = 2.96GPa

R_y/R_x	b/R_y	**Ply lay-up**				
[0°/90°]						
1	plate	0.4762	2.9535	8.3970	10.2132	11.2391
	0.25	0.6855	2.7364	4.2186	6.6554	9.0469
[0°/90°/0°]						
1	plate	0.9862	6.1131	9.9849	10.9231	15.7281
	0.25	1.2256	2.8839	6.6393	8.0653	11.5233
[90°/0°/90°]						
1	plate	0.3174	1.9690	5.5996	11.0498	11.4226
	0.25	0.5376	2.6395	4.9535	6.3930	10.0631
[0°/90°/0°/90°]						
1	plate	0.6778	4.2030	11.4073	11.9184	12.1588
	0.25	0.9058	3.4671	5.5555	8.1916	11.3568
[0°/90°/90°/0°]						
1	plate	0.9434	5.8477	10.0824	11.0935	16.2837
	0.25	1.1835	3.1394	6.6128	8.2571	11.9698
[0°/90°/0°/90°/0°/90°/0°/90°/0°/90°]						
1	plate	0.7194	4.4608	11.6137	12.2693	12.6963
	0.25	0.9515	3.6143	5.8265	8.4974	11.7952

Table 4.21 shows the variation of non-dimensional frequency parameter with the variation of aspect ratio (a / b). As the aspect ratio increases, the non-dimensional frequency parameter first slightly increases and then decreases gradually for all the stacking sequences except in the two-layer stacking sequence

which decreases with increase in the aspect ratio. The non-dimensional frequency is higher in the symmetric cross-ply compared to the antisymmetric lay-ups.

Table 4.21: Variation of non-dimensional frequency parameter with aspect ratio for cross-ply twisted cantilever plates with different ply lay-ups

$\Phi = 15°$, b/h = 250

E_{11} = 141.0GPa, E_{22} = 9.23GPa, ν_{12} = 0.313, G_{12} = 5.95GPa, G_{23} = 2.96GPa.

a/b	0°/90°	0°/90°/0°/90°	0°/90°/90°/0°	0°/90°/0°/90°/ 0°/90°/0°/90°
0.5	0.4763	0.6777	0.9432	0.7193
1	0.4762	0.6778	0.9434	0.7194
2	0.4761	0.6777	0.9433	0.7193
3	0.4761	0.6776	0.9431	0.7193

Table 4.22: Variation of frequency in Hz with b/h ratio for square cross-ply twisted cantilever plates with different ply lay-ups

a = b = 500mm, $\Phi = 15°$

E_{11} = 141.0GPa, E_{22}= 9.23GPa, ν_{12} = 0.313, G_{12} =5.95GPa, G_{23} = 2.96GPa.

b/h	0°/90°	0°/90°/0°/90°	0°/90°/90°/0°	0°/90°/0°/90°/ 0°/90°/0°/90°
25	57.0919	81.0384	112.2152	85.9569
50	28.6166	40.7011	56.5779	43.1930
100	14.3176	20.3741	28.3497	21.6242
200	7.1601	10.1903	14.1829	10.8159
250	5.7282	8.1526	11.3472	8.6532
300	4.8690	6.9300	9.6455	7.3554

The variation of the frequencies in hertz for different cross-ply stacking sequences with increasing width to thickness ratio (b/h ratio) is shown in Table

4.22. It is seen that as the thickness of the plate decreases the frequency in hertz is decreasing due to decrease of stiffness. This is seen to be true for both symmetric and antisymmetric cross-ply stacking sequences.

The effect of curvature on the non-dimensional frequency parameter is next studied. The width to radius of curvature ratio (b/R_y) is taken as 0.25. Cylindrical, spherical and hyperbolic paraboloid twisted shells are analyzed and results compared with those of the twisted plate for various cross-ply stacking sequences. The angle of twist in all cases is taken as 15°. The results are tabulated in Table 4.23. The introduction of curvature increases the non-dimensional frequency parameter as compared with that of the twisted plate. This suggests an increase in the stiffness with introduction of curvature. Spherical twisted shells show the highest frequency parameters for a particular stacking sequence. For example, for the two layer antisymmetric ply lay-up, the non-dimensional frequency is 44% more than the twisted plate, followed by the cylindrical twisted panels (36.7% more than the twisted plate) and hyperbolic paraboloidal twisted panels (30.9% more than the twisted plate).

Table 4.23: Variation of non-dimensional frequency parameter with geometry for cross-ply twisted cantilever plates with different ply lay-ups

a/ b = 1, h = 2 mm, b/R_y = 0.25

E_{11}= 141.0GPa, E_{22} = 9.23GPa, υ_{12}= 0.313, G_{12} = 5.95GPa, G_{23} = 2.96GPa

No.of Layers	Plate	Cylindrical shell	Spherical shell	Hyperbolic Paraboloid shell
0°/90°	0.4762	0.6510	0.6856	0.6234
0°/90°/90°/0°	0.9434	1.1688	1.1835	1.1406
0°/90°/0°/90°	0.6778	0.8791	0.9058	0.8507
0°/90°/0°/90°/0°/ 90°/0°/90°	0.7194	0.9262	0.9515	0.8976

Table 4.24 shows the variation of the non-dimensional frequency parameter with the degree of orthotropy of the twisted cross-ply square plate with various laminate stacking sequences. The angle of twist is assumed as 15°. It is seen that as the degree of orthotropy increases, the non-dimensional frequency parameter decreases.

Table 4.24: Variation of non-dimensional frequency parameter with degree of orthotropy of different square cross-ply twisted cantilever plates

a/b = 1, h = 2mm

υ_{12} = 0.313, G_{12} = 5.95GPa, G_{23} = 2.96GPa

E_1/E_2	0°/90°	0°/90°/0°/90°	0°/90°/90°/0°	0°/90°/0°/90°/0°/90°/0°/90°
10	0.5258	0.6973	0.9473	0.7340
25	0.4343	0.6629	0.9407	0.7086
40	0.4067	0.6537	0.9391	0.7020

The studies are then extended to the buckling study of cross-ply laminated cantilever twisted panels. The buckling loads are computed for square laminated cross-ply twisted cantilever plates for different angles of twist and different ply orientations as shown in Table 4.25. One symmetric and three antisymmetric cross-ply lay-ups were chosen. It is seen that as the angle of twist increases, the non-dimensional buckling load decreases. The untwisted plate has the highest non-dimensional buckling load for all stacking sequences. The introduction of twist to an untwisted plate is hence seen to give lesser non-dimensional buckling load values. An angle of twist of 10° introduced to the cross-ply panel decreases the buckling load by about 2.2% in all cases. The non-dimensional buckling load at 30° angle of twist is around 20% lesser than that of the untwisted plate. Also, comparing the antisymmetric lay-ups, for a particular angle of twist, the non-dimensional buckling load increases as the number of layers increases.

Table 4.25: Variation of non-dimensional buckling load with angle of twist for square cross-ply plates with different ply lay-ups

a/b =1, b/h = 250

E_{11}= 141.0GPa, E_{22} = 9.23GPa, υ_{12}= 0.313, G_{12} = 5.95GPa, G_{23} = 2.96Gpa

Angle of twist	**Non-dimensional buckling load**			
	0°/90°	**0°/90°/0°/90°**	**0°/90°/90°/0°**	**0°/90°/0°/90°/ 0°/90°/0°/90°**
0°	0.7106	1.4432	2.7891	1.6254
10°	0.6949	1.4078	2.7273	1.5860
20°	0.6473	1.3114	2.5405	1.4774
30°	0.5689	1.1526	2.2329	1.2985

The buckling load for different laminations of a square cylindrical and spherical shell with angle of twist of 15° is presented in Table 4.26. The buckling load is found to decrease with increase of R/a ratio for all the cross-ply lay-ups for both cylindrical and spherical shells. The symmetric arrangement of the plies shows the greatest non-dimensional buckling load for a particular R/a ratio. For R/a values up to 10, the spherical twisted shell shows greater buckling load than the cylindrical twisted shell, but at higher R/a values, the trend is reversed. Comparing only the antisymmetric cross-ply panels, the buckling load is seen to increase as the number of layers increases for the same R/a ratio.

Table 4.26: Variation of non-dimensional buckling load with R/a ratio for square cylindrical and spherical twisted cross-ply shells

a/b =1, Φ = 15°, h = 2mm

E_{11}= 141.0GPa, E_{22} = 9.23GPa, υ_{12} = 0.313, G_{12} =5.95GPa, G_{23} = 2.96Gpa

R/a	0°/90°		$0^o/90^o/0°/90°$		$0^o/90^o/90^o/0^o$		$0^o/90^o/0^o/90^o$ $/0^o/90^o/0^o/90^o$	
	C	S	C	S	C	S	C	S
5	0.9349	0.9710	1.7780	1.8170	3.2768	3.3189	1.9867	2.0258
10	0.7511	0.7523	1.4897	1.4909	2.8392	2.8400	1.6736	1.6748
20	0.6955	0.6954	1.4005	1.4003	2.7003	2.6997	1.5766	1.5763
50	0.6782	0.6781	1.3729	1.3728	2.6578	2.6576	1.5466	1.5465
100	0.6757	0.6757	1.3689	1.3689	2.6515	2.6515	1.5422	1.5421

C – cylindrical, S-spherical

The values of non-dimensional buckling loads are compared for square twisted plates and square twisted spherical shells with angle of twist of 15° and are shown in the Table 4.27. The spherical shell gives higher buckling load than the plate for all the ply lay-ups.

The variation of the non-dimensional buckling load with aspect ratio of the twisted square cantilever plate is shown in Table 4.28. The angle of twist is taken as 15°. As the aspect ratio increases, non-dimensional buckling load decreases. This is observed for all the ply orientations. The non-dimensional buckling load for the rectangular plate with a/b =3 is about 88% less than the square plate for the antisymmetric panels.

Table 4.27: Non-dimensional buckling load for square cross-ply twisted plates and spherical twisted shells (b/R_y = 0.25) with different ply lay-ups

a /b =1, Φ = 15°**,** h = 2mm

E_{11}= 141.0 GPa, E_{22} = 9.23GPa, υ_{12} = 0.313, G_{12} = 5.95GPa, G_{23} = 2.96GPa

R_y/R_x	b/R_y	Lay-up
1.0		**[0°/90°]**
	plate	0.6750
	0.25	1.1606
1.0		**[0°/90°/0°]**
	plate	2.8953
	0.25	3.9331
1.0		**[90°/0°/90°]**
	Plate	0.2999
	0.25	0.6972
1.0		**[0°/90°/0°/90°]**
	plate	1.3676
	0.25	2.0683
1.0		**[0°/90°/90°/0°]**
	plate	2.6494
	0.25	3.6377
1.0		**[0°/90°/0°/90°/0°/90°/0°/90°]**
	plate	1.5407
	0.25	2.2908

Table 4.28: Variation of non-dimensional buckling load with aspect ratio for cross-ply twisted cantilever plates with different ply lay-ups

b/h = 250, Φ = 15°

E_{11} = 141.0GPa, E_{22}= 9.23GPa, ν_{12} = 0.313, G_{12} =5.95GPa, G_{23} = 2.96GPa.

a/b	0°/90°	0°/90°/0°/90°	0°/90°/90°/0°	0°/90°/0°/90°/ 0°/90°/0°/90°
0.5	2.7010	5.4706	10.5967	6.1628
1	0.6750	1.3676	2.6494	1.5407
2	0.1687	0.3418	0.6621	0.3851
3	0.0750	0.1519	0.2941	0.1711

Table 4.29 shows the variation of buckling load with b / h ratio. The angle of twist is taken as 15°. As the thickness of the twisted plate decreases, the buckling load decreases for all the ply orientations.

Next, the variation of non-dimensional buckling load for different shell geometries is studied and is shown in Table 4.30. The b /R_y ratio is taken as 0.25 and angle of twist as 15°. It is observed that introduction of curvature in the plate increases the non-dimensional buckling load. For a particular stacking sequence, the spherical twisted panel shows the highest non-dimensional buckling load while the plate shows the least non-dimensional buckling load. This is observed for both the symmetric as well as antisymmetric lay-ups. For the two layer lay-up, the non-dimensional buckling load of the cylindrical twisted panel is 57.9% greater than that of the twisted plate, while the spherical twisted panel is 71.9% more and the hyperbolic paraboloidal twisted panel is 42.1% more than that of the twisted plate. Also for antisymmetric stacking sequences, the buckling load increases with increase in the number of layers.

Table 4.29: Variation of buckling load in N/m with b/h ratio for square cross-ply twisted cantilever plates with different ply lay-ups

a =0.5m. b = 0.5m, Φ =15°

E_{11} = 141.0GPa, E_{22} = 9.23GPa, ν_{12} = 0.313, G_{12} = 5.95GPa, G_{23} = 2.96GPa

b/h	0°/90°	0°/90°/0°/90°	0°/90°/90°/0°	0°/90°/0°/90°/0°/90°/0°/90°
25	198626.08	401251.03	772946.51	451723.41
50	24895.47	50400.31	97499.37	56770.53
100	3114.36	6308.38	12217.06	7106.66
200	389.40	788.89	1528.23	888.75
250	199.38	403.94	782.54	455.08
300	122.45	248.08	480.61	279.49

Table 4.30: Variation of non-dimensional buckling load with geometry for square cross-ply twisted cantilever panels with different ply lay- ups

a = b = 500mm, h = 2mm, b /R_y = 0.25, Φ = 15°

E_{11} = 141.0GPa, E_{22}= 9.23GPa, ν_{12} = 0.313, G_{12} = 5.95GPa, G_{23} = 2.96GPa

Lay-up	Plate	Cylindrical shell	Spherical shell	Hyperbolic paraboloid shell
[0°/90°]	0.6750	1.0664	1.1606	0.9590
[0°/90°/0°/90°]	1.3676	1.9733	2.0683	1.8100
[0°/90°/90°/0°]	2.6494	3.5434	3.6377	3.3054
[0°/90°/0°/90°/0°/90°/0°/90°]	1.5407	2.1968	2.2908	2.0202

The variation of the non-dimensional buckling load with the degree of orthotropy is studied next and is shown in Table 4.31. With the increasing E_1/ E_2

ratio, the non-dimensional buckling load is found to increase for all the cross-ply twisted plates. Angle of twist is taken as 15° for the twisted plates.

Table 4.31: Variation of non-dimensional buckling load with degree of orthotropy (E_1/E_2) for different square cross-ply twisted cantilever plates

a /b = 1, b/h = 250, Φ =15°

E_{11} = 141.0GPa, E_{22}= 9.23GPa, ν_{12} = 0.313, G_{12} =5.95GPa, G_{23} = 2.96GPa

E_1/E_2	0°/90°	0°/90°/0°/90°	0°/90°/90°/0°	0°/90°/0°/90°/ 0°/90°/0°/90°
10	0.5384	0.9474	1.7486	1.0497
15	0.6682	1.3459	2.6030	1.5153
25	0.9190	1.7435	4.3116	2.4461
40	1.2890	3.3315	6.8744	3.8421

4.6.4: Dynamic stability studies

The parametric instability studies are carried out for uniaxially loaded laminated composite cross-ply pretwisted panels with static component of load to consider the effect of various parameters.

The non-dimensional excitation frequency $\Omega = \overline{\Omega} a^2 \sqrt{(\rho / E_{22} h^2)}$ is used throughout the dynamic instability studies, where $\overline{\Omega}$ is the excitation frequency in radians/second.

Numerical results are presented for symmetric as well as anti-symmetric cross-ply laminated pretwisted cantilever panels with different combinations of lamination parameters and geometry including angle of twist, b/h ratio, aspect ratio and curvature.

The variation of the instability regions of twisted cross-ply cantilever plates/panels for different ply orientations and for varying angles of twist are

studied. The dynamic instability regions are plotted for cross-ply four layer [0°/90°/90°/0°] twisted plate with varying angle of twist i.e. ϕ = 0°, ϕ =15° and ϕ = 30°. The static load factor is taken as 0.2. As shown in Figure 4.7, the onset of instability occurs earlier with introduction of twist (ϕ =10°) in the untwisted panel (ϕ = 0°). With increase of twist angle from ϕ =10° to ϕ = 30°, the onset of instability occurs earlier for this lamination sequence and ply orientation. As can be observed from the figure, the widths of the instability region also decrease slightly as the angle of twist decreases.

Similar behaviour is observed in studies of antisymmetric cross-ply two layer [0°/90°] and 8 layer [0°/90°/0°/90°/0°/90°/0°/90°] twisted plates.

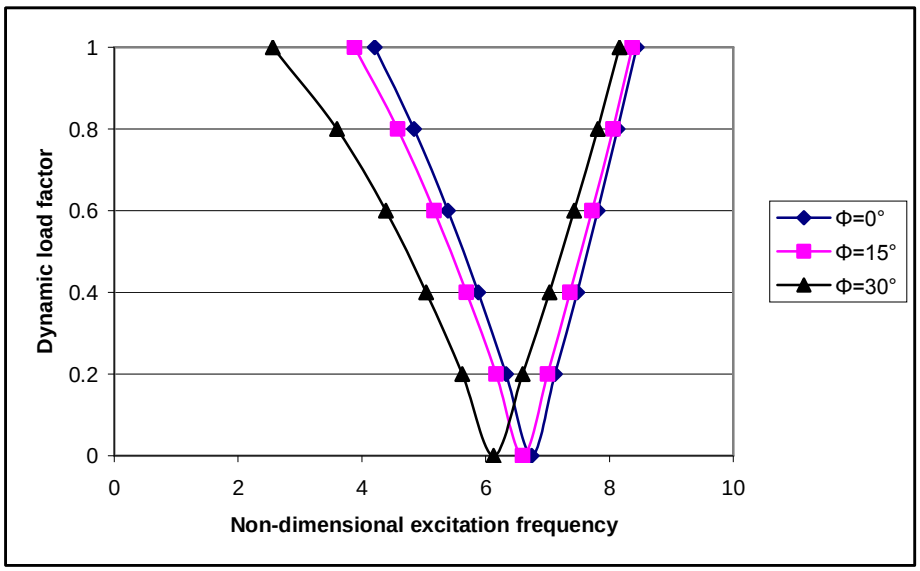

Figure 4.7: Variation of instability region with angle of twist of the four-layer cross-ply twisted plate [0°/90°/90°/0°], a/b =1, ϕ = 0°, 15°and 30°, α = 0.2.

To study the effect of number of layers on the dynamic instability regions, two layer [0°/90°], four layer [0°/90°/0°/90°] and eight layer [0°/90°/0°/90°/0°/90°/0°/90°] cross-ply twisted panels with angle of twist taken as 15° were studied. The static load factor is taken as 0.2. As observed from Figure 4.8, the two layer panel reaches dynamic instability earliest and the eight layer cross-ply reaches dynamic instability latest. The width of the instability region is

different with two layer lay-up showing most width and the eight layer cross-ply twisted plate showing the least width.

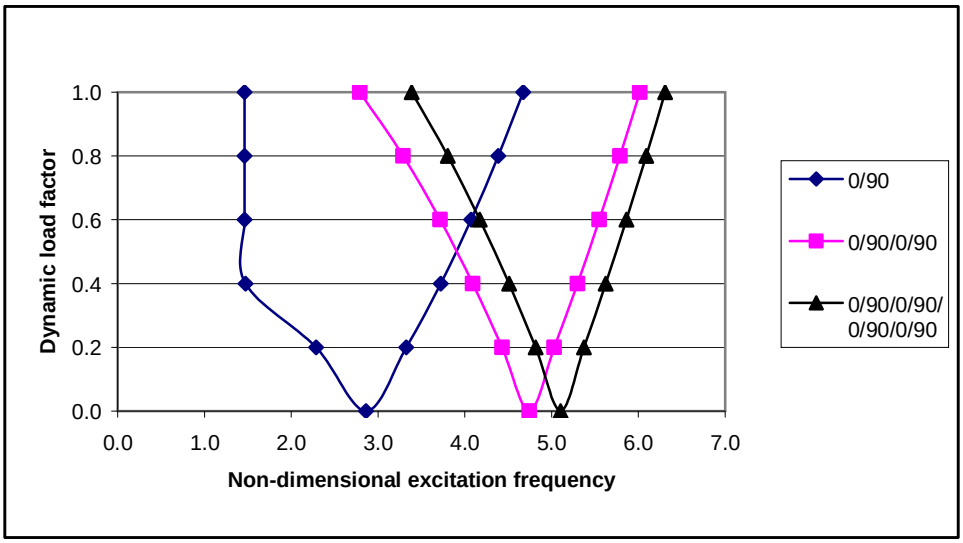

Figure 4.8: Variation of instability regions with number of layers of the cross-ply twisted plate (2, 4, and 8 layers), a/b =1, ϕ =15°, α = 0.2.

Figure 4.9 shows the dynamic instability regions for cross-ply four layer [0°/90°/90°/0°] twisted plate with varying static load factor α = 0.0, α = 0.2, α = 0.4 and α = 0.6 for angle of twist ϕ =15°. The instability occurs earlier for higher static load factor and the width of instability zones decreases with decrease in static load factor. The same behaviour is observed for cross-ply 2 layer [0°/90°] and 8 layer [0°/90°/0°/90°/0°/90°/0°/90°] (Figure 4.10) twisted panel with angle of twist of 15°.

The dynamic instability regions have been plotted in Figure 4.11 for four layer symmetric cantilever cross-ply plates of aspect ratios a/b = 0.5, 1.0 and 1.5. The width of the dynamic instability region is less in a/b = 0.5, and it increases from a/b = 0.5 to 1.5. As shown in figure 4.11, the onset of instability occurs later for a/b = 1 than a/b = 1.5 but before a/b = 0.5 i.e. excitation frequency decreases with increase of aspect ratio. Similar behaviour is noticed in the two and eight layer antisymmetric cross-ply twisted plates.

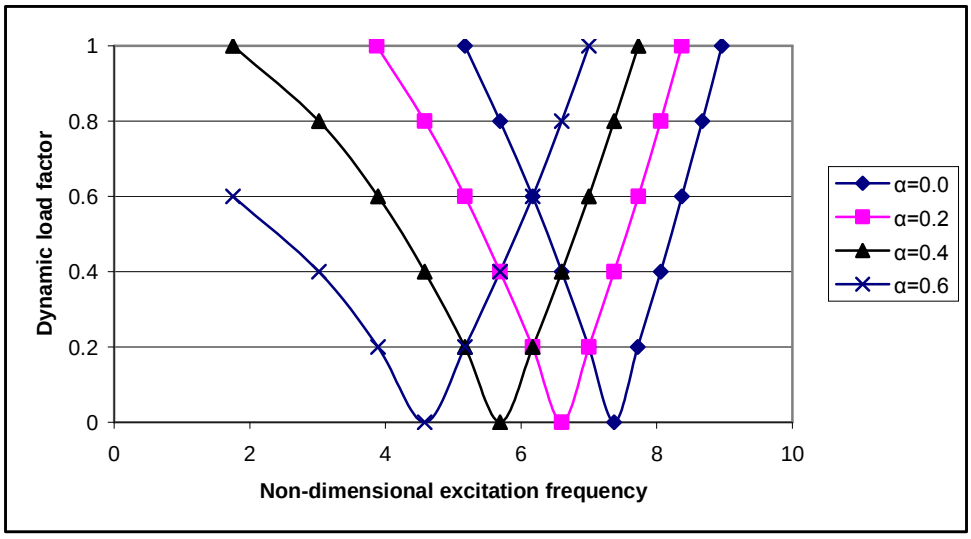

Figure 4.9: Variation of instability region with static load factor of a cross-ply twisted plate [0°/90°/90°/0°], a/b =1, ϕ =15°, α = 0.0, 0.2, 0.4 and α = 0.6.

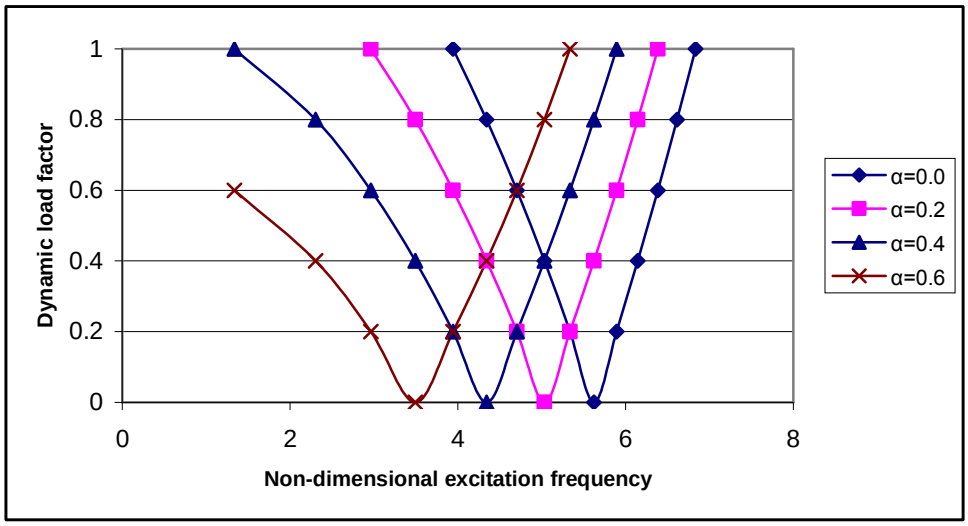

Figure 4.10: Variation of instability region with static load factor of a cross-ply twisted plate, [0°/90°/0°/90°/0°/90°/0°/90°], a/b =1, ϕ =15°, α = 0.0, 0.2, 0.4, 0.6.

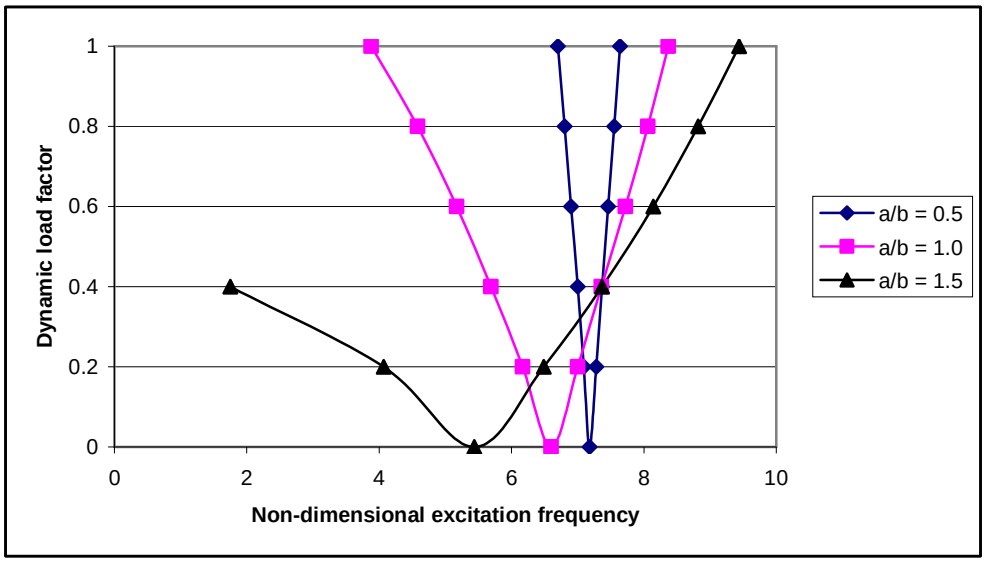

Figure 4.11: Variation of instability region with aspect ratio of the cross-ply twisted plate [0°/90°/90°/0°], ϕ =15°, α = 0.2, a/b = 0.5, 1.0 and 1.5

The effect of b/h ratio (width to thickness ratio) on the instability regions is now analysed for uniform loading with static component. Dynamic instability regions are studied for 2 layer [0°/90°], 4 layer [0°/90°/90°/0°] and 8 layer [0°/90°/0°/90°/0°/90°/0°/90°] twisted cross-ply plates. The plots for the four layer and eight layer cross-ply twisted plates are as shown in figures 4.12 and 4.13 respectively. The onset of instability occurs with a lesser excitation frequency for thin plates and occurs later as the thickness increases. The width of instability regions is also more for thinner plates than thicker plates, i.e., width of instability regions is more for b/h = 300.

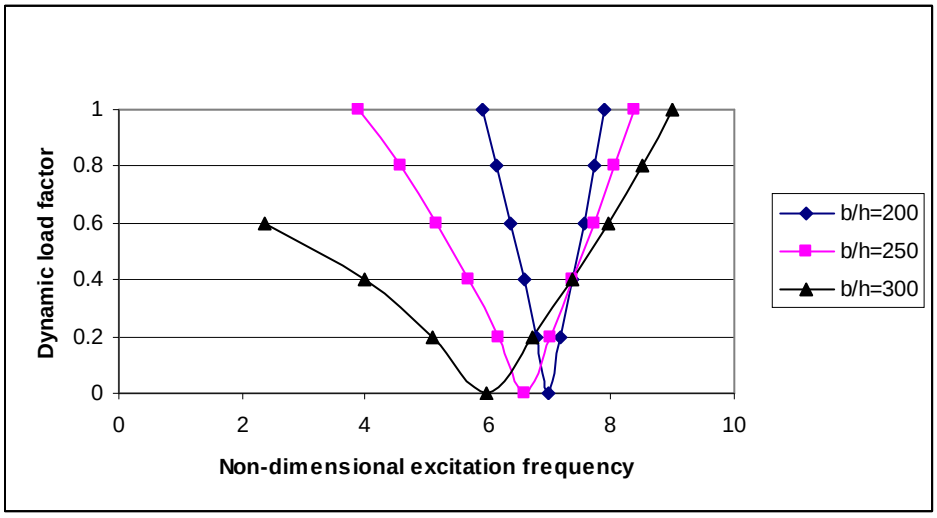

Figure 4.12: Variation of instability region with b/h ratio of the four layer cross-ply twisted plate [0°/90°/90°/0°], a/b =1, ϕ =15°, α = 0.2, b/h = 200, 250 and 300

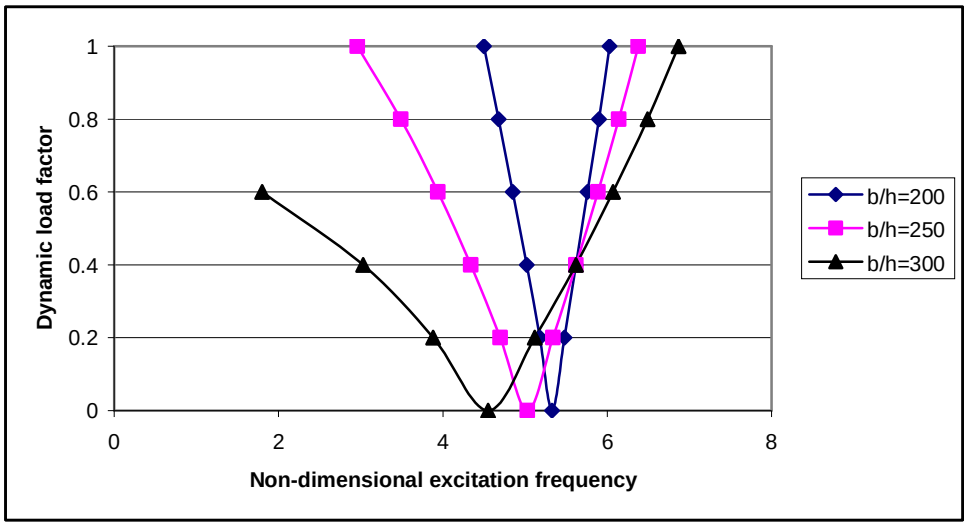

Figure 4.13: Variation of instability region with b/h ratio of the cross-ply twisted plate [0°/90°/0°/90°/0°/90°/0°/90°], a/b =1, ϕ =15°, α = 0.2, b/h = 200, 250 and 300

Dynamic instability regions are plotted for 2 layer [0°/90°], 4 layer [0°/90°/0°/90°] and 8 layer [0°/90°/0°/90°/0°/90°/0°/90°] twisted cross-ply cylindrical panels ($b/R_y = 0.25$), spherical panels ($b/R_x = 0.25$, $b/R_y = 0.25$) and hyperbolic paraboloid panels ($b/R_x = -0.25$, $b/R_y = 0.25$) , as shown in figures 4.14, 4.15 and 4.16 respectively. From these figures, it is seen that the onset of instability regions occurs later for eight layer anti-symmetric as compared to two

layer and the four layer antisymmetric twisted panel for all the three cases. The width of instability regions is higher for the two layer stacking sequence as compared to the four layer and eight layer ply orientations in all the three twisted cross-ply geometries (cylindrical, spherical and hyperbolic).

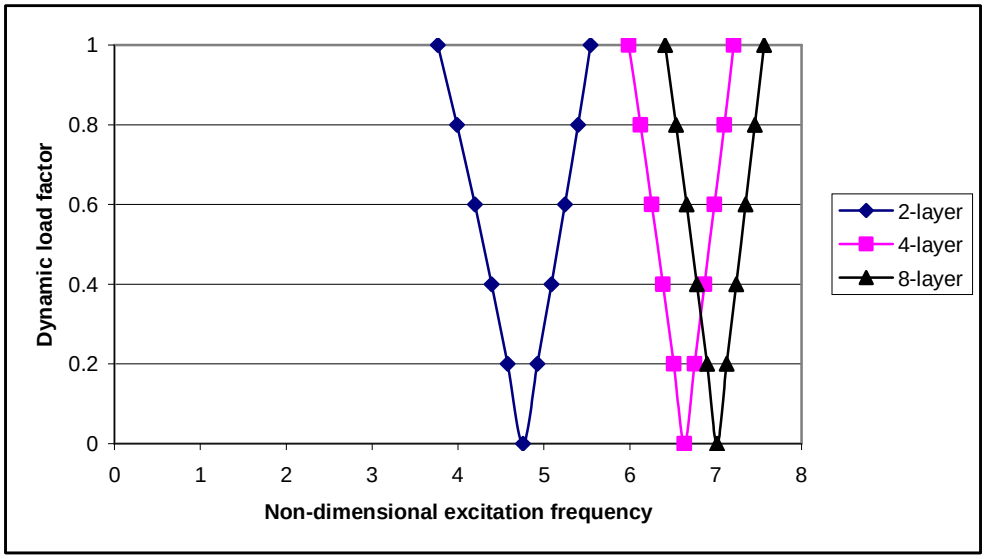

Figure 4.14: Variation of instability regions with number of layers of the cross-ply twisted cylindrical panel, a/b =1, ϕ =15 °, α = 0.2 and b/R_y = 0.25

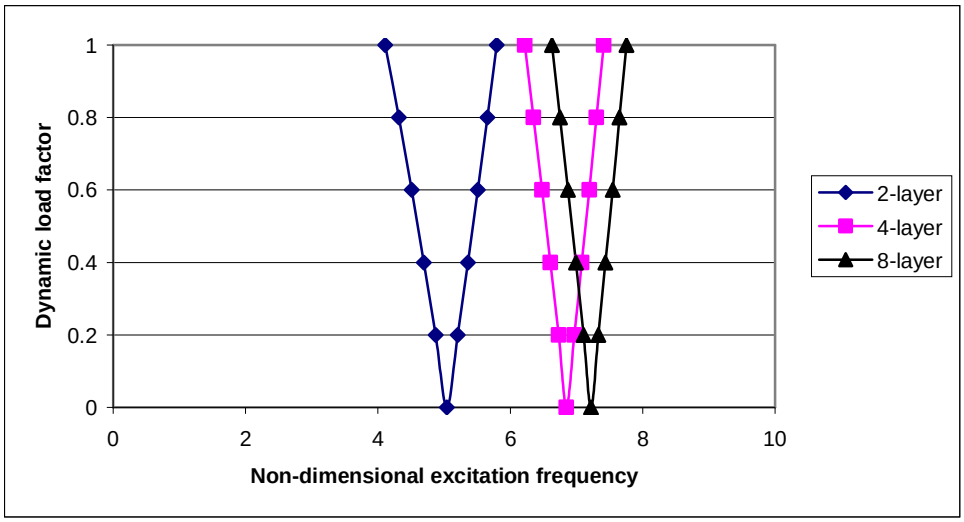

Figure 4.15: Variation of instability region with number of layers of the cross-ply twisted spherical panel, a/b =1, ϕ =15°, α = 0.2 and b/R_y = 0.25, b/R_x = 0.25

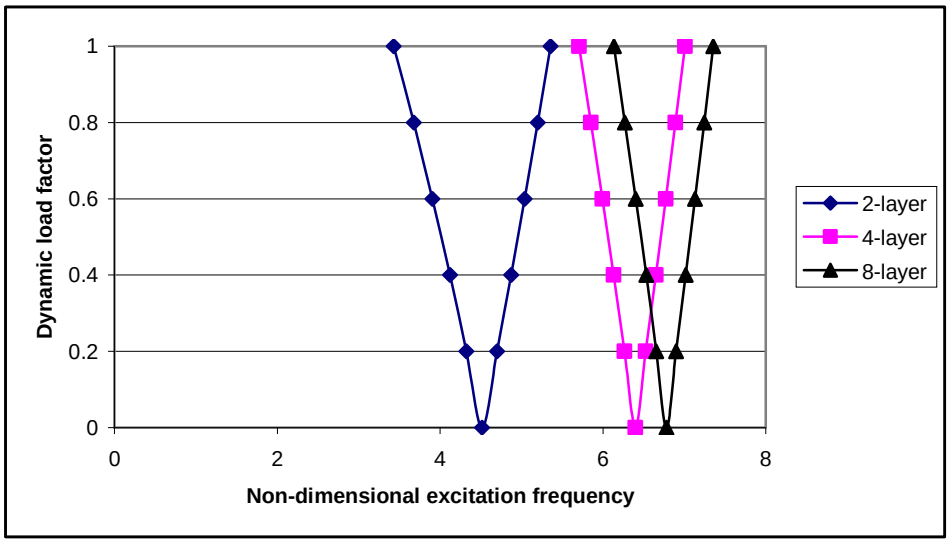

Figure 4.16: Variation of instability regions with number of layers of the cross-ply twisted hyperbolic panel, a/b =1, ϕ =15°, α = 0.2 and b/R_y = 0.25, b/R_x = −0.25

The studies are then extended to investigate the effect of geometry. The dynamic instability regions of composite two layer (0°/90°) and four layer (0°/90°/90°/0°) cross-ply cantilever twisted panels with different geometries, i.e. cylindrical (b/R_y = 0.25), spherical (b/R_x = 0.25, b/R_y = 0.25) and hyperbolic paraboloidal (b/R_x = −0.25, b/R_y = 0.25), for a particular twist (ϕ =15°) are compared. As observed from figures 4.17 and 4.18, the onset of instability occurs later for cylindrical panels than the hyperbolic paraboloidal curved panels. The width of instability regions is smaller for cylindrical panels than hyperbolic twisted panels. However, the spherical twisted panels show slightly later onset of dynamic instability as compared to these two. The onset of instability of laminated composite twisted cylindrical panels occurs earlier than twisted spherical panels but later than twisted hyperbolic panels. Similar behaviour is noticed in the four layer symmetric and eight layer antisymmetric cross-ply twisted panels. The four layer lay-up shows much larger excitation frequencies

than the two or eight layer antisymmetric twisted cross-ply panels for a particular shell geometry. The earliest instability frequency is shown by plates in all cases.

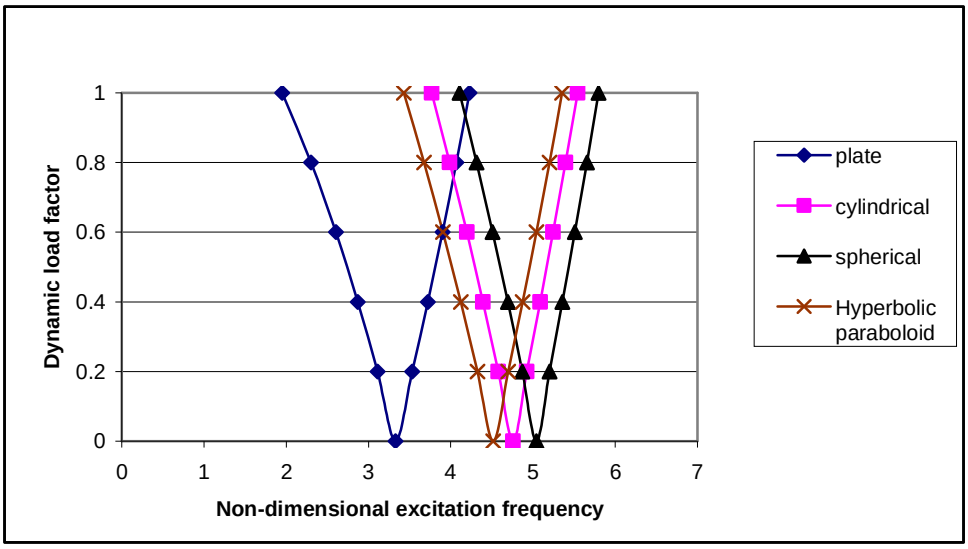

Figure 4.17: Variation of instability region with curvature for a cross-ply twisted cantilever panel [0°/90°], a/b =1, ϕ =15°, α = 0.2, b/R_y = 0.25

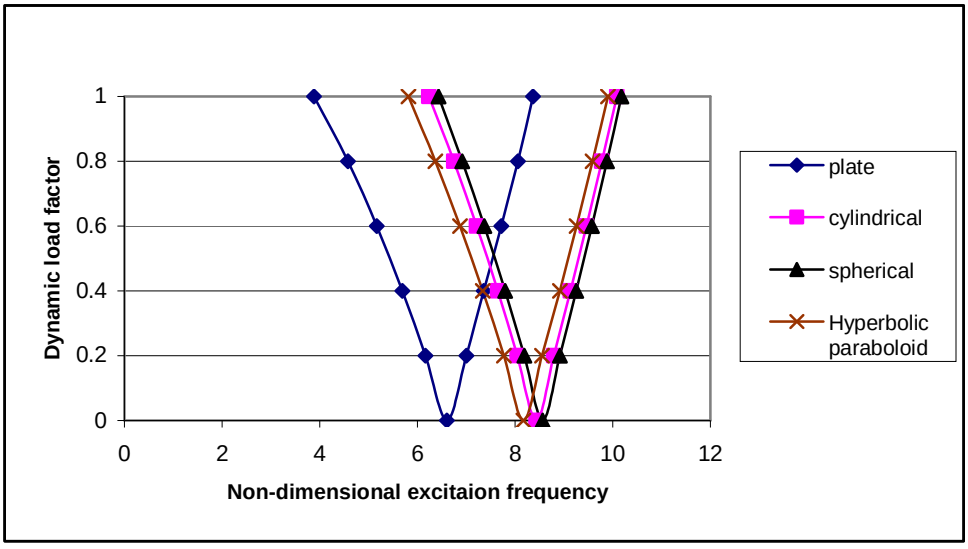

Figure 4.18: Variation of instability region with curvature for a cross-ply twisted cantilever panel [0°/90°/90°/0°], a/b =1, ϕ =15°, α = 0.2, b/R_y = 0.25

The variation of dynamic instability region of twisted cantilever plates for different matrix fiber combinations of the laminates is next studied. Dynamic

instability regions are plotted for the four layer cross-ply [0°/90°/90°/0°] plate as shown in Figure 4.19. The onset of instability occurs earlier for lesser E_1/E_2 ratio. The width of the instability region is more or less the same. The same behaviour is observed for the antisymmetric cross-ply two layer [0°/90°] and eight layer [0°/90°/0°/90°/0°/90°/0°/90°] twisted plates.

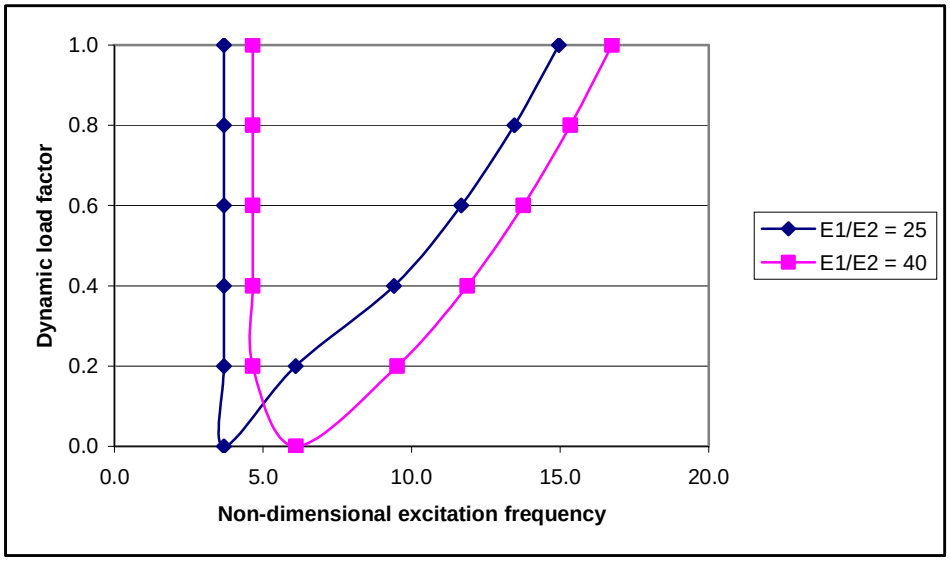

Figure 4.19: Variation of instability region with degree of orthotropy of the cross-ply twisted cantilever panel [0°/90°/90°/0°], a/b =1, ϕ =15°, α = 0.2.

4.7: Angle-ply twisted cantilever panels

The studies are extended further to examine in detail the effects of various parameters on the vibration and stability of laminated composite, pretwisted angle-ply cantilever plates/panels. The study has been carried out extensively for vibration, buckling and parametric resonance characteristics of symmetric and antisymmetric angle-ply lay-ups.

The geometrical and material properties of the twisted panels (unless otherwise stated) are

a = b = 500mm, h = 2mm, ρ = 1580 kg/ m^3

E_{11} = 141.0GPa, E_{22} = 9.23GPa, ν_{12} = 0.313, G_{12} = 5.95GPa, G_{23} = 2.96GPa.

4.7.1: Non-dimensionalization of parameters

Non-dimensional frequency $\varpi = \omega a^2 \sqrt{\frac{\rho}{E_{11} h^2}}$

Non-dimensional buckling load $\lambda = \frac{N_x b^2}{E_{22} h^3}$

The non-dimensional excitation frequency $\Omega = \overline{\Omega} a^2 \sqrt{(\rho / E_{22} h^2)}$ (unless otherwise stated) is used throughout the dynamic instability studies, where $\overline{\Omega}$ is the excitation frequency in radians/second.

4.7.2: Boundary conditions

The clamped (C) boundary condition of the laminated composite twisted angle-ply panel using the first order shear deformation theory is:

u = v = w = θ_x = θ_y = 0 at the left edge.

4.7.3: Vibration and buckling studies

The first four natural frequency parameters for twisted angle-ply cantilever plates having different ply orientations and angles of twist are obtained. Table 4.32 shows these parameters for a three layer [θ, -θ, θ] laminate having a square planform and a thickness ratio (b/h) of 250. Plates with two different angles of twist were studied, i.e., Φ = 15° and 30° in addition to the untwisted plate (i.e. Φ = 0°). The fiber orientation angle is varied from 0° to 90° with an increment of 15°. It is seen that the fundamental frequency decreases with increase in the angle of twist for the 0°/-0°/0°, 75°/-75°/75° and 90°/-90°/90° stacking sequence. For the other stacking sequences the fundamental frequency first increases and then decreases with increase in the angle of twist. The maximum fundamental frequencies are observed when the fibers are perpendicular to the clamped edge

(i.e. $\theta = 0°$) in all cases. Also introducing twist to the panel decreases the frequency parameter as compared to the untwisted panel.

Table 4.32: Variation of non-dimensional free vibration frequencies with angle of twist and ply orientation of angle-ply(θ,-θ,θ) pretwisted cantilever plates

a = b = 500mm, h = 2mm

E_{11} = 141.0GPa, E_{22}= 9.23GPa, ν_{12} = 0.313, G_{12} =5.95GPa, G_{23} = 2.96GPa.

Φ	θ	Non-dimensional free vibration frequencies			
		Mode 1	Mode 2	Mode 3	Mode 4
0	0	1.0176	1.3188	2.5406	5.2331
	15	0.8596	1.3707	2.7513	5.3634
	30	0.6360	1.4196	3.0686	4.0886
	45	0.4476	1.3615	2.7157	3.4475
	60	0.3235	1.1523	1.9947	3.3501
	75	0.2701	0.9078	1.6876	2.9875
	90	0.2601	0.7971	1.6293	2.7521
15	0	1.0037	6.2217	9.3270	10.8862
	15	0.9334	5.7193	9.5061	11.1801
	30	0.7493	4.5043	8.7582	10.4013
	45	0.5271	3.1325	7.5445	8.4461
	60	0.3496	2.1034	5.9566	7.0459
	75	0.2698	1.6660	4.7452	6.6898
	90	0.2566	1.5914	4.5259	6.4686
30	0	0.9568	5.7824	16.3619	17.1346
	15	0.8929	5.3721	15.7032	16.4388
	30	0.7214	4.2968	12.5646	14.7185
	45	0.5100	3.0169	8.9282	12.3703
	60	0.3381	2.0168	6.0177	11.6466
	75	0.2581	1.5584	4.6387	9.2944
	90	0.2446	1.4800	4.4022	8.8036

The free vibration frequencies of the four lowest modes of vibration of composite angle-ply pretwisted cantilever curved panels (twisted plate with camber) are presented in Table 4.33. For a particular stacking sequence, as the angle of twist increases, the non-dimensional fundamental frequency decreases in all cases. There is significant increase in non-dimensional frequencies of higher modes with increase in the angle of twist. As shown in Table 4.33, the non-dimensional fundamental frequency of the twisted curved panel decreases with introduction of twist. Comparing the frequencies in Table 4.32 with that given in Table 4.33, it is also observed that introducing curvature to the plate increases the stiffness and hence the non-dimensional frequency.

Table 4.34 shows the variation of non-dimensional fundamental frequency with increasing R_y /b ratio. The angle of twist of all the panels is taken as 15°. It is observed that as the R_y /b ratio increases, the non-dimensional frequency parameter decreases for all the ply orientations.

The effects of variation of aspect ratio are studied for a three layer twisted plate with the angle of twist taken as 15° and are shown in Table 4.35. It can be seen that as the aspect ratio increases for a particular ply orientation, the non-dimensional frequency decreases suggesting a decrease in stiffness. For the 0° ply orientation, there is a slight increase after which the frequency parameter decreases with increase in aspect ratio. For both 0° and 90° lay-ups the difference in non-dimensional frequency parameter is marginal with the changing aspect ratio as compared to the other stacking sequences.

Table 4.33: Variation of non-dimensional free vibration frequencies with angle of twist and ply orientation of angle-ply(θ/-θ/θ) pretwisted cantilever panels

a = b = 500mm, h = 2mm, b/ R_y = 0.25

E_{11} = 141.0GPa, E_{22} = 9.23GPa, ν_{12} = 0.313, G_{12} = 5.95GPa, G_{23} = 2.96GPa.

Non dimensional frequency, $\varpi = \omega a^2 \sqrt{(\rho / E_{11} h^2)}$

Φ	θ	Non-dimensional free vibration frequencies			
		Mode 1	Mode 2	Mode 3	Mode 4
0	0	2.1125	2.3497	5.2505	5.5324
	15	2.2111	2.6650	5.9996	6.1109
	30	2.0677	2.9741	5.7551	6.7037
	45	1.7227	2.8244	4.9103	6.8087
	60	1.3974	2.3210	4.8870	6.2691
	75	1.1461	2.0354	4.5636	6.2666
	90	1.0344	1.9189	4.1643	6.2689
15	0	1.2250	5.6794	10.1520	11.2324
	15	1.3432	6.3001	10.3559	11.5056
	30	1.2706	5.9930	9.1797	10.9543
	45	1.0426	4.8964	8.0115	9.6814
	60	0.7627	3.6345	7.5997	8.7788
	75	0.5393	2.6940	7.2031	7.4241
	90	0.4219	2.1820	5.6302	7.1798
30	0	1.0443	5.9535	14.5770	18.0224
	15	1.0628	6.0468	15.2957	17.4549
	30	0.9376	5.3306	14.0577	15.0780
	45	0.7247	4.1385	11.2988	12.5670
	60	0.5070	2.9318	8.2728	11.7349
	75	0.3542	2.0703	5.8907	10.9149
	90	0.2957	1.7354	4.9074	9.2144

Table 4.34: Variation of non-dimensional free vibration frequencies with R_y/b ratio of square angle-ply(θ/-θ/θ) pretwisted cantilever panels

a = b = 500mm, h = 2mm, Φ = 15°

E_{11} = 141.0GPa, E_{22}= 9.23GPa, ν_{12} = 0.313, G_{12} =5.95GPa, G_{23} = 2.96GPa

R_y / b	Ply orientation (θ) in Degrees						
	0	**15**	**30**	**45**	**60**	**75**	**90**
5	1.1639	1.2404	1.1409	0.9134	0.6548	0.4601	0.3687
10	1.0529	1.0526	0.9091	0.6862	0.4704	0.3355	0.2909
20	1.0168	0.9806	0.8169	0.5950	0.3989	0.2929	0.2665
50	1.0058	0.9490	0.7730	0.5511	0.3660	0.2761	0.2583
100	1.0042	0.9406	0.7606	0.5385	0.3572	0.2724	0.2570

Table 4.35: Variation of non-dimensional frequency with aspect ratio of laminated composite angle-ply(θ/-θ/θ) pretwisted cantilever plates

h = 2mm, Φ = 15°

E_{11} = 141.0GPa, E_{22}= 9.23GPa, ν_{12} = 0.313, G_{12} =5.95GPa, G_{23} = 2.96GPa.

Aspect ratio a/b	Ply orientation (θ) in Degrees						
	0	**15**	**30**	**45**	**60**	**75**	**90**
0.5	1.0036	0.9358	0.7604	0.5427	0.3599	0.2717	0.2567
1	1.0037	0.9334	0.7493	0.5271	0.3496	0.2698	0.2566
2	1.0034	0.9294	0.7291	0.4916	0.3298	0.2669	0.2564
3	1.0032	0.9256	0.7061	0.4610	0.3170	0.2654	0.2563

In Table 4.36, the effects of the thickness ratio (b/h) are studied for various three layer angle-ply twisted plates with angle of twist taken as 15°. As

the thickness of the shell decreases, the frequency is decreasing in all cases. The 0° ply stacking sequence shows the highest frequency for all b/h values. It is also observed that for a particular b/h ratio, the frequency decreases as the ply angle increases.

Table 4.36: Variation of frequency in Hz with b/h ratio for square laminated composite angle-ply(θ/-θ/θ) pretwisted cantilever plates

a = b = 500mm, Φ = 15°

E_{11} = 141.0GPa, E_{22}= 9.23GPa, ν_{12} = 0.313, G_{12} =5.95GPa, G_{23} = 2.96GPa.

b /h	Ply orientation (θ) in Degrees						
	0	**15**	**30**	**45**	**60**	**75**	**90**
25	119.562	107.0002	81.6985	55.7453	38.8318	32.0182	30.7998
50	60.2136	54.9709	43.0171	29.5242	19.9827	16.0887	15.4194
100	30.1632	27.8230	22.0956	15.3747	10.2498	8.0759	7.7129
200	15.0895	14.0105	11.2212	7.8785	5.2273	4.0525	3.8576
250	12.0725	11.2273	9.0130	6.3401	4.2048	3.2457	3.0864
300	10.2621	9.5535	7.6820	5.4102	3.5875	2.7610	2.6236

The effect of degree of orthotropy on the non-dimensional frequency parameter is studied and shown in Table 4.37. As shown, increasing the degree of orthotropy decreases the non-dimensional fundamental frequency for all ply stacking sequences.

Table 4.37: Variation of non-dimensional frequency with degree of orthotropy of square angle-ply(θ/-θ/θ) pretwisted cantilever plates

a = b = 500mm, Φ = 15°

ν_{12} = 0.313, G_{12} = 5.95GPa, G_{23} = 2.96GPa

E_1/E_2	Ply orientation (θ) in Degrees						
	0	**15**	**30**	**45**	**60**	**75**	**90**
10	1.0055	1.0163	1.0096	0.9292	0.7467	0.4867	0.3177
15	1.0040	0.9897	0.9333	0.8157	0.6295	0.4000	0.2591
25	1.0028	0.9663	0.8629	0.7057	0.5126	0.3128	0.2005
40	1.0021	0.9514	0.8161	0.6297	0.4295	0.2501	0.1584

The study is extended to the study of the buckling characteristics of angle-ply laminated composite twisted cantilever panels. First of all, the effect of increasing angle of twist on non-dimensional buckling load of twisted cantilever three-layer angle-ply plates with varying ply orientations (0° to 90°) is studied. Square plates are used. The plate analyzed is a three-layer laminate. The ply orientation is increased from 0° to 90° in steps of 15°. The buckling loads tend to decrease with increase of lamination angle from 0° to 90° for untwisted and twisted plates. From Table 4.38, it is observed that the buckling load in general decreases with increase in twist angle from untwisted (0°) to an angle of twist of 30°. However, in the case of the 15°, 30°, 45°, and 60° ply lay-ups, the buckling load first increases and then decreases with increasing angle of twist. So the buckling behaviour of twisted plates is quite different from the untwisted plates.

For all the cantilever twisted plates, for this lamination sequence, (θ,-θ, θ), 0° seems to be the preferential ply orientation for maximum non-dimensional buckling loads.

Table 4.38: Variation of non-dimensional buckling load with angle of twist of square angle-ply(θ/-θ/θ) pretwisted cantilever plates

a = b = 500mm, h = 2mm

E_{11} = 141.0GPa, E_{22}= 9.23GPa, ν_{12} = 0.313, G_{12} =5.95GPa, G_{23} = 2.96GPa

Angle of twist in degrees	**Ply orientation (θ) in Degrees**						
	0	**15**	**30**	**45**	**60**	**75**	**90**
0	3.1557	2.0719	1.0759	0.5371	0.2971	0.2195	0.2060
15	2.9985	2.5824	1.6325	0.7900	0.3481	0.2147	0.1959
30	2.5273	2.1958	1.4147	0.6962	0.3075	0.1829	0.1652

Then the buckling studies are extended to laminated composite twisted plates with camber (b/ R_y = 0.25) as shown in Table 4.39. Here again panels of square plan form are used. Comparing buckling loads of Table 4.38 and Table 4.39, it is seen that the buckling loads have significantly increased with introduction of curvature in the panel. However the buckling load decreases significantly when the angle of twist increases from 0° to 30° for the curved panel.

The buckling loads are then computed for a thick (b/h=20) pretwisted cantilever plate as shown in Table 4.40. The non-dimensional buckling loads for thick twisted plates (b/h = 20) are less in comparison with thin pre twisted plates (b/h = 250). The buckling load decreases with increase in angle of twist and 0° seems to be preferential ply orientation for all categories of thick twisted plates.

Table 4.39: Variation of non-dimensional buckling load with angle of twist of square angle-ply(θ/-θ/θ) pretwisted cantilever plates with camber

a = b = 500mm, h = 2mm, b/R_y = 0.25

E_{11} = 141.0GPa, E_{22}= 9.23GPa, ν_{12} = 0.313, G_{12} =5.95GPa, G_{23} = 2.96Gpa

Angle of twist in degrees	Ply orientation (θ) in Degree						
	0	**15**	**30**	**45**	**60**	**75**	**90**
0	14.4381	12.5799	11.6314	9.8141	6.8799	4.6547	3.8417
15	3.9293	4.8098	4.2486	2.8036	1.4581	0.7231	0.4497
30	2.8406	2.9473	2.2650	1.3279	0.6431	0.3163	0.2231

Table 4.40: Variation of non-dimensional buckling load with angle of twist of angle-ply(θ/-θ/θ) pretwisted thick cantilever plates

a/b =1, b /h = 20

E_{11} = 141.0GPa, E_{22}= 9.23GPa, ν_{12} = 0.313, G_{12} =5.95GPa, G_{23} = 2.96GPa

Angle of twist in degrees	Ply orientation (θ) in Degree						
	0	**15**	**30**	**45**	**60**	**75**	**90**
0	3.1078	2.0155	1.0399	0.5207	0.2917	0.2183	0.2055
15	2.9484	2.1964	1.1920	0.5528	0.2868	0.2082	0.1951
30	2.4775	2.0042	1.1701	0.5380	0.2553	0.1766	0.1644

As observed in Table 4.41, increasing the aspect ratio of the twisted plate decreases the non-dimensional buckling load. This is true for all ply orientations.

Then the study is extended to plates with aspect ratio a/b = 3 (Table 4.42). The study analyses effects of varying angle of twist. Comparing Tables 4.41 and 4.42, it is observed that the buckling loads tend to decrease significantly with increase of aspect ratio. However for this geometry of pretwisted cantilever plates, the non-dimensional buckling load tends to decrease with increase of angle of twist except for the 15°, 30°, 45° and 60° ply lay-ups which first increase and then decrease. 0^0 seems to be the preferential ply orientation for all plates. The behaviour is hence quite similar to that of square twisted plates.

Table 4.41: Variation of non-dimensional buckling load with aspect ratio of laminated composite angle-ply(θ/-θ/θ) pretwisted cantilever plates

h = 2mm, Φ = 15°

E_{11} = 141.0GPa, E_{22}= 9.23GPa, ν_{12} = 0.313, G_{12} =5.95GPa, G_{23} = 2.96GPa

Aspect ratio a/b	**Ply orientation (θ) in Degrees**						
	0	**15**	**30**	**45**	**60**	**75**	**90**
0.5	11.9958	10.3819	6.7625	3.4047	1.5062	0.8744	0.7846
1	2.9985	2.5824	1.6325	0.7900	0.3481	0.2147	0.1959
2	0.7491	0.6393	0.3794	0.1624	0.7546	0.0524	0.0489
3	0.3327	0.2812	0.1547	0.0627	0.0313	0.0231	0.0217

Table 4.42: Variation of non-dimensional buckling load with angle of twist of rectangular angle-ply(θ/-θ/θ) pretwisted cantilever plates

h = 2mm, a/ b = 3, Φ = 15°

E_{11} = 141.0GPa, E_{22} = 9.23GPa, ν_{12} = 0.313, G_{12} = 5.95GPa, G_{23} = 2.96GPa.

Angle of twist in Degree	Ply orientation (θ) in Degree						
	0	**15**	**30**	**45**	**60**	**75**	**90**
0	0.3499	0.2012	0.0937	0.0479	0.0298	0.0240	0.0229
15	0.3327	0.2812	0.1547	0.0627	0.0313	0.0231	0.0217
30	0.2805	0.2404	0.1412	0.0595	0.0279	0.0196	0.0183

Table 4.43 shows the variation of non-dimensional buckling load with increasing width to thickness ratio of the angle-ply twisted plate (Φ =15°). It is seen that as the b /h ratio increases, i.e., thickness decreases, the non-dimensional buckling load is increasing for all the ply orientations.

The variation of the non-dimensional buckling load with increasing E_1 / E_2 ratio is studied in Table 4.44. As the E_1 / E_2 ratio increases, the non-dimensional buckling load increases, except for the 90/-90/90 stacking sequence where it is found to decrease with increase in the E_1 / E_2 ratio.

Table 4.43: Variation of non-dimensional buckling load with b/h ratio of square angle-ply (θ/-θ/θ) pretwisted cantilever plates

a = b = 500mm, Φ = 15°

E_{11} = 141.0GPa, E_{22}= 9.23GPa, ν_{12} = 0.313, G_{12} =5.95GPa, G_{23} = 2.96GPa

b /h	Ply orientation (θ) in Degrees						
	0	15	30	45	60	75	90
25	2.9656	2.2698	1.2561	0.5760	0.2915	0.2089	0.1953
50	2.9894	2.4380	1.4378	0.6569	0.3084	0.2106	0.1956
100	2.9960	2.5239	1.5501	0.7261	0.3254	0.2122	0.1957
200	2.9981	2.5717	1.6160	0.7771	0.3425	0.2140	0.1958
250	2.9985	2.5824	1.6325	0.7900	0.3481	0.2147	0.1959
300	2.9987	2.5891	1.6437	0.7985	0.3520	0.2152	0.1959

Table 4.44: Variation of non-dimensional buckling load with degree of orthotropy of angle-ply(θ/-θ/θ) pretwisted cantilever plates

a = b = 500mm, Φ = 15°

ν_{12} = 0.313, G_{12} = 5.95GPa, G_{23} = 2.96GPa

E_1/E_2	Ply orientation (θ) in Degrees						
	0	15	30	45	60	75	90
10	1.9697	2.0121	1.9744	1.6661	1.0800	0.4620	0.1965
15	2.9460	2.8627	2.5415	1.9394	1.1568	0.4683	0.1960
25	4.8985	4.5482	3.6265	2.4258	1.2811	0.4775	0.1957
40	7.8273	7.0483	5.1776	3.0788	1.4338	0.4873	0.1955

4.7.4: Dynamic stability studies

Numerical results are presented for anti-symmetric angle-ply laminated pretwisted cantilever panels with different combinations of lamination parameters and geometry including angle of twist, b/h ratio, aspect ratio and curvature.

The dynamic stability regions are plotted for angle-ply [30°/-30°/30°/-30°] twisted flat panel with different angles of twist i.e. ϕ = 0°, ϕ =15° and ϕ = 30°. As shown in Figure 4.20, the onset of instability occurs earlier with introduction of twist (ϕ =15°) in the untwisted panel (ϕ = 0°). With increase of twist angle from ϕ =15° to ϕ =30°, the onset of instability occurs earlier with wider instability regions, for this lamination sequence and ply orientation.

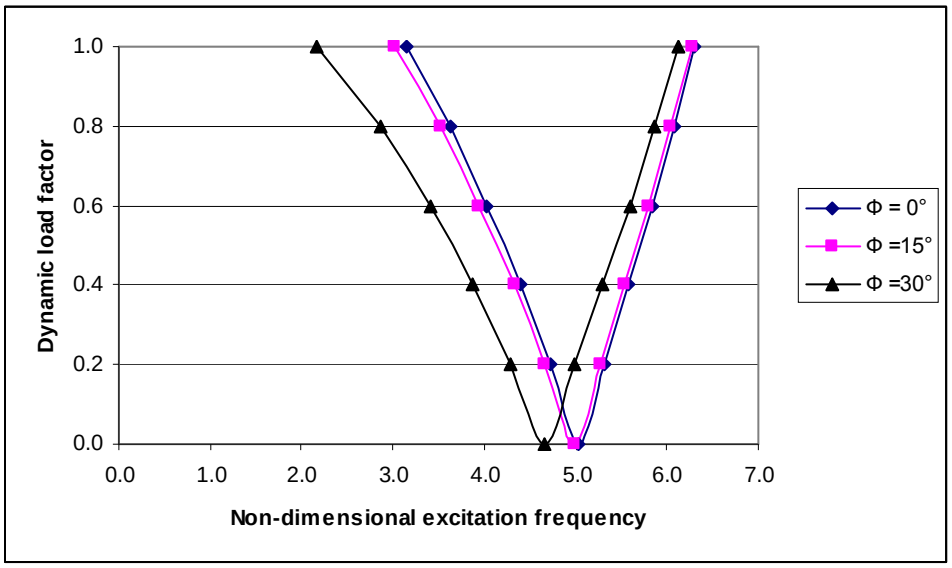

Figure 4.20: Variation of instability region with angle of twist of the angle-ply flat panel [30°/-30°/30°/-30°] , a/b =1, ϕ = 0°, 15°and 30°, α = 0.2.

The instability regions are also analysed for pretwisted two, four and eight layer anti-symmetric angle-ply panels for ply angle 45°/-45° as shown in Figure 4.21 to study the effect of number of layers. The static load factor is taken as 0.2. The onset of instability occurs later with more number of layers due to the bending stretching coupling.

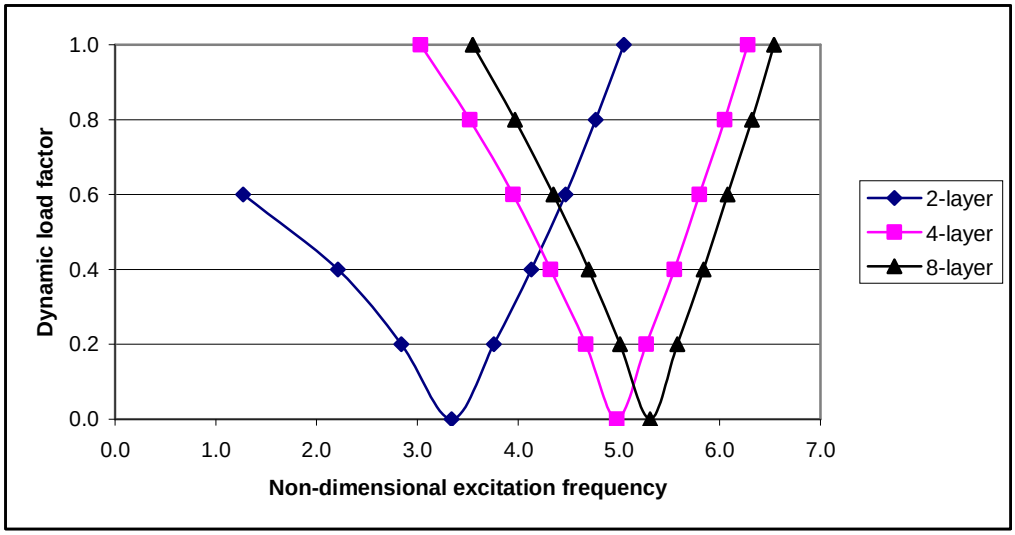

Figure 4.21: Variation of instability region with number of layers of the angle- ply twisted panel, a/b=1, b/h =250, ϕ = 15°, α = 0.2.

The variation of instability regions with static load factor (α) for a twisted anti-symmetric angle-ply panel of square plan-form and twisting angle ϕ =15° is shown in Figure 4.22. As observed in Figure 4.22, the instability occurs earlier and the width of instability zones expands with increase in static load factor from 0.0 to 0.6.

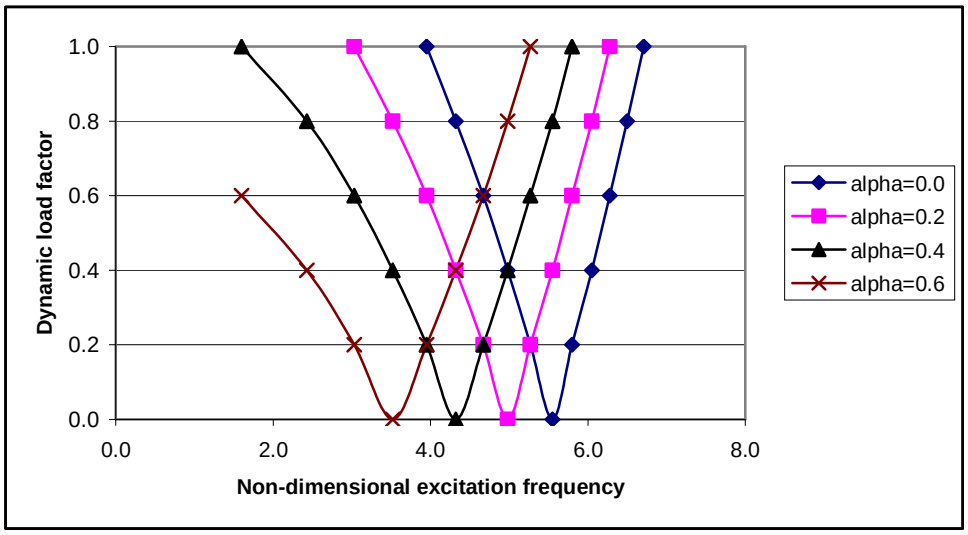

Figure 4.22: Variation of instability region with static load factor of an angle-ply twisted panel [30°/-30°/30°/-30°], a/b =1, ϕ =15°, α = 0.0, 0.2, 0.4 and α = 0.6.

The variations of instability regions with ply orientation of angle-ply [$\theta/-\theta/\theta/-\theta$] cantilevered pretwisted (ϕ =15°) panels for uniform loading with static component is shown in Figure 4.23. The static load factor is taken as 0.2. As observed, the onset of instability occurs earlier for ply orientations of 60°, 75° and 90°. The instability occurs much later for ply orientation of 0° and 15°. The ply orientation 0° seems to be the preferential ply orientation for this lamination sequence and twisting angle. Thus the ply orientation significantly affects the onset of instability region and the width of instability zones. The variation of instability regions shows asymmetric behaviour unlike the results of dynamic stability of simply supported, square and untwisted angle-ply plates by Chen and Yang [1990]. This may be due to the un-symmetry in boundary conditions and twisting of the panels.

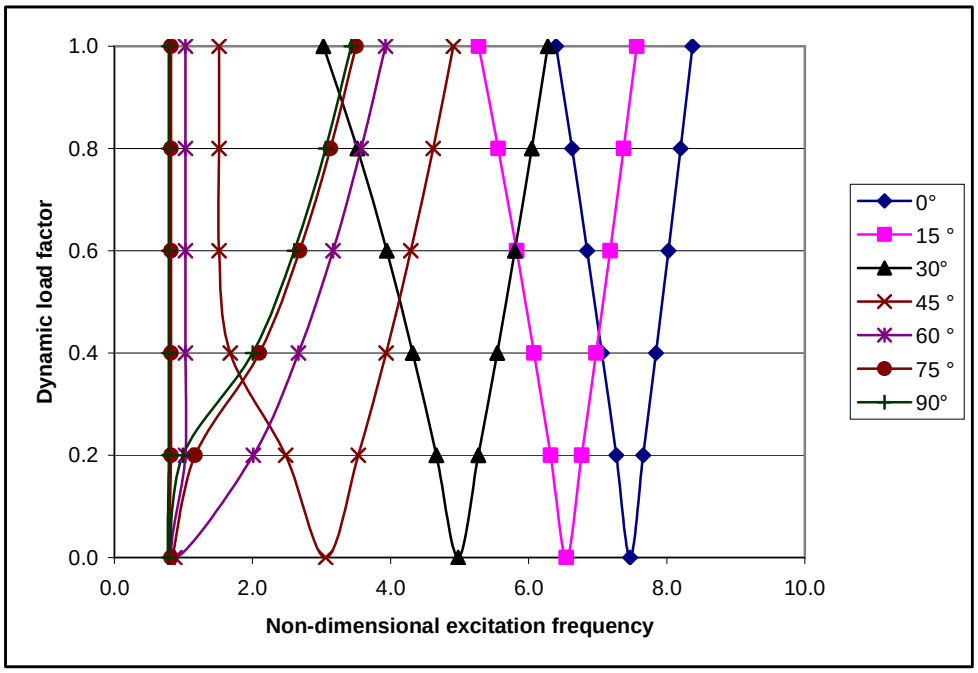

Figure 4.23: Variation of instability region with ply orientation of an angle-ply twisted panel [θ/−θ/θ/−θ], a/b =1, ϕ =15°, α = 0.2, θ = 0° to 90°.

The dynamic instability regions have been plotted for cantilever angle-ply twisted panels of aspect ratios a/b =1, 2 and 4 as shown in Figure 4.24. The angle of twist is fixed at 15° and static load factor is taken as 0.2. As shown in the figure, the excitation frequency decreases from square (a/b =1) to rectangular panels (a/b = 2 and 4) with increase of aspect ratio.

The effect of b/h ratio on the instability regions has been studied for uniform loading with static component. As observed in Figure 4.25, the onset of instability occurs with a higher excitation frequency with increase in the thickness of panels from b/h = 300 to b/h = 200. The width of instability regions is also more for thinner panels than thicker panels.

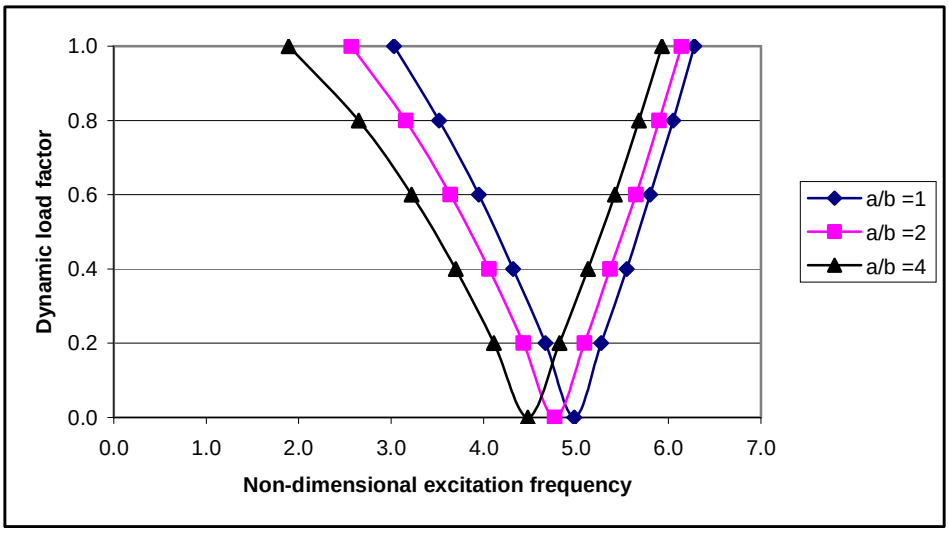

Figure 4.24: Variation of instability region with aspect ratio of the angle-ply twisted panel [30°/-30°/30°/-30°], a/b =1, 2 and 4, ϕ =15°, α = 0.2.

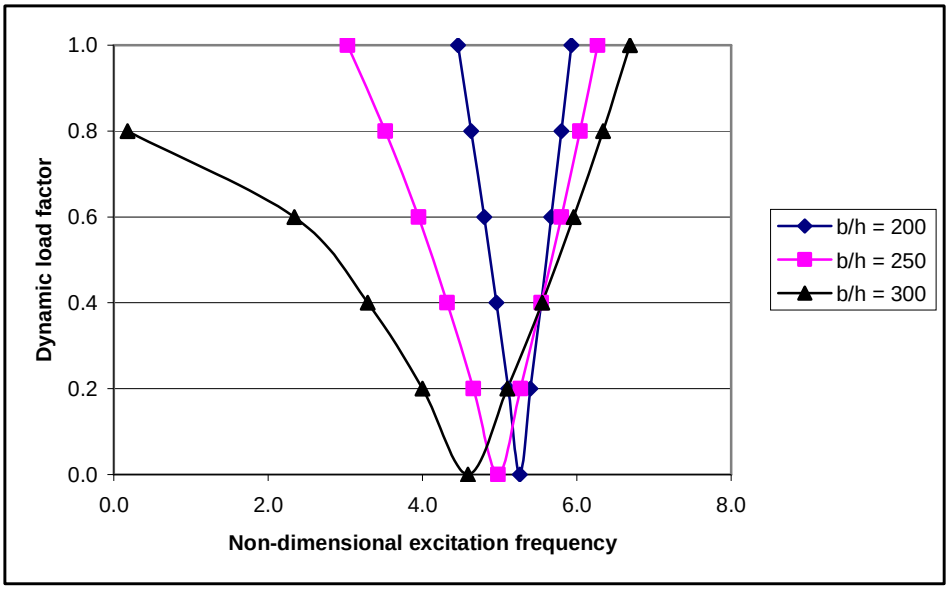

Figure 4.25: Variation of instability region with b/h ratio of the angle-ply twisted panel [30°/-30°/30°/-30°], a/b =1, b/h = 200, 250, 300, ϕ =15°, α = 0.2.

The variation of instability regions is studied for anti-symmetric angle-ply pretwisted cylindrical panels ($b/R_y = 0.25$) to study the effect of angle of twist on the curved panel. As seen from Figure 4.26, there is significant deviation of the instability behaviour of twisted cylindrical panels than that of untwisted panels.

The onset of instability of twisted cylindrical panels occurs much earlier than untwisted cylindrical panels. The widths of the instability regions increase with increase of angle of twist in the panel.

Similar behaviour is also observed for the variation of instability region of twisted spherical and hyperbolic paraboloidal panels with the angle of twist. The variations of dynamic instability regions with angle of twist for a four layer angle-ply spherical and hyperbolic paraboloid twisted panel are studied and the plots are shown in figures 4.27 and 4.28. As the angle of twist increases, the onset of instability occurs earlier and this behaviour is noticed for both shell geometries. The excitation frequency is however much lesser for the hyperbolic paraboloid twisted panel as compared to the spherical twisted panel.

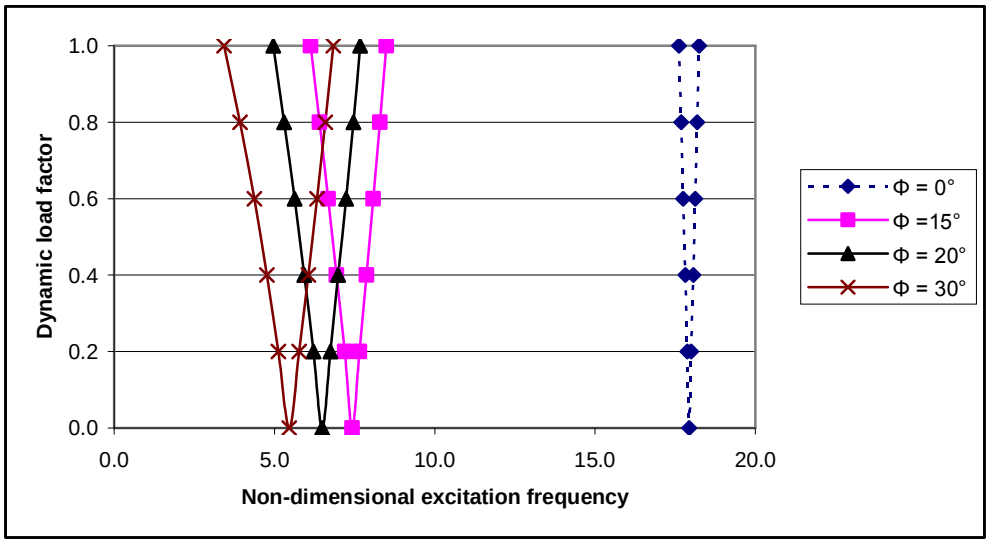

Figure 4.26: Variation of instability region with angle of twist of the angle-ply cylindrical twisted panel [30°/-30°/30°/-30°], a/b =1, ϕ = 0°, 15° and 30°, α = 0.2, b/R_y = 0.25

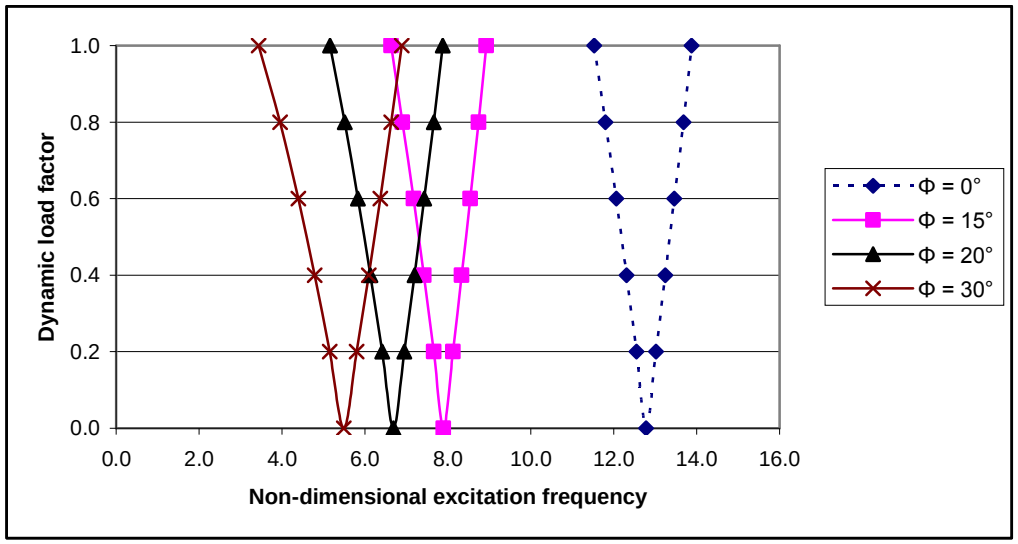

Figure 4.27: Variation of instability region with angle of twist of the angle-ply spherical twisted panel [30°/-30°/30°/-30°], a/b =1, ϕ = 0°, 15° and 30°, α = 0.2, b/R_y = 0.25, b/R_x = 0.25

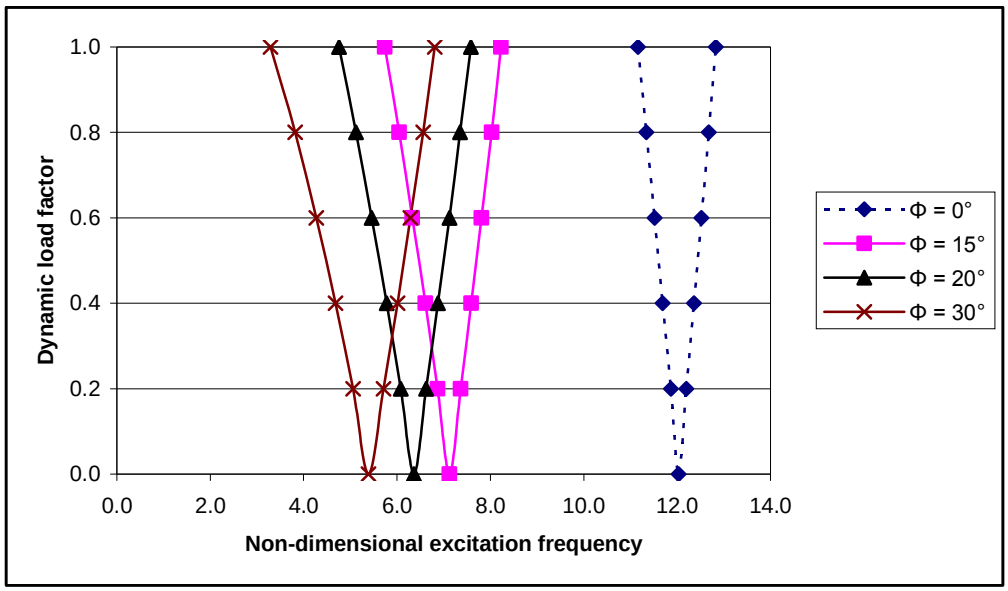

Figure 4.28: Variation of instability regions with angle of twist of the angle-ply hyperbolic paraboloidal twisted panel [30°/-30°/30°/-30°] a/b =1, ϕ = 0°, 15° and 30°, α = 0.2, b/R_y = 0.25, b/R_x = −0.25

The studies were then extended to compare the dynamic instability regions of a laminated composite twisted angle-ply four layer(30°/-30°/30°/-30°**)** cantilever curved panel with different geometries, i.e., cylindrical ($b/R_y = 0.25$), spherical ($b/R_x = 0.25$, $b/R_y = 0.25$) and hyperbolic paraboloidal ($b/R_x = -0.25$, $b/R_y = 0.25$) panels, for a particular twist ($\phi = 15°$), to study the effect of curvature. As observed from Figure 4.29, the onset of instability regions occurs later for cylindrical panels than the flat panels due to addition of curvature. The width of instability regions is smaller for cylindrical panels than flat panels. However, the spherical pretwisted panels show small increase of non-dimensional excitation frequency over the cylindrical pretwisted panels. The onset of instability of laminated composite pretwisted hyperbolic paraboloidal curved panels occurs earlier to pretwisted cylindrical panels but after flat panels.

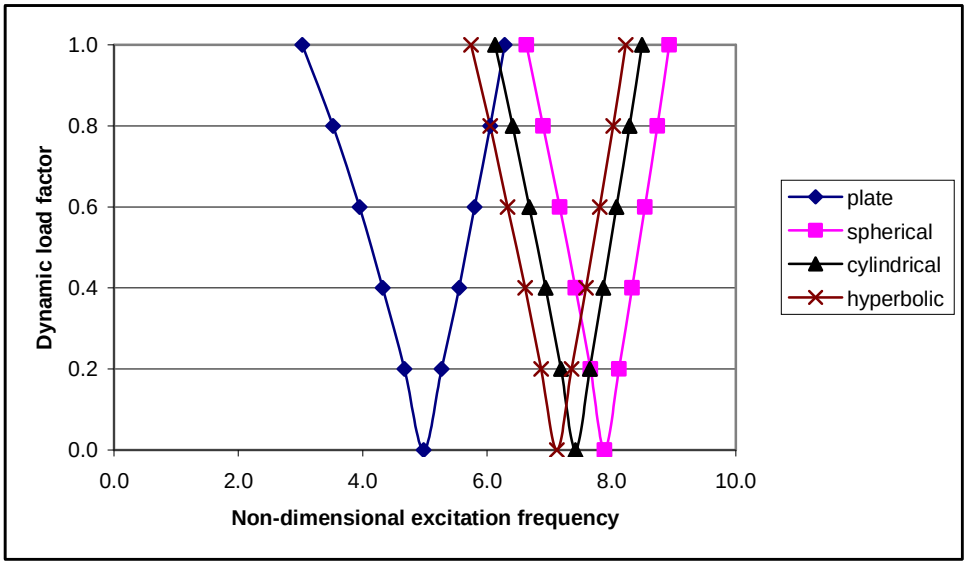

Figure 4.29: Variation of instability region with geometry for an angle-ply twisted panel [30°/-30°/30°/-30°], a/b =1, ϕ =15°, α = 0.2, b/R_y = 0.25.

As observed from figure 4.30, as the E_1/E_2 ratio increases, the onset of instability for the plate is delayed.

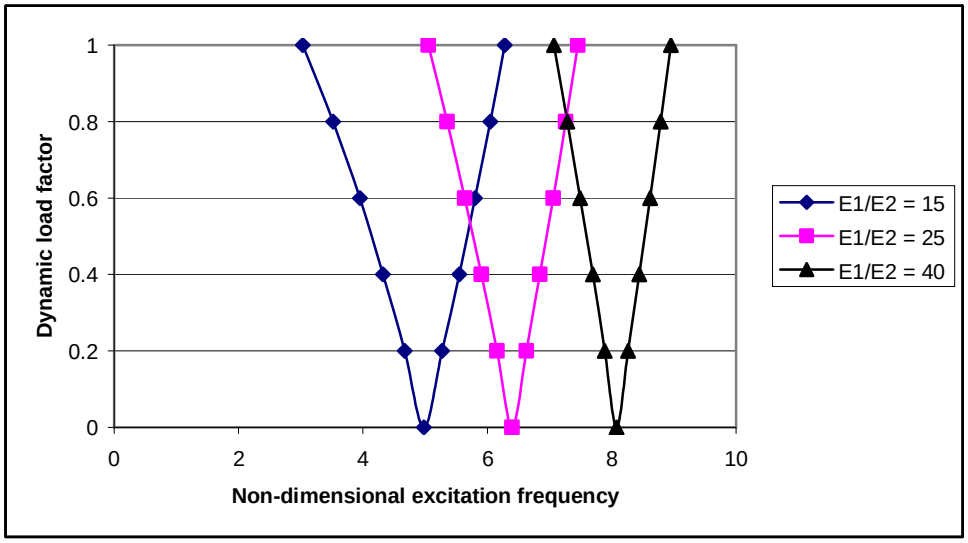

Figure 4.30: Variation of instability region with degree of orthotropy for an angle-ply twisted panel [30°/-30°/30°/-30°], a/b =1, ϕ =15°, α = 0.2, h = 2mm.

CHAPTER 5

CONCLUSIONS

The present work deals with the study of the vibration, buckling and parametric resonance characteristics of homogeneous, cross-ply and angle-ply laminated composite twisted cantilever panels. The formulation is based on the first order shear deformation theory, taking into account transverse shear and rotary inertia effects. A finite element procedure using an eight-node isoparametric quadratic shell element is employed in the present analysis with five degrees of freedom per node. The development of regions of instability arises from Floquet's theory developed by Bolotin and the boundaries of the primary instability regions with period 2T, where $T = 2\pi/\Omega$ which are of practical importance have been determined to study the effect of various parameters of the laminated composite twisted panels on the dynamic instability regions.

Results are presented for the vibration, buckling and dynamic stability characteristics for isotropic, cross-ply and angle-ply laminated composite twisted cantilever panels. The effects of various geometrical parameters like angle of twist, aspect ratio, shallowness ratio and lamination details (for composite panels) on the vibration and stability characteristics of isotropic and laminated composite(cross-ply and angle-ply) twisted cantilever panels has been analysed.

The conclusions are presented separately for these three cases.

5.1: Isotropic twisted panels

The effect of various parameters on the vibration and stability characteristics of the isotropic twisted panel has been studied. The results can be summarized as follows.

- Introduction of an angle of twist of 10° to the untwisted plate is seen to reduce the fundamental frequency parameter by 0.5%. It is also seen that as the angle of twist increases, the lowest non-dimensional frequency parameter decreases.

- Introducing a curvature to the twisted panel increases the non-dimensional frequency parameter suggesting an increase in the stiffness of the panel due to addition of curvature.

- The frequency parameter of the twisted isotropic panel decreases as the aspect ratio increases.

- As the thickness of the plate decreases, the frequency of vibration in Hz decreases.

- Twisted curved panels with various geometries were also studied and it is observed that all the twisted panels with curvature have greater frequency parameter than the flat twisted panel. The fundamental frequency parameter is highest for the spherical twisted panel and is 35.1% greater than the twisted flat panel.

- The lowest non-dimensional buckling load decreases as the angle of twist of the plate increases. Introduction of an angle of twist of 10° to the untwisted plate decreases the buckling load by 1.9% and at an angle of twist of 30°, the decrease in the lowest buckling load is as much as 18% compared to the untwisted panel.

- The buckling load significantly increases with introduction of curvature to the plate. The buckling load for an untwisted square cylindrical panel is 726.9% more than the untwisted square plate. The buckling load of the cylindrical cantilever panel decreases as the angle of twist increases.

- As the R_y /b ratio increases, the non-dimensional buckling load decreases.

- Increasing the aspect ratio is found to decrease the non-dimensional buckling load of the twisted panel.

- An increase in the b/h ratio of the twisted panel contributes to a decrease in the buckling load.

- The instability occurs at lower excitation frequency as the angle of twist of the panel increases and the width of the instability region is found to decrease as the angle of twist decreases.

- The effect of static load factor variation on the dynamic instability region shows that the instability occurs earlier for higher static load factor and the width of instability zones decreases with the decrease in the static load factor. The variation was studied changing the static load factor α from 0.2 to 0.6 for angle of twist ϕ =15°.

- As the R_y /b ratio increases, the instability occurs at an earlier frequency and the width of the instability region increases.

- Increase in the b/h ratio causes the instability to occur earlier and the width of the instability region to increase.

- Comparing twisted curved panels with different geometries, it is seen that the onset of instability occurs earlier for the flat panel. It occurs at a higher excitation frequency for cylindrical panels than the hyperbolic paraboloidal twisted panels and at a still higher excitation frequency for the spherical twisted panel, though the spherical and cylindrical twisted

panels show little difference of excitation frequencies for instability. The width of the instability region is marginally smaller for the cylindrical panel than the hyperbolic paraboloid twisted panel.

5.2: Cross-ply twisted cantilever panels

The study has been carried out extensively for vibration, buckling and parametric resonance characteristics of symmetric and anti-symmetric cross-ply lay-ups. Two, four and eight layer antisymmetric lay-ups as well as a four layer symmetric cross-ply lay-up are taken for the study.

- ❖ It is found that as the angle of twist increases for a particular cross-ply orientation, the frequency parameter decreases. This is true for both the symmetric as well as antisymmetric cross-ply stacking sequences.

- ❖ As the R/a ratio increases, the non-dimensional frequency parameter decreases. Also for a particular cross-ply orientation and low R/a ratio, the spherical shell shows slightly higher frequency parameter than the cylindrical shell. Hence introduction of curvature increases the non-dimensional frequency parameter suggesting an increase in the stiffness of the shell with curvature.

- ❖ As the aspect ratio increases, the non-dimensional frequency parameter first slightly increases and then decreases gradually for all the stacking sequences except in the two-layer stacking sequence which decreases with increase in the aspect ratio.

- ❖ With decrease in the thickness of the plate, the frequency in Hz decreases. This is seen to be true for both symmetric and antisymmetric cross-ply stacking sequences.

- ❖ As the degree of orthotropy increases, the non-dimensional frequency parameter decreases.

- The introduction of twist to an untwisted plate is also seen to give lesser non-dimensional buckling load values. Comparing the antisymmetric lay-ups, for a particular angle of twist, the non-dimensional buckling load increases as the number of layers increases.

- The analysis of the non-dimensional buckling load for different laminations of a square cylindrical and spherical shell with angle of twist of 15° shows that the buckling load is found to decrease with increase of R/a ratio for all cross-ply lay-ups. The symmetric arrangement of the plies shows the greatest non-dimensional buckling load for a particular R/a ratio.

- It is observed that introduction of curvature to the plate increases the non-dimensional buckling load. Comparing a square spherical twisted panel and a square twisted plate, the buckling load is greater for the spherical twisted panel.

- Increase of aspect ratio is found to decrease the non-dimensional buckling load.

- As the thickness of the twisted plate decreases, the buckling load decreases for all the ply orientations

- With the increasing E_1/ E_2 ratio, the non-dimensional buckling load is found to increase for all the cross-ply twisted plates.

- The onset of instability occurs earlier with introduction of twist (ϕ =10°) in the untwisted panel (ϕ = 0°). With increase of twist angle from ϕ =10° to ϕ = 30°, the instability frequency decreases and the widths of the instability region also decrease slightly as the angle of twist decreases.

- To study the effect of number of layers on the dynamic instability regions, two layer [0°/90°], four layer [0°/90°/0°/90°] and eight layer

[0°/90°/0°/90°/0°/90°/0°/90°] cross-ply twisted panels with angle of twist taken as 15° were studied. The static load factor is taken as 0.2. The two layer panel reaches dynamic instability earliest and the eight layer cross-ply reaches dynamic instability latest. The width of the instability region is different with two layer lay-up showing most width and the eight layer cross-ply twisted plate showing the least width. This behaviour is also noticed for the twisted spherical, cylindrical and hyperbolic paraboloidal twisted panel where again the effect of number of layers is studied.

- The instability occurs earlier for higher static load factor and the width of instability zones decreases with decrease in static load factor.

- As the aspect ratio increases, the instability occurs earlier and the width of the instability region increases.

- The onset of instability occurs with a lesser excitation frequency for thin plates and occurs later as the thickness increases. The width of instability regions is also more for thinner plates than thicker plates.

- The onset of instability of laminated composite twisted cylindrical panels occurs earlier than twisted spherical panels but later than twisted hyperbolic panels. The width of instability regions is smaller for cylindrical panels than hyperbolic twisted panels. Similar behaviour is noticed in the four layer symmetric and eight layer antisymmetric cross-ply twisted panels. The four layer lay-up shows much larger excitation frequencies than the two or eight layer antisymmetric twisted cross-ply panels for a particular shell geometry. The earliest instability frequency is shown by plates in all cases.

- The instability frequency increases as the E_1/E_2 ratio increases.

5.3: Angle-ply twisted cantilever panels

The studies are finally extended to examine in detail the effects of various parameters on the stability of laminated composite, pretwisted angle-ply cantilever plates/panels. The study has been carried out extensively for vibration, buckling and parametric resonance characteristics of symmetric and antisymmetric angle-ply lay-ups. For the vibration and buckling studies, three layer symmetric angle-ply panels with varying ply orientation (0° to 90°) were studied while for buckling studies four layer antisymmetric lay-up is assumed.

- The first frequency parameter decreases with increase in the angle of twist for the 0°/-0°/0°, 75°/-75°/75° and 90°/-90°/90° stacking sequence. For the other stacking sequences the first frequency first increases and then decreases with increase in the angle of twist. The maximum fundamental frequencies are observed when the fibers are perpendicular to the clamped edge (i.e. $\theta = 0°$) in all cases. Also introducing twist to the plate decreases the frequency parameter as compared to the untwisted plate.

- For plates with camber, for a particular stacking sequence, as the angle of twist increases, the non-dimensional fundamental frequency decreases in all cases. There is significant increase in non-dimensional frequencies of higher modes with increase in the angle of twist.

- Introducing curvature to the plate increases the stiffness and hence the non-dimensional frequency.

- As the R_y /b ratio increases, the non-dimensional frequency parameter decreases for all the ply orientations.

- As the aspect ratio increases for a particular ply orientation, the non-dimensional frequency decreases suggesting a decrease in stiffness.

- As the thickness of the shell decreases, the frequency in Hz is decreasing in all cases. The 0° ply stacking sequence shows the highest frequency for all b/h values. It is also observed that for a particular b/h ratio, the frequency decreases as the ply angle increases.

- Increasing the degree of orthotropy decreases the non-dimensional fundamental frequency for all ply stacking sequences.

- The buckling loads tend to decrease with increase of lamination angle from 0° to 90° for untwisted and twisted plates.

- The buckling load in general decreases with increase in twist angle from untwisted (0°) to an angle of twist of 30°. However in the case of the 15°, 30°, 45°, and 60° ply lay-ups, the buckling load first increases and then decreases with increasing angle of twist. So the buckling behaviour of twisted plates is quite different from the untwisted plates.

- For all the cantilever twisted plates, for this lamination, (θ,-θ, θ), 0° seems to be the preferential ply orientation for maximum non-dimensional buckling loads.

- The buckling load decreases with increase in angle of twist and 0° seems to be preferential ply orientation for all categories of thick twisted plates

- The buckling loads significantly increase with introduction of curvature in the panel. However the buckling load decreases significantly when the angle of twist increases from 0° to 30° for the curved panel.

- Increasing the aspect ratio of the twisted plate decreases the non-dimensional buckling load. This is true for all ply orientations.

- As the b /h ratio increases, i.e., thickness decreases, the non-dimensional buckling load is increasing for all the ply orientations

- As the E_1 / E_2 ratio increases, the non-dimensional buckling load increases, except for the 90/-90/90 stacking sequence where it is found to decrease with increase in the E_1 / E_2 ratio.

- The onset of instability occurs earlier with introduction of twist (ϕ =15°) in the untwisted panel (ϕ = 0°). With increase of twist angle from ϕ =15° to ϕ =30°, the onset of instability occurs earlier with wider instability regions.

- The onset of instability occurs later with more number of layers due to the bending stretching coupling.

- Varying the static load factor from 0.0 to 0.6, it is observed that the instability occurs earlier and the width of instability zones expands with increase in static load factor.

- The angle of the ply was also varied keeping static load factor as 0.2 and angle of twist as 15°. As observed, the onset of instability occurs earlier for ply orientations of 60°, 75° and 90°. The instability occurs much later for ply orientation of 0° and 15°. The ply orientation 0° seems to be the preferential ply orientation for this lamination sequence and twisting angle. Thus the ply orientation significantly affects the onset of instability region and the width of instability zones. The variation of instability regions shows asymmetric behaviour.

- The excitation frequency decreases from square (a/b =1) to rectangular panels (a/b = 2 and 4) with increase of aspect ratio.

- The onset of instability occurs with a higher excitation frequency with increase in the thickness of panels from b/h = 300 to b/h = 200. The width of instability regions is also more for thinner panels than thicker panels.

- There is significant deviation of the instability behaviour of twisted cylindrical panels than that of untwisted panels. The onset of instability of twisted cylindrical panels occurs much earlier than untwisted cylindrical panels. The widths of the instability regions increase with increase of angle of twist in the panel. Similar behaviour is also observed for the variation of instability region of twisted spherical and hyperbolic paraboloidal panels with the angle of twist. The excitation frequency is however much lesser for the hyperbolic paraboloid twisted panel as compared to the spherical twisted panel.

- Different geometries of a twisted panel are analysed keeping the ply orientation, static load factor and angle of twist constant. The onset of instability regions occurs later for cylindrical panels than the flat panels due to addition of curvature. The width of instability regions is smaller for cylindrical panels than flat panels. However, the spherical pretwisted panels show small increase of non-dimensional excitation frequency over the cylindrical pretwisted panels. The onset of instability of laminated composite pretwisted hyperbolic paraboloidal curved panels occurs earlier to pretwisted cylindrical panels but after flat panels.

- As the E_1/E_2 ratio increases, the onset of instability for the plate is delayed.

In general it is seen that for both the homogeneous and laminated composite twisted cantilever panels, there is a decrease in the non-dimensional frequency parameter and non-dimensional buckling load with increase in the angle of twist and increase in aspect ratio. There is a decrease in frequency and buckling load with decrease in thickness of the twisted square panel. For laminated composite twisted panels, as the degree of orthotropy increases, the non-dimensional frequency parameter and non-dimensional buckling load decreases. Introduction of curvature increases the stiffness leading to greater non-dimensional frequency and buckling load.

For both homogeneous and laminated composite twisted cantilever panels, the instability occurs earlier with wider instability regions as the angle of twist, static load factor, aspect ratio and b/h ratio increase. It occurs with higher excitation frequency and a wider instability zone as curvature is introduced, keeping angle of twist constant. The instability occurs later with less wider regions with increase in the number of layers for laminated composite cantilever twisted panels. For the angle-ply twisted panel, the instability occurs much later with narrower zones as the ply angle decreases.

From the above studies, it may be concluded that the instability behaviour of composite twisted cantilever panels is greatly influenced by the geometry, material, angle of twist and lamination parameters. So, this can be used to the advantage of tailoring during design of composite twisted cantilever panels.

5.4: Scope for further work

The possible extensions to the present work are as presented below:

- The present investigation can be extended to dynamic stability studies of twisted panels subjected to non-uniform loading.
- Since cantilever twisted panels form an important aspect of the study of turbomachinery blades, the study may also be extended to study the effects of rotation to the cantilever twisted panels.
- The panels in this study are of uniform thickness and width. Hence the effect of varying thickness and width may also be incorporated in this study.
- Material non-linearity may also be taken into account in further parametric studies of twisted cantilever panels.
- The effects of damping on the instability regions of twisted cantilever panels may also be studied.
- There is also scope to study variation of the instability regions by experimental methods.

REFERENCES

1. **Abbas, B.** (1979): Simple finite elements for dynamic analysis of thick pretwisted blades, *Aeronautical Journal*, Vol.**83**, pp. 450-453.
2. **Ansari, K.A.** (1975): Nonlinear vibrations of a rotating pretwisted blade, *Computers and Structures*, Vol.**5** (2-3), pp. 101-118.
3. **Beres, D.P.** (1974): Vibration analysis of skewed cantilever systems: Helicoidal Shells and plates, Ohio State University, Ph.D. Thesis.
4. **Bert, C.W.**, and **Birman, V.** (1988): Parametric instability of thick orthotropic circular cylindrical shells, *Acta Mechanica*, Vol.**71**, pp.61-76.
5. **Bhumbla, R.**, **Kosmatka, J.B.**, and **Reddy, J.N.** (1990): Free vibration behaviour of spinning shear deformable plates composed of composite materials, *AIAA Journal*, Vol.**28**(11), pp.1962-1970.
6. **Bolotin, V.V.** (1964): The dynamic stability of elastic systems, Holden-Day, San Francisco.
7. **Bossak, M.A.J.,** and **Zienkiewicz, O.C.** (1973): Free vibrations of initially stressed solids with particular reference to centrifugal force effects in rotating machinery, *Journal of Strain Analysis*, Vol. **8** (4), pp. 245-252.
8. **Carnegie, W.** (1957): Static bending of pretwisted cantilever blades, *Proceedings of the Institution of Mechanical Engineers*, Vol.**171** (32), pp. 873- 894.
9. **Carnegie, W.** (1959[a]): Vibrations of pretwisted cantilever blading, *Proceedings of the Institution of Mechanical Engineers*, Vol.**173** (12), pp. 343- 374.
10. **Carnegie, W.** (1959[b]): Vibrations of rotating cantilever blading: Theoretical approaches to the frequency problem based on energy methods, *Journal of Mechanical Engineering Science*, Vol.**1** (3), pp. 235-240.
11. **Carnegie, W.** (1962): Vibrations of pretwisted cantilever blading: An additional effect due to torsion, *Proceedings of the Institution of Mechanical Engineers*, Vol.**176** (13), pp. 315- 322.

12. **Carnegie, W.** (1964): Vibrations of pretwisted cantilever blading allowing for rotary inertia and shear deflection, *Journal of Mechanical Engineering Science*, Vol.**6** (2), pp. 105-109.
13. **Carnegie, W.** (1966): A note on the application of the Variational method to derive the equations of dynamic motion of a pretwisted cantilever blade mounted on the periphery of a rotating disc allowing for shear deflection, rotary inertia and torsion bending, *Bulletin of Mechanical Engineering Education*, Vol.**5**, pp. 221- 223.
14. **Carnegie, W.,** and **Dawson, B.** (1969[a]): Modal curves of pretwisted beams of rectangular cross-section, *Journal of Mechanical Engineering Science*, Vol.**11** (1), pp. 1–13.
15. **Carnegie, W.,** and **Dawson, B.** (1969[b]): Vibration characteristics of straight blades of asymmetrical aerofoil cross-section, *Aeronautical Quarterly*, Vol.**20**, pp. 178-190.
16. **Carnegie, W.,** and **Dawson, B.** (1971): Vibration characteristics of pretwisted blades of asymmetrical aerofoil cross-section, *Aeronautical Quarterly*, Vol.**22**, pp. 257- 273.
17. **Carnegie, W.,** and **Thomas, J.** (1972): The coupled bending–bending vibration of pretwisted tapered blading, *Journal of Engineering Industry*, Vol.**94** (1), pp. 255–266.
18. **Cederbaum, G**. (1991): Dynamic instability of shear deformable laminated plates, *AIAA Journal*, Vol.**29** (11), pp.2000-2005.
19. **Chamis, C.C.** (1977): Vibration characteristics of composite fan blades and comparison with measured data, *Journal of Aircraft*, Vol.**14** (7), pp.644-647.
20. **Chamis, C.C.,** and **Lynch, J.E.** (1974): High-tip speed fiber composite compressor blades: Vibration and strength analysis, NASA Lewis Research Center, Cleveland, Ohio, Rept. No. NASA-TM-X-71589.
21. **Chamis, C.C.,** and **Minich, M.D.** (1975): Structural response of a fiber composite compressor fan blade airfoil, Rept. No. NASA-TM-X-71623.

22. **Chandiramani, N.K., Shete, C.D.,** and **Librescu, L.I.** (2003): Vibration of higher-order-shearable pretwisted rotating composite blades, *International Journal of Mechanical Sciences*, Vol.**45** (12), pp.2017-2041.
23. **Chandrashekhara, K.** (1989)**:** Free vibrations of anisotropic laminated doubly curved shells, *Computers and Structures*, Vol.**33** (2), pp.435-440
24. **Chen L.W.**, and **Jeng, C. H**. (1993): Vibrational analyses of cracked pretwisted blades, *Computers and Structures*, Vol.**46** (1-3), pp.133-140.
25. **Chen, L.-W**., and **Peng, W.-K.** (1995): Dynamic stability of rotating blades with geometric non-linearity, *Journal of Sound and Vibration*, Vol.**187** (3), pp.421-433.
26. **Chen, L.-W.,** and **Yang, J.Y.** (1990): Dynamic stability of laminated composite plates by the finite element method, *Computers and Structures*, Vol.**36** (5), pp.845-851.
27. **Choi, S.-T.,** and **Chou, Y.-T.** (2001): Vibration analysis of elastically supported turbomachinery blades by the modified differential quadrature method, *Journal of Sound and Vibration*, Vol. **240**(5), pp.937-953.
28. **Cook, R.D**. (1989): Concepts and applications of finite element analysis, *John Wiley and Sons*.
29. **Crispino, D.J.,** and **Benson, R.C.** (1986): Stability of twisted orthotropic plates, *International Journal of Mechanical Sciences*, Vol. **28** (6), pp. 371-379.
30. **Dawson, B.** (1968): Coupled bending-bending vibrations of pretwisted cantilever blading treated by the Rayleigh–Ritz energy method, *Journal of Mechanical Engineering Science*, Vol.**10**, pp. 381–388.
31. **Dey, Partha,** and **Singha, M.K.** (2006): Dynamic stability analysis of composite skew plates subjected to periodic in-plane load, *Thin- walled Structures*, Vol. **44**(9), pp. 937-942.
32. **Dokainish, M.A.**, and **Rawtani, S.** (1969): Vibration analysis of pretwisted cantilever plates, *Transactions of Canadian Aeronautics and Space Institute*, Vol.**2**, pp. 95-100.

33. **Dokainish, M.A.**, and **Rawtani, S.** (1971): Vibration analysis of rotating cantilever plates, *International Journal of Numerical Methods in Engineering*, Vol.**3**, pp. 233-248.
34. **El Chazly, N.M.** (1993): Static and dynamic analysis of wind turbine blades using the finite element method, *Computers and Structures*, Vol.**48** (2), pp. 273-290.
35. **Ganapathi, M.**, **Varadan, T.K.**, and **Balamurugan, V.** (1994): Dynamic instability of laminated composite curved panels using finite element method, *Computers and Structures*, Vol. **53**(2), pp. 335-342.
36. **Gupta, K**., and **Rao, J.S.** (1978[a]): Torsional vibrations of pretwisted cantilever plates, *Journal of Mechanical Engineering Design, Transactions of the ASME*, Vol.**100** (3), pp. 528-534.
37. **Gupta, R.S.**, and **Rao, S.S.** (1978[b]): Finite element eigenvalue analysis of tapered and twisted Timoshenko beams, *Journal of Sound and Vibration*, Vol.**56** (**2**), pp. 187–200.
38. **He, L.-H., Lim, C.W.**, and **Kitipornchai, S.** (2000): A non-discretized global method for free vibration of generally laminated fiber-reinforced pretwisted cantilever plates, *Computational Mechanics*, Vol.**26**, pp.197-207.
39. **Henry, R.,** and **Lalanne, M.** (1974): Vibration analysis of rotating compressor blades, *Journal of Engineering in Industry, Transactions of the ASME*, Vol.**96**, pp. 1028-1035.
40. **Hernried, A.G.**, and **Bian, W.M.**(1993): A finite element approach for determining the frequencies and dynamic response of twisted, nonuniform rotating blades with small or no precone, *Computers and Structures*, Vol.**48** (5), pp.925-933.
41. **Hu, X.X.**, and **Tsuiji, T.** (1999): Free vibration analysis of rotating twisted cylindrical thin panels, *Journal of Sound and Vibration*, Vol.**222** (2), pp.209-224.

42. **Hu, X.X., Sakiyama, T., Matsuda, H.,** and **Morita, C.** (2002): Vibration of twisted laminated composite conical shells, *International Journal of Mechanical Sciences*, Vol.**44** (8), pp.1521-1541.
43. **Hu, X.X., Sakiyama, T., Lim, C.W., Xiong, Y., Matsuda, H.**, and **Morita, C**. (2004): Vibration of angle-ply laminated plates with twist by Rayleigh-Ritz procedure, *Computer Methods in Applied Mechanics and Engineering*, Vol.**193**, Issues 9-11, pp. 805-823.
44. **Kar, R. C.,** and **Neogy, S.**(1989): Stability of a rotating, pretwisted, non-uniform cantilever beam with tip mass and thermal gradient subjected to a non-conservative force, *Computers and Structures*, Vol.**33**(2), pp. 499-507.
45. **Karada, V.** (1984): Finite element dynamic analysis of blade shear center effects on practical bladed disks, *Journal of Sound and Vibration*, Vol.**94**(2), pp.183-197.
46. **Karmakar, A.,** and **Sinha, P.K.** (1997): Finite element free vibration analysis of rotating laminated composite pretwisted cantilever plates, *Journal of Reinforced plastics and composites*, Vol. **16(**16), pp 1461-1490.
47. **Kee, Y.-J**., and **Kim J.-H**. (2004): Vibration characteristics of initially twisted rotating shell type composite blades, *Composite Structures*, Vol. **64**(2), pp.151-159.
48. **Kielb, R.E., Leissa, A.W., Macbain, J.C.,** and **Carney, K.S**. (1985[a]): Joint research effort on vibrations of twisted plates, *NASA Reference Publication*, pp.1150.
49. **Kielb, R.E., Leissa, A.W.,** and **Macbain, J.C.** (1985[b]): Vibrations of twisted cantilever plates – a comparison of theoretical results, *International Journal of Numerical Methods in Engineering*, Vol.**21**, pp.1365.
50. **Kielb, R.E., Macbain, J.C.,** and **Leissa, A.W.** (1985[c]): Vibrations of twisted cantilevered plates – experimental investigation, *ASME Journal of Engineering for Gas Turbines and Power, Vol.* **107**, pp.187-196.

51. **Kuang, Jao-Hwa** and **Hsu, Ming-Hung** (2002): The effect of fiber angle on the natural frequencies of orthotropic composite pretwisted blades, *Composite Structures*, Vol. **58** (4), pp. 457-468.
52. **Lapid, A.J.**, **Kosmatka, J.B.**, and **Mehmed, O.** (1993): Behaviour of spinning laminated composite plates with initial twist-experimental vibrations, strain, and deflection results, *AIAA/ASME/ASCE/AHS/ASC Structures, Structural Dynamics, and Materials Conference, 34th and AIAA/ASME Adaptive Structures Forum, La Jolla, CA, Apr. 19-22, 1993, Technical Papers. Pt. 1 (A93-33876 13-39)*, pp. 255-265.
53. **Lee, J.J.**, **Yeom, C.H.**, and **Lee, I.** (2002): Vibration analysis of twisted cantilevered conical composite shells, *Journal of Sound and Vibration*, Vol.**255** (5), pp.965-982.
54. **Leissa, A.W.** (1980): Vibrations of turbine engine blades by shell analysis, *The Shock and Vibration Digest*, Vol. **12**(11), pp. 3-10.
55. **Leissa, A.W.** (1981): Vibrational aspects of rotating turbomachinery blades, *Applied Mechanics Review*, Vol.**34** (5), pp. 629-635.
56. **Leissa, A.W.,** and **Ewing, M.S.** (1983): Comparison of beam and shell theories for the vibrations of thin turbomachinery blades, ASME *Journal of Engineering for Power*, Vol.**105**, pp. 383-392.
57. **Leissa, A.W.** and **Jacob, K.I.** (1986): Three dimensional vibrations of twisted cantilevered parallelpipeds, *Journal of Applied Mechanics,* Vol.**53**, pp.614-618.
58. **Leissa, A.W., Lee, J.K.**, and **Wang, A.J.** (1981): Vibrations of cantilevered shallow cylindrical shells of rectangular planform, *Journal of Sound and Vibration*, Vol.**78** (3), pp.311-328.
59. **Leissa, A.W., Lee, J.K.**, and **Wang, A.J**. (1982): Rotating blade vibration analysis using shells, ASME *Journal of Engineering for Power*, Vol.**104**, pp. 296-302.

60. **Leissa, A.W., Lee, J.K.**, and **Wang, A.J.** (1983): Vibrations of cantilevered doubly curved shallow shells, *International Journal of Solids and Structures*, Vol.**19** (5), pp. 411-424.
61. **Leissa, A.W., Lee, J.K.**, and **Wang, A.J.** (1984): Vibrations of twisted rotating blades, ASME Journal of Vibration, Acoustics, Stress Reliability Design, Vol.**106**(2), pp. 251-257.
62. **Leissa, A.W., Macbain, J.C.,** and **Kielb, R.E.** (1984): Vibrations of twisted cantilevered plates – summary of previous and current studies, *Journal of Sound and Vibration*, Vol.**96** (2), pp.159-173.
63. **Leissa, A.W.,** and **Qatu, M.S.** (1991): Equations of elastic deformation for laminated composite shallow shells, *Journal of Applied Mechanics*, Vol.**58**, pp.181-188.
64. **Lim, C.W.,** and **Liew, K.M.** (1993): Vibration of pretwisted cantilever trapezoidal symmetric laminates, *Acta Mechanica*, Vol.**111**, numbers 3-4, pp. 193-208.
65. **Lin, Chung-Yi,** and **Chen, Lien-Wen** (2003): Dynamic stability of rotating pretwisted blades with a constrained damping layer, *Composite Structures*, Vol. **61**(3), pp. 235-245.
66. **Macbain, J.C.** (1975): Vibratory behaviour of twisted cantilevered plates, *Journal of Aircraft*, Vol.**12** (4), pp. 343-349.
67. **McGee, O.G.,** and **Chu, H.R.** (1994): Three-dimensional vibration analysis of rotating laminated composite blades, *Journal of Engineering for Gas Turbines and Power*, Vol.**116**, pp.663-671.
68. **Mockensturm, E.M**. (2001): The elastic stability of twisted plates, *Journal of Applied Mechanics, Transactions of the ASME*, Vol. **68** (4), pp. 561-567.
69. **Moita, J.S.**, **Soares, C.M.M.**, and **Soares, C.A.M.**(1999) : Buckling and dynamic behaviour of laminated composite structures using a discrete higher-order displacement model, *Computers and Structures*, Vol. **73**, Issues 1-5, pp. 407- 423.

70. **Moorthy, J., Reddy, J.N., and Plaut, R.H.** (1990): Parametric instability of laminated composite plates with transverse shear deformation, *International Journal of Solids and Structures*, Vol. **26**(7), pp 801-811.
71. **Nabi, S. M.**, and **Ganesan, N.** (1993): Vibration and damping analysis of pretwisted composite blades, *Computers and Structures*, Vol. **47**(2), pp. 275-280.
72. **Nabi, S. M.**, and **Ganesan, N.** (1996): Comparison of beam and plate theories for free vibrations of metal matrix composite pretwisted blades, *Journal of Sound and Vibration*, Vol.**189** (2), pp. 149-160.
73. **Naim, K.,** and **Ghazi, A.F.** (1990): A triangular shell element for vibration analysis of cambered and twisted fan blades, *Finite Elements in Analysis and Design*, Vol.**6** (4), pp.287-301.
74. **Ng, T.Y., Lam, K.Y.,** and **Reddy, J.N.** (1998): Dynamic stability of cross-ply laminated composite cylindrical shells, *International Journal of Mechanical Engineering Sciences*, Vol. **40**(8), pp. 805-823.
75. **Parhi, P.K.**, **Bhattacharyya, S.K.,** and **Sinha, P.K.** (1999): Dynamic analysis of multiple delaminated composite twisted plates, *Aircraft Engineering and Aerospace Technology*, Vol. **71**, pp.451-461.
76. **Petericone, R.,** and **Sisto, F.** (1971): Vibration characteristics of low aspect ratio compressor blades, *ASME Journal of Engineering for Power*, Vol.**93** (1), pp.103-112.
77. **Qatu, M.S.**, and **Leissa, A.W**. (1991): Vibration studies for laminated composite twisted cantilever plates, *International Journal of Mechanical Science*, Vol. **33**(11), pp. 927-940.
78. **Ramamurti, V.,** and **Kielb, R.** (1984): Natural frequencies of twisted rotating plates, *Journal of Sound and Vibration*, Vol.**97** (3), pp. 429-449.
79. **Ramamurti, V.**, and **Sreenivasamurthy, S.** (1980): Dynamic stress analysis of rotating twisted and tapered blades, *Journal of Strain Analysis*, Vol.**15**, pp.117-126.

80. Rand, O., and **Barkai, S.M**. (1997): A refined nonlinear analysis of pretwisted composite blades, *Composite Structures*, Vol.**39** (1-2), pp.39-54.

81. Rao, J.S. (1972): Flexural vibration of pretwisted tapered cantilever blades, *Journal of Engineering Industry*, Vol.**94 (**1), pp. 343–346.

82. Rao, J.S. (1973): Natural frequencies of Turbine blading- a survey, *Shock and Vibration Digest*, Vol.**5** (10), pp.3-16.

83. Rao, J.S. (1977[a])**:** Turbine blading excitation and vibration, *Shock and Vibration Digest*, Vol.**9** (3), pp.15-22.

84. Rao, J.S. (1977[b]): Coupled vibrations of turbomachine blading, *Shock and Vibration Bulletin*, Vol.**47**, pp.107–125.

85. Rao, J.S. (1980): Turbomachine blade vibration, *Shock and Vibration Digest*, Vol.**12** (2), pp.19-26.

86. Rao, J.S. (1992): *Advanced Theory of Vibration*, Wiley, New York, 1992, pp. 330–338.

87. Rao, J.S., and **Gupta, K.** (1987): Free vibrations of rotating small aspect ratio pretwisted blades, *Mechanism and Machine Theory*, Vol.**22**(2), pp.159-167.

88. Rawtani, S., and **Dokainish, M.A.** (1972): Pseudo-static deformation and frequencies of rotating turbomachinery blades, *AIAA Journal*, Vol.**10** (11), pp. 1397-1398.

89. Ray, K., and **Kar, R. C.** (1995): Dynamic stability of a pretwisted, three layered symmetric sandwich beam, *Journal of Sound and Vibration*, Vol. **183**(4), pp.591-606.

90. Reddy, J. N. (2004): *Mechanics of Laminated Composite plates and Shells*, CRC Press, Washington, D.C.

91. Rosen, A. (1991): Structural and dynamic behaviour of pretwisted rods and beams, *Applied Mechanics Review*, Vol.**44** (12), pp.483-515.

92. Sahu, S.K., and **Datta, P.K.** (2000): Dynamic instability of laminated composite rectangular plates subjected to non-uniform harmonic in-plane edge loading, *Journal of Aerospace Engineering*, Proceedings of the Institution of Mechanical Engineers, Part G, **214**, pp.295-312.

93. Sahu, S.K., and **Datta, P.K.** (2001): Parametric resonance characteristics of laminated doubly curved shells subjected to non-uniform loading, *Journal of Reinforced Plastics and Composites*, Vol.**20** (18), pp.1556-1576.

94. Sahu, S.K., and **Datta, P.K.** (2003): Dynamic stability of laminated composite curved panels with cutouts, *Journal of Engineering Mechanics*, ASCE, **129**(11), pp.1245-1253.

95. Sreenivasamurthy, S., and **Ramamurti, V.** (1980): Effect of tip mass on the natural frequencies of a rotating pretwisted cantilever plate, *Journal of Sound and Vibration*, Vol.**70** (4), pp.598-601.

96. Sreenivasamurthy, S., and **Ramamurti, V.** (1981): A parametric study of vibration of rotating pretwisted and tapered low-aspect ratio cantilever plates, *Journal of Sound and Vibration*, Vol.**76** (3), pp.311-328.

97. Subrahmanyam, K.B., and **Rao, J.S. (**1982): Coupled bending–bending vibrations of pretwisted tapered cantilever beams treated by the Reissner method, *Journal of Sound and Vibration*, **Vol. 82** (4), pp. 577–592.

98. Thirupathi, S.R., Seshuz, P., and **Naganathany, N.G**. (1997): A finite element static analysis of smart turbine blades, *Smart Materials and Structures*, Vol.**6** (5), pp. 607-615.

99. Thomas, J., and **Sabuncu, M**. (1979): Finite element analysis of rotating pretwisted asymmetric cross-section blades, *ASME Design Engineering Technical Conference*, 79-DET-95, pp.1-12.

100. Toda, A. (1971): An investigation of flexural vibrations of pretwisted rectangular plates, Ohio State University, M.S.Thesis.

101. Tsuiji, Tsuneo, and **Sueoka, Teiyu** (1987): Free vibrations of pretwisted plates (Fundamental Theory), *JSME International Journal*, Vol. **30,** pp. 958-962.

102. Walker, K.P. (1978): Vibrations of cambered Helicoidal Fan blades, *Journal of Sound and Vibration*, Vol. **59**(1), pp. 35-57.

103. White, J.F., and **Bendiksen, O.O.** (1987): Aeroelastic behaviour of low aspect ratio metal and composite blades, *Journal of Engineering Gas Turbines and Power, Transactions of the ASME*, Vol.**109**, pp 168-175.

104. Yang, S. M., and **Tsao, S. M.** (1997): Dynamics of a pretwisted blade under nonconstant rotating speed, *Computers and Structures*, Vol. **62**(4), pp. 643-651.

105. Yoo, H.H., **Kwak, J.Y.**, and **Chung, J**. (2001): Vibration analysis of rotating pretwisted blades with a concentrated mass, *Journal of Sound and Vibration*, Vol. **240**(5), pp.891-908.

106. Yoo, H.H., Park, J.H., and **Park, J.** (2001): Vibration analysis of rotating pretwisted blades, *Computers and Structures*, Vol. **79**(19), pp 1811-1819.

APPENDIX

Programme features and flow chart

For the present analysis, codes are developed in FORTRAN 77. The program can be used for both homogeneous and laminated composite cases. The finite element procedure involves three basic steps which may be summarized as:

- Preprocessor
- Processor
- Post processor

The different functions are given in Figure 6.1

Preprocessor

This module of the programme reads the input data which includes the geometry of the twisted panel, boundary conditions of the twisted panel, material properties(isotropic or composite), loading configuration, static and dynamic load factor, etc. Also in this module, the finite element mesh is generated including node numbers, nodal coordinates, nodal connectivity and active degrees of freedom of each node. Finally it creates an array for all the elements which comprises the kinematic, geometric and material properties.

Processor

The processor module generates the element plane, bending and geometric stiffness matrices and the consistent mass matrix. These are assembled into global

stiffness and mass matrices using skyline technique. The global load vector is also prepared. Then an eigen value subroutine using subspace iteration technique is used to determine the eigen values for free vibration, buckling and dynamic stability analyses.

Postprocessor

In this part of the programme all the input data are echoed to check their accuracy. The outputs obtained from the various analyses are also printed. The results are stored in a series of separate output files for each category of problem analysed and the values used to prepare the tables and graphs.

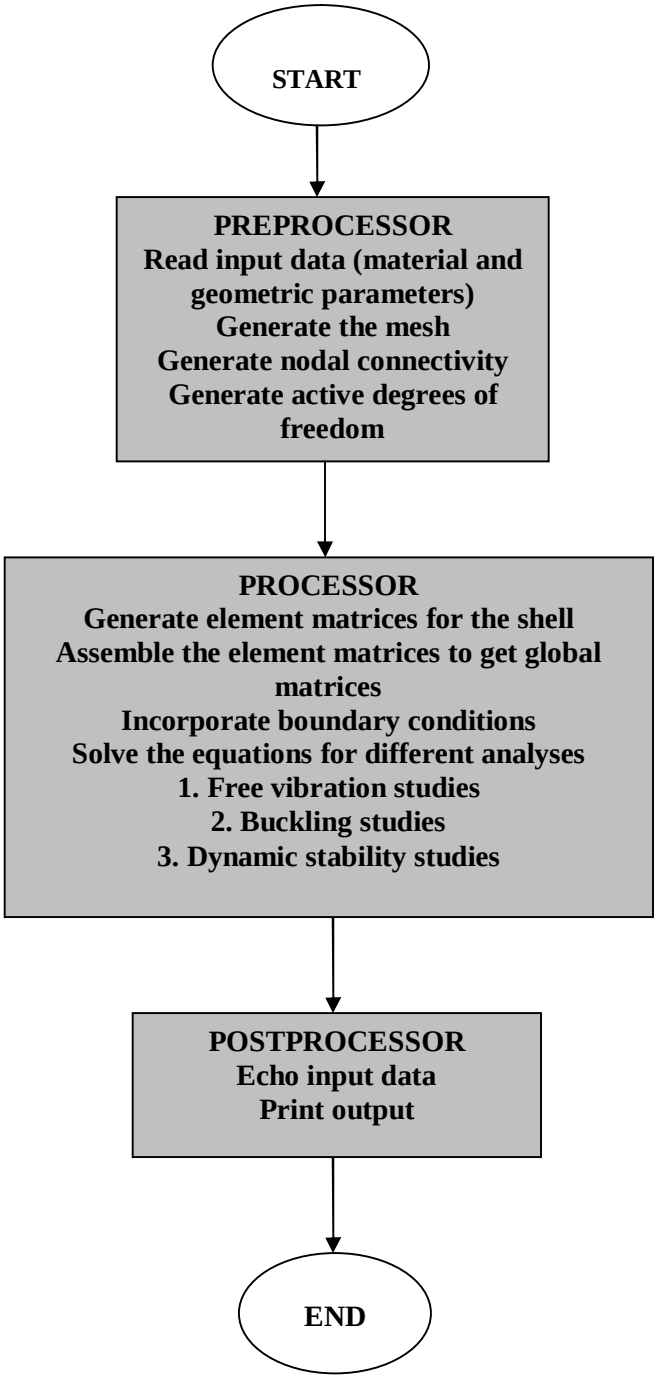

Figure 6.1: Flow chart of computer programme